Pairing and Condensation in Ultracold Quantum Gases

THESIS SUBMITTED FOR THE DEGREE OF DOCTOR OF PHILOSOPHY (SCIENCE) OF JADAVPUR UNIVERSITY

Raka Dasgupta
SATYENDRANATH BOSE NATIONAL CENTRE
FOR BASIC SCIENCES
BLOCK-JD, SECTOR III, SALT LAKE
KOLKATA 700 098, INDIA

August, 2012

CERTIFICATE FROM THE SUPERVISOR

This is to certify that the thesis entitled **"Pairing and Condensation in Ultracold Quantum Gases."** submitted by Smt. **Raka Dasgupta**, who got her name registered on **August 5, 2009** for the award of **Ph.D. (Science) degree** of **Jadavpur University**, is absolutely based upon her own work under the supervision of **Professor Jayanta Kumar Bhattacharjee** at **S. N. Bose National Centre For Basic Sciences, Kolkata, India** and that neither this thesis nor any part of it has been submitted for either any degree/diploma or any other academic award anywhere before.

JAYANTA KUMAR BHATTACHARJEE
Senior Professor
(Supervisor)

Date :

Department of Theoretical Sciences
S N Bose National Centre For Basic Sciences,
Block JD, Sector III, Salt Lake, Kolkata 700098
India.

To My Parents

And

To Sayan

"Around here, however, we don't
look backwards for very long.
We keep moving forward, opening up new doors and
doing new things, because we're curious
and curiosity keeps leading us down new paths."

-Walt Disney

ACKNOWLEDGEMENTS

First of all, I would like to thank Prof. J. K. Bhattacharjee for being such an amazing supervisor and mentor. His command over almost all the branches of physics, his deep insight that goes into every analytical problem that he puts his mind on, and his infectious passion for the subject played a key role in giving shape to this work. He gave me all the freedom to pursue problems in my own way. Yet, whenever I seemed to enter a blind alley, he was there to lift my spirit and show me the right track. Working with him has introduced me to various aspects of ultracold atom physics, and most importantly, taught me to appreciate the underlying beauty of this subject. I take immense pride in being his student.

I would like to express my sincere gratitude to Prof. Krishnendu Sengupta. His lectures on many-body physics served as the gateway for me to enter this fascinating field. I worked with him in a collaborational project, and that was an excellent learning experience for me. His vast knowledge of the subject and his enthusiasm for trying out newer routes has always remained as a great inspiration for me.

It is a pleasure to acknowledge my collaborators : Dr. Arnab Das, Dr. Analabha Roy and Sanhita Modak; and Arghya Dutta, my junior in our research group. Discussions and interactions with all of them have enriched me.

I had the opportunity of meeting Prof. Prashanta Panigrahi, Prof. Hiranmaya Mishra, Prof. Dilip Angom, Dr. Rajdeep Sensarma, Prof. Carlos Sa de Melo, Prof. Sandro Stringari, Dr. Masud Haque in various national and international conferences on cold atom physics. Discussions with them have helped me to acquire a better understanding of the subject. I was fortunate to be able to interact with Prof. Wolfgang Ketterle when he visited our institute. His way of explaining the difficult concepts in ultracold fermionic pairing by means of simple and beautiful analogies is something I would never forget.

I am grateful to Dr. Simon Gardiner who hosted my visit to his group in Durham University, U.K. That was my first hands-on session with computational cold atom physics, and my first visit to an actual BEC lab.

I would like to mention that my stay in S. N. Bose institute has been the most wonderful and fruitful phase of my life. For the first few months after joining this institute my research life was not all smooth sailing. It was my seniors: Tamoghna-da, Arya-da, Sagar-da, Arnab-da and Ankush-da who dragged me out of that rough patch. It was on their suggestion that I requested Prof. Bhattacharjee to be my thesis advisor. That indeed was the turning point for me.

The love and support I received from all my seniors, batchmates and juniors is something I shall cherish forever. I was lucky to have friends like Swastika, Indrakshi, Amartya, Sirshendu, Rudranil, Hena and others in the institute. With them being around, it was like living in an extended family.

I must thank our Director, Prof. A K Raychaudhuri for the way he motivated the students to strive for excellence. The administration, faculty and staff of our institute have always extended their helping hands to me. The coordination with Jadavpur University has entirely been handled by Mr. Sunish Kumar Deb and I thank him for his assistance.

I take this opportunity to thank my teachers in Siliguri Girls' High School, and my professors in Jadavpur University. Their contribution to my academic career has been an overwhelming one. I would like to acknowledge my physics friends from other research institutes/ universities : Shreyoshi, Hridis, Amit and Amit-da, who provided valuable support throughout this period. Talking to people like Sudipto-da, Aditi-di, Shankha, Souradip often provided me the much-needed breather, and helped me to cope with the stress in a researcher's life.

I am grateful to all my family members for their love and support. A special thanks to my in-laws for being so caring and understanding of my studies and research.

I am thankful to Sayan who came forward to share my dreams, and not only insisted but also ensured that I put my research above everything else. In him, I found a loving friend and a caring husband with whom I share the same passion for literature, art, theatre and music. Together, it has been a wonderful journey all the way.

I cannot thank my parents enough for always being there by my side. My father Dr. Dhruba Dasgupta who himself was a professor of physics, has always taken a keen interest in my studies and research. To me, he is the best teacher ever. My mother Nandita Dasgupta is the pillar of strength for me. It was their love and support that kept me going for all these years, and I am sure that it would be the same for the years to come.

Raka Dasgupta

List of Publications

1. **Stability of the breached pair state for a two-species fermionic system in the presence of Feshbach resonance**
   Raka Dasgupta, Phys. Rev. A. **80**, 063623, (2009)

2. **Stability of a gapless state for population-imbalanced fermionic systems**
   Raka Dasgupta, Physics Teacher (Quarterly Journal of Indian Physical Society) **51**, numbers 3-4, (2009)

3. **Effects of three-body scattering processes on BCS-BEC crossover**
   Raka Dasgupta, Phys. Rev. A, **82**, 063607,2010

4. **Dynamics as a probe for population-imbalanced fermionic systems**
   Raka Dasgupta and J. K. Bhattacharjee, arXiv:1110.4092v1
   (communicated to European Journal of Physics B)

5. **Periodic dynamics of Fermi superuids in the BCS regime**
   Analabha Roy, Raka Dasgupta, Sanhita Modak, Arnab Das, and K. Sengupta (to be communicated soon).

Contents

List of Figures

Chapter 1

Introduction

" Deep in the sea
all molecules repeat
the patterns of one another
till complex new ones are formed.
They make others like themselves
and a new dance starts."

-From a poem by Richard Feynman

1.1 Superfluidity, Superconductivity and Cooper Pairs

The story of superconductivity and superfluidity is an old one. It dates back to the early 20th century. However, this is one tale that never lost its freshness and charm, for, generations of scientists have retold it, and enriched it in their own ways.

Superconductivity was discovered in 1911 when the resistance of mercury was observed to go to zero below a critical temperature [1]. This was quite unprecedented, at least from the classical point of view. Indeed, superconductivity is novel in the sense that it is a quantum phenomenon that has manifestation even in the classical macroscopic world. These resistance-less or frictionless flows are nothing but manifestations of quantum mechanical effects that take place at very low temperatures. To observe these fascinating phenomena, one has to go deep down in the low temperature regime, so that the thermal de Broglie wavelength exceeds the interparticle separation in a gas and become compa-

rable or greater than it. This is precisely the reason why low temperatures are special. People thus got excited by the idea of exploring physical systems near absolute zero, and started working on ultracold atomic gases. Today, scientists are extensively studying ultracold Bose and Fermi gases, and theories and experiments are going hand in hand.

The discovery of superconductivity was followed by another important achievement. The superfluid phase of liquid Helium-4 was revealed in 1938 when the viscosity of the liquid below the λ point (2.17 K) was measured [2,3]. Later, Helium-3, the fermionic Helium isotope, was also found to be superfluid at a much lower temperature than Helium-4 [4].Then in the eighties, high-temperature superconductors in Copper-oxide compounds were discovered, thus adding to the family of superconducting materials [5].
The family became even bigger when it was discovered that there are many other physical systems that display superfluid properties such as neutron stars, excitons in semiconductors, atomic nuclei. All these systems are characterized by frictionless flow and quantized vorticity. If the system is electrically charged, it is called a superconductor. On the other hand, if it is charge-neutral, then it is termed as a superfluid.

One of the theories put forward to explain superfluidity and superconductivity was that of Bose-Einstein condensation (BEC) of bosonic particles. BEC is a consequence of the quantum statistics of bosons, which are particles with integer spin, and it results in a macroscopic occupation of a single quantum state [6]. This state of matter was first predicted by Albert Einstein in 1924-1925 on the basis of the new statistics introduced by Satyendra Nath Bose. Fritz London proposed in 1938 that superfluid properties of Helium-4 came from Bose-Einstein condensation of bosonic Helium-4 atoms.

The complete microscopic theory of superconductivity was proposed in 1957 by Bardeen, Cooper and Schrieffer, which is known as the BCS theory. This was based on the suggestion by Cooper in 1956 that a pair of fermions in the presence of a filled Fermi sea will form a bound pair in the presence of an arbitrarily small attractive interaction [7]. The result predicted the formation of a minimum excitation energy, or energy gap, in the conductor below a critical temperature T_c. Many properties of conventional superconductors

could be understood as consequences of this energy gap, and the BCS picture was hailed as a successful theory of superconductivity.

In a system of charge-neutral uldracold atom gas, the relevant property is not superconductivity, but superfluidity. The first insight into the theory of superfluidity came from F. London, Lev Landau, V. L. Ginzburg and R. P. Feynman [8, 9]. However, to capture the the microscopic details of superfluid transitions, one has to take resort of the BCS theory. For example, although phenomenologies of the superfluid states of Helium-4 and Helium-3 are very similar, the actual mechanisms are not the same. This is reflected in the fact that superfluidity occurs in liquid Helium-4 at much higher temperatures than the transition temperature of Helium-3. Since Helium-4 atoms are bosons, their superfluidity can be regarded as a consequence of Bose-Einstein condensation in an interacting system. On the other hand, Helium-3 atoms are fermions, and the superfluid transition in this system is best described by formation of Cooper pairs, as in the BCS theory of superconductivity [10, 11].

1.2 Bose Einstein Condensation

In the last section we used the term 'Bose Einstein Condensation'. In a nutshell, a Bose-Einstein condensate is a state of matter of a dilute gas of weakly interacting bosons trapped in an external potential and cooled to temperatures of the order of nano or picokelvin. Under such conditions, a large fraction of the bosons occupy the lowermost quantum state of the external potential. At that point quantum effects become apparent even on a macroscopic scale, and the condensate can be described quite successfully by a mean field theory.

As already mentioned, Bose Einstein Condensation was predicted by Einstein in 1924 on the basis of ideas given by Satyendra Nath Bose on photons. Its consequence was that if a system of particles obey the Bose counting system, i.e., the Bose statistics, and if the total number of particles is conserved, there should be a temperature below which a finite fraction of the particles would condense into the same state [6]. Einstein's original prediction was for non-interacting systems. Later, when superfluidity in Helium-4 was

observed below the λ point, Fritz London suggested that although the system is strongly interacting, it is actually Bose Einstein Condensation which has taken place in the system. It is the emergence of BEC which is responsible for the superfluid properties [12].

Amongst the scientific community, the interest in the theory of Bose Einstein Condensation was rekindled after its experimental realization. The first gaseous condensate was achieved by Eric Cornell and Carl Wieman in 1995 at the University of Colorado at Boulder NIST-JILA lab.They used a gas of Rubidium atoms for the experiment and cooled it to 170 nanokelvin (nK) ($1.7X10^{-7}$ K). About four months later, the MIT group led by Wolfgang Ketterle [13] created a condensate of ^{23}Na. Ketterle's condensate had about a hundred times more atoms. His experiment yielded several significant results including the observation of quantum mechanical interference between two different condensates. For their achievements Cornell, Wieman, and Wolfgang Ketterle received the 2001 Nobel Prize in Physics.

More experiments followed. A group led by Randall Hulet at Rice University created a condensate of lithium atoms only one month after the JILA work [14]. The novelty with this experiment was that unlike Sodium or Rubidium, Lithium has attractive interactions which causes the condensate to be unstable. Thus it would collapse for most of the atoms. Hulet and co-workers stabilized the condensate in a subsequent experiment by applying quantum pressure from trap confinement for up to about 1000 atoms.

One of the most noteworthy features of these trapped Bose gases is that they are inhomogeneous and finite-sized systems, the number of atoms ranging typically from a few thousands to several millions. In typical BEC experiments the atoms are confined in magnetic traps and cooled down to extremely low temperatures, of the order of nano or picokelvins. The first evidence for condensation can be captured by time of flight measurements. The atoms are left to expand by switching off the confining trap and then imaged with optical methods. A sharp peak in the velocity distribution is then observed below a certain critical temperature, which is counted as a clear signature of BEC.

In most cases, the confining traps can be approximated by harmonic potentials. The

trapping frequency, ω_{ho}, provides also a characteristic length scale for the system, $a_{ho} = [\hbar/m\omega_{ho}]^{1/2}$ [12], of the order of a few microns in the available samples. Density variations occur on this scale. This marks a sharp contrast to other systems, like for instance superfluid helium, where the effects of inhomogeneity take place on a microscopic scale fixed by the interatomic distance. In the case of ^{87}Rb and , ^{23}Na the size of the system is enlarged as an effect of repulsive two-body forces and the trapped gases can become almost macroscopic objects, directly measurable with optical methods.

The initial experiments with alkali BEC could be perfectly described by existing theories. However, the progress in experimental techniques became so fast, that soon they started posing new questions to the theorists as well. Moreover, recent work in the field of BEC became relevant for the outstanding theoretical questions not only in atomic physics, but also in condensed matter physics. For example, experiments achieved BEC with much stronger interatomic interactions than typical alkali gases, and that influenced the studies of all strongly correlated systems. furthermore, these interactions could even be tuned externally by applying magnetic fields [15, 16]. Another breakthrough came when phase transition to the highly-correlated Mott insulator state was observed through studies of quantum gases in optical lattice potentials [17]. All these opened up new vistas for BEC-studies in particular, and cold atom physics in general.

1.3 Cold Fermions

The achievement of Bose-Einstein-Condensation (BEC) in trapped, dilute, weakly interacting atomic gases [13, 14] started a whole new era of atomic physics. Over the past decade, the quest for the demonstration of BEC has redefined itself, and discovered new exciting challenges. The natural extension of this work was the search for quantum degeneracy in Fermions, particles with half-integer spins.

In practice, fermions did not lag much behind bosons when it comes to experimental considerations involving their cooling. After the first experimental report on cooling a dilute Fermi gas to temperatures where quantum statistics are already pronounced, by DeMarco and Jin [18], this field became even more popular. Soon it started attracting large interest both from theoretical and experimental sides.

At the same time as the creation of the first strongly interacting Bose gases, people started applying the techniques used to create alkali BECs to the other class of quantum particles, fermions. To create an ultracold Fermi gas, experimenters applied the same cooling techniques as those used to obtain BEC, but instead of the bosonic atom, such as ^{87}Rb or ^{23}Na, they used its fermionic counterpart. The two such stable alkali atoms are ^{40}K and ^{6}Li. However, there was a problem dealing with fermions. As a consequence of the quantum statistics of fermions, the s-wave collisions required for standard evaporative cooling method could not occur at ultracold temperatures in a gas of identical fermions. The solution to this problem was to introduce a second particle to ensure the evaporative cooling, either another hyperfine state of that particular fermionic atom or an entirely different species. The first fermionic candidate which successfully entered the quantum degenerate regime was ^{40}K, created at JILA in 1999 [18]. Unlike Bose gas, no phase transition was observed here. But the experimental signatures clearly deviated from classically predicted results when the Fermi gas was cooled below the Fermi temperature. More experiments on Fermi systems followed, using a wide variety of cooling techniques. [19–22].

After the creation of a normal Fermi gas of atoms, the next target was to form a superfluid out of a paired Fermi gas, keeping in mind the analogy with conventional superconductors consisting of Cooper pairs. It was thought that just like the s-wave pairing occurring between spin-up and spin-down electrons in superconductors, a pairing would play the pivotal role in a two-component atomic gas with an equal Fermi energy for each component. Such a two-component gas was realized using an equal mixture of alkali atoms in two different hyperfine spin states. However, it was soon found out that for typical interatomic interactions the temperatures required to reach a BCS-like state were far too low compared to achievable temperatures at that time. Soon a method was devised. Stoof et al. noted that the interaction between ^{6}Li atoms was large compared to typical values ($|a| \sim 2000a_0$), as well as attractive, bringing the BCS transition temperature closer to realistic temperatures [23]. It was then recognized that by means of a type of scattering resonance, known as a Feshbach resonance, the interaction strength could be varied arbitrarily. By changing the magnetic field, the system can even be taken to the

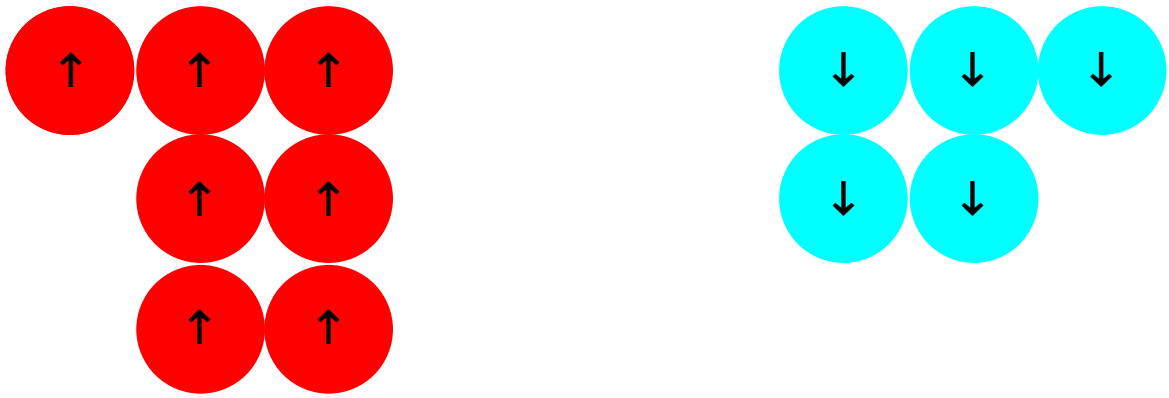

Figure 1.1: Population-imbalanced fermionic system

strong coupling regime. Popularly this is known as the BCS-BEC crossover.

1.4 Population Imbalanced Fermions

It is a well established fact that superfluidity and superconductivity in fermionic systems arise from pairing of fermions. This the reason why these phenomena are often described as the Bose condensations of Cooper pairs formed out of those fermions.

In fermionic systems, Cooper pairs are made of fermions of different species. For example in superconductors they are electrons of opposite spins and opposite momenta. For a cold atom system, they are atoms belonging to different species, or, alternatively, belonging to two different hyperfine states of the same atom. It is obvious that the most favorable situation for pairing is when the two species of fermions have the same population, so that every fermion can find its partner and there is no unpaired fermion in the ground state. The physics of pairing and resultant superfluidity under such condition is well described by the BCS theory.

However, when the two fermion species have different densities, the physics of pairing no more goes the BCS way. In any paired superfluid state formed under such situation, some of the majority fermions will necessarily be unpaired. The question to be addressed then reduces to -"How would the system accommodate these unpaired fermions? " An early suggestion was given by Fulde and Ferrell [24] and Larkin and Ovchinnikov [25]

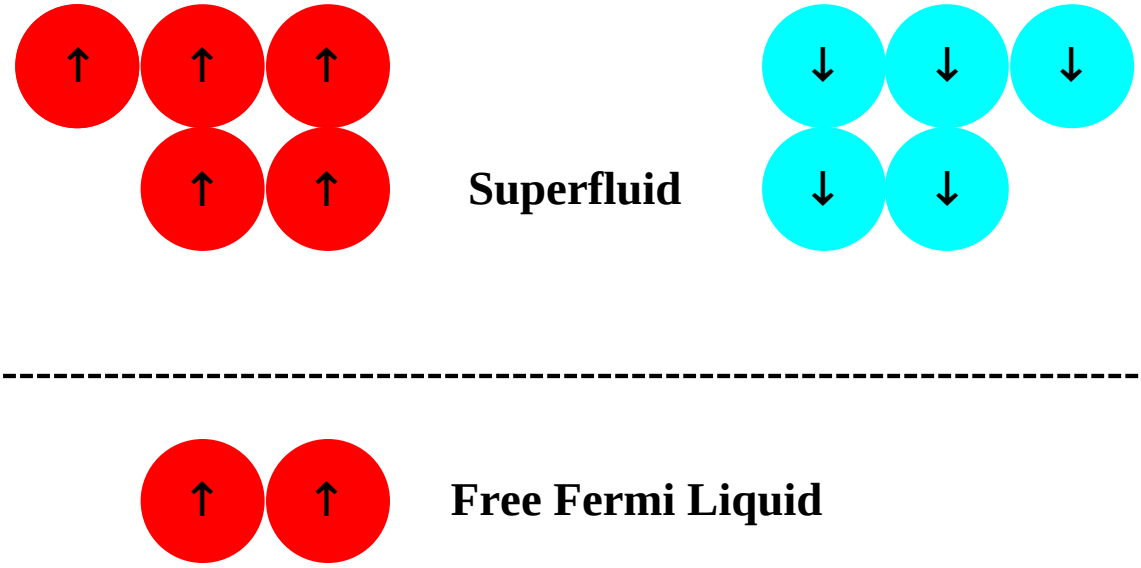

Figure 1.2: Phase separated imbalanced system

who argued that the Cooper pairs may condense into either a single finite momentum state, or a state that is a superposition of finite-momentum states. Such states are known collectively as the Fulde-Ferrell- Larkin-Ovchinnikov (FFLO) state.

Another example of the population-imbalanced pairing is the Sarma state, or the breached pair phase. Sarma [26], in the early studies of superconductivity, predicted a spatially isotropic, homogeneous and uniform state with gapless excitation modes in the presence of a magnetic field. A similar gapless phase was discussed in the context of population-imbalanced cold fermionic system [27, 28]. However, for weak coupling BCS theory, this gapless breached pair state marks the maximum of the thermodynamic potential, and thus, cannot be the stable ground state of the system. This is the well-known Sarma instability. In the last few years, several mechanisms were put forward to avoid this instability [29–33] . Another place where pairing between unbalanced fermion species arises is quark and nucleon pairing in high density quark or nuclear matter, such as in the core of a neutron star. There the origin of density imbalance is due to the difference in the rest mass of quarks or nucleons that form the pairs; when the different pairing species are in chemical equilibrium.

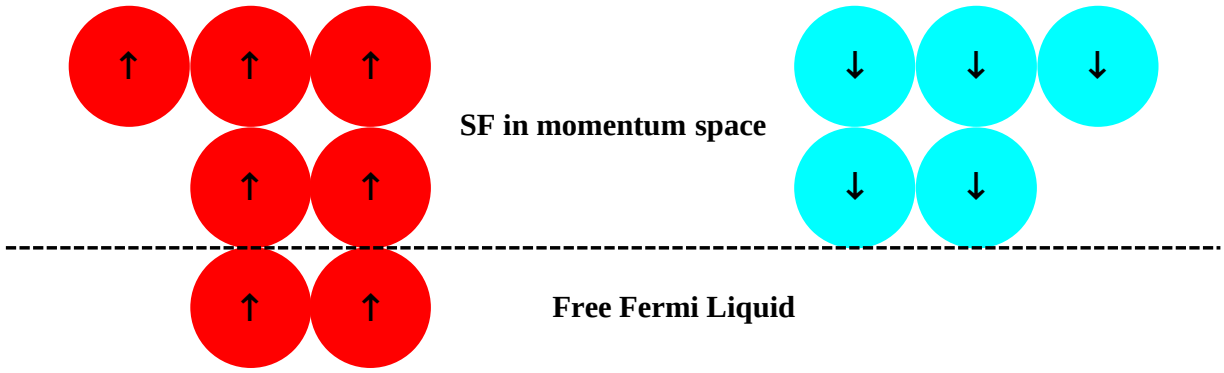

Figure 1.3: Breached Pair system

1.5 BCS-BEC Crossover

The problem of BCS-BEC crossover is also an old one, having been studied in a variety of contexts in the 80s and 90s [34–37], although recent experimental realization through ultracold Fermi gases [38–40] has led to a revival of interest in the subject. The basic idea behind this problem is simple: a system of fermions with weak attractive interaction is known to form large overlapping Cooper pairs of zero center of mass momentum and zero net spin. In charged systems, this leads to superconductivity, while neutral systems show superfluid behavior. The system in this limit is well described by the BCS mean field theory of superconductivity. If the strength of this fermion-fermion interaction is gradually increased, As the attraction goes beyond a point, bound states can be formed [41–43]. If the attraction is increased much beyond this point, tightly bound bosonic molecules with a large binding energy would appear. A many body system of these bosons would then undergo Bose Einstein condensation (BEC) at sufficiently low temperatures. The challenge is then to find a single theory which can describe the entire regime from the BCS to the BEC limit .

BCS-BEC crossover was first addressed way back in 1969, in the seminal work of Eagles [44]. Later, using a variational prescription, Leggett [34] showed that as the coupling strength is increased, the superconducting BCS ground state at zero temperature smoothly evolves into a BEC state of tightly bound molecules. Nozieres and Schmitt-

Rink [35] and M. Randeria [36, 37] extended the analysis to a finite temperature. Since then, various aspects of the crossover problem has been widely investigated over the years.

So the crucial point is, one needs a handle over the fermion-fermion coupling. The interaction potential between the atoms depend on their internal states leading to a two-channel problem. For example, when there is a spin- singlet and a spin triplet state, The effective interaction in the triplet channel can be tuned by changing the energy of a bound state in the singlet channel relative to the scattering states in the triplet channel with a magnetic field. The scattering cross section in the singlet channel becomes maximal when the bound state energy crosses the energy of the lowest scattering state in the singlet channel. This phenomenon is called the Feshbach resonance.

In a simplified picture, a Feshbach resonance occurs when the energy of a bound state of the interatomic potential is equal to the kinetic energy of a colliding pair of atoms. Assuming a finite kinetic energy, such a degeneracy can occur only when the bound state exists in a potential that has a higher threshold energy than that of the colliding atom pair. This condition can be satisfied in ultracold gases of alkali atoms, due to the low collision energy of the atoms and the existence of atomic hyperfine structure. Since the different hyperfine states generally possess different spin configurations and magnetic moments, one can sometimes tune the bound state energy into resonance with the colliding atom energy via the different Zeeman shifts in an external magnetic field. Assuming that both colliding atoms are in the lower hyperfine state, it may happen that an interatomic potential associated with the upper hyperfine state supports a bound state nearby in energy.

If two atoms begin an elastic collision in the lower channel with kinetic energy much smaller than the hyperfine splitting, the atoms cannot have the energy to go to the upper channel because. Thus, the upper channel is energetically "closed", while the lower channel is termed to be "open".

Resonance scattering occurs when a bound state of the potential is very close to the collision energy of the atoms. The colliding atoms then can make a transition to the bound state and stay there for a short time before moving apart again after the collision. An enormous change in the scattering process occurs when the two levels have exactly the

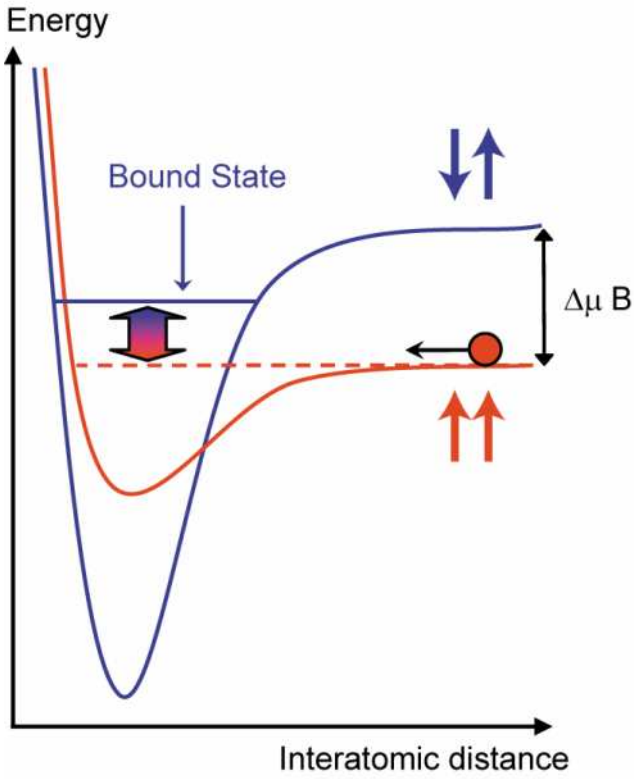

Figure 1.4: Feshbach resonance (Figure credit: Webpage of Ketterle group, MIT)

same energy, which causes the elastic cross section and scattering length to reach infinite values. In a Feshbach resonance, one can adjust the energy of a bound state relative to the collision energy just by tuning the magnetic field. Even though the bound state exists in a different interatomic potential from that of the colliding atoms, the variable bound state energy can have an immense influence on the atom-atom scattering length.

From the coupled-channels scattering theory of Feshbach resonances, one can derive an approximate analytic expression for the variation of the scattering length [12]

$$a = a_{bg}(1 - \frac{\Gamma}{H - H_0}) \tag{1.1}$$

It follows that as a is negative when there is no bound state, it tends to $-\infty$ at the onset of the bound state and to $+\infty$ just as the bound state stabilizes. It remains positive but decreases in value as the interaction becomes increasingly strong. The magnitude of a_s is

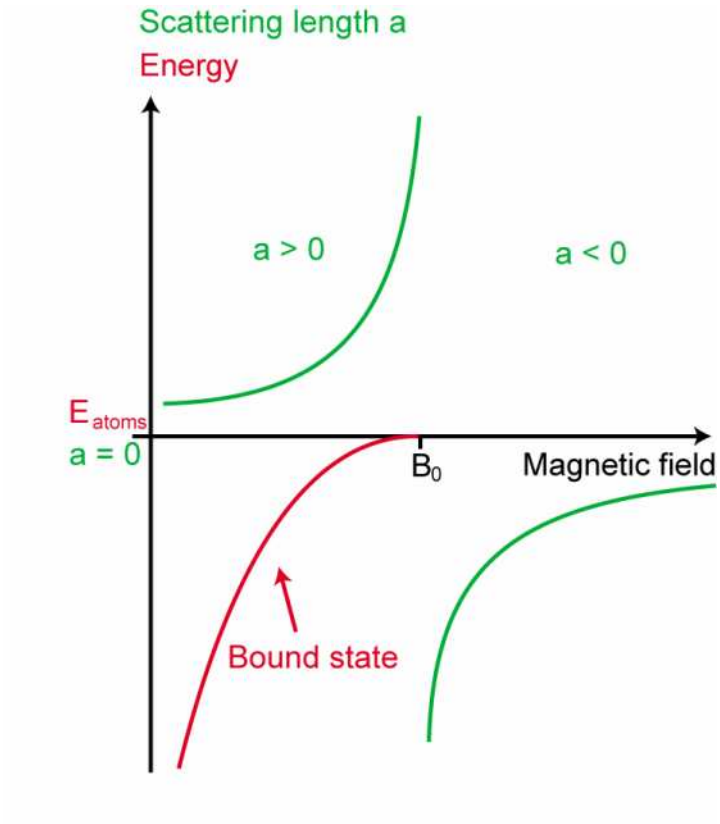

Figure 1.5: BCS-BEC crossover (Figure credit: Webpage of Ketterle group, MIT)

small in both the extreme BCS and BEC limits, but with opposite signs. Although the two-body scattering length changes abruptly at the unitarity ($|a_S| = \infty$), in the N-body problem, superfluid properties vary smoothly through this point.

1.6 Dynamical Studies

The dynamical properties are extremely important attributes of ultracold atomic gases. In the recent years, scientists have started to explore Fermi and Bose systems from this perspective as well. The discovery that the interparticle interaction can be tuned via Feshbach resonance has led to much advances in this front, and both the BCS-BEC crossover and the dynamics of the condensate fraction were investigated.

The expansion of Bose and Fermi superfluids after the sudden release of the confining

potential has been extensively studied by experimentalists, and the collective excitations of these systems have been duly probed. In fact, it started with the first generation of experiments on trapped Bose-Einstein Condensates. Once the trap potential was suddenly switched off, the imaging of the expanding cloud highlighted many features of the condensate, like the bimodal structure of the Bose system at finite temperature and the anisotropy of the expanded gas. Experiments with weakly coupled Fermi gases followed suit and collective excitations were measured. Ultracold Li^6 atoms were proved to be excellent candidates for all these experiments because when the BCS-BEC crossover is achieved, Li^6 gas shows a good amount of stability in the molecular regime.

As for the theorists, both the equilibrium and non-equilibrium aspects of the ultracold system dynamics have been important. Although dynamical studies were going on for a long time addressing various quantum systems, the advancement in the experiments with ultracold atoms rekindled the interest in this field. This is mostly because the Feshbach-tuned experiments now enabled the scientists to have a good control over the parameters in the quantum Hamiltonians. Thus, ultracold atom gases provided a wonderful test bed for many-body quantum theories.

1.6.1 Quench Dynamics

The high tunability associated with ultracold atom experiments have also opened up new avenues for studying nonequilibrium quantum dynamics of many-body systems. In these experiments, one can change the system parameters rapidly, and study the quantum evolution that follows. As a matter of fact, it is not always possible for to vary parameters (like the magnetic field in Feshbach resonance) adiabatically throughout the experiment, and abrupt changes in the parameter value has to be taken into account. Nonadiabatic dynamics has been investigated for the superfluid to Mott insulator quantum phase transition, and for the BCS-BEC crossover as well.

In most of these cases where the system parameters are changed or quenched rapidly, a standard quench picture or prescription holds. It is assumed that the system is prepared in the ground state of an initial Hamiltonian H, and as the sudden change takes place, a different Hamiltonian H' takes over. However, the change is so fast that the system

does not even "realize" at that time that a change has taken place, and the ground state remains unaltered., only now it evolves under the influence of the new Hamiltonian. For all calculations, the ground state is now expanded in terms of the eigenstates of the new Hamiltonian.

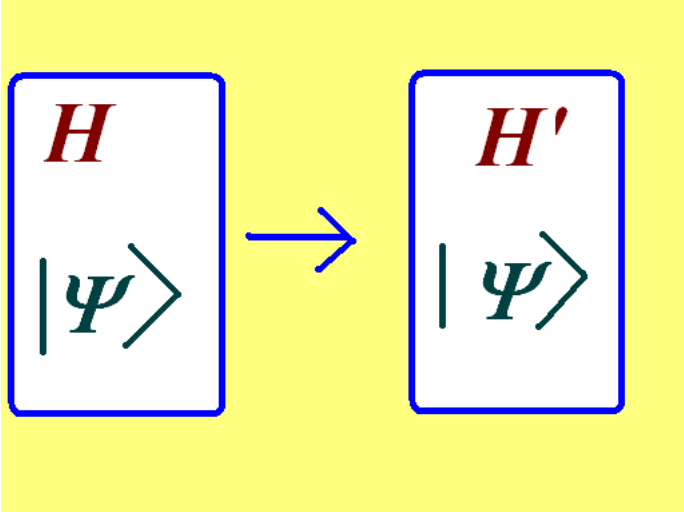

Figure 1.6: Quench mechanism

Quenches are important from the standpoint of scaling laws and universality. In adiabatic evolutions across a critical point, a universal scaling property arises. Similarly, if a system is quenched through a quantum phase transition, several quantities (like the quasiparticle excitation energy, fidelity susceptibility etc.) scale in a definite fashion, tallying with the universality of the system.

Even when there are no actual phase transitions in the system, a tuning of the parameters in the system Hamiltonian can lead to a certain "level crossing" : the system can now either stay in the ground state or jump to the excited state. This dynamics is usually described by the Landau-Zener process.

1.6.2 Natural Dynamics of the System

The study of the collective excitation modes of a many-body system is also very useful. It sheds light on the system for both equilibrium and far-from-equilibrium cases. Near equilibrium, the fluctuations in the system variable that arises due to small perturbations

is either periodic or decaying. Since the collectives modes are stable there, a growth cannot be present in this dynamics.

The study of the excitation modes, even in the linearized approximation, holds the key to the understanding of many important properties of the system. S. Nascimbene et al. [45] in their paper on collective oscillations of an imbalanced Fermi gas puts it very nicely : "The study of the low-lying excitation modes of a complex system can be a powerful tool for investigation of its physical properties. For instance, Earths structure has been probed using the propagation of seismic waves in the mantle, and the ripples in space-time propagated by gravitational waves can be used as probes of extreme cosmic phenomena." Ultracold atom systems are no exceptions. Measurement of low energy modes of bosonic or fermionic systems has indeed been of much use to probe manifestations of superfluidity, or to study vortex lattices [46, 47].

1.7 About this Thesis

The work reported in this thesis is divided into four major chapters: Chapter 2-Chapter 5. The first two of them deal with static properties of ultracold atom systems, while the last two investigate dynamic properties.

In chapter 2, we discuss the phenomenon of fermionic pairing and BCS-BEC crossover for a population-imbalanced fermionic system in the presence of Feshbach resonance, where the resonantly-paired fermions combine to form bosonic molecules. In addition to the fermion-fermion coupling and the Feshbach interaction, we also take into account the scattering of Cooper pairs by newly formed bosons near the resonance. Thus, it is essentially the study of a three-body process.

In chapter 3, we study a population-imbalanced two-species fermionic system. There are, as discussed earlier, suggestions of various possible superfluid states that can accommodate those excess fermions. We focus on one such particular state : the Sarma phase or Breached Pair state. It had been argued earlier that this state marks the maximum of thermodynamic potential for the weak-coupling regime, and therefore, cannot be a stable configuration. This is termed as the Sarma instability. Here we try to address an important question in this line : if instead of only the weak-coupling BCS side we consider

the entire BCS-BEC crossover path, can we have a region where the breached pair state might become stable?

With chapter 4, we turn to the dynamics of superfluid systems. We focus here on fast quench dynamics,i.e., the evolution of the system after one of the system parameter is changed rapidly. We feel that this is really important if one tries to draw a parallel with actual cold atom experiments. We talk about both linear quenches and periodically driven quenches in the context of a BCS superfluid.

Chapter 5 is also about dynamical studies. This time we study the natural dynamics of population-imbalanced ultracold Fermi systems. Our aim is to use the results obtained from this analysis to probe monentum space structures of the imbalanced configuration. In fact, it is extremely difficult for present-day experiments to detect the exotic phases that appear from the imbalanced pairing, and it is almost impossible to resolve their momentum-space structures. We believe that the study of dynamical properties can go a long way in determining the momentum space structures of two-species fermions with mismatched Fermi surfaces. This is the motivation behind chapter 5.

In chapter 6, we summarize all our findings, and talk about the future directions that can emerge from our work.

So the essential questions that we have addressed in this thesis are:

- What happens to the BCS-BEC crossover picture if additional three-body interactions are taken into account?

- For a population-imbalanced two-species fermionic system, how are the excess fermions accommodated? If we consider the breached pair state as a possible candidate for representing such a system, can we identify the conditions which make it a stable one?

- How do the system parameters scale for a superfluid system undergoing linear quench dynamics?

- What happens if a periodic drive is introduced in the quench Hamiltonian for the

BCS superfluid?

- In a system of fermions capable of forming bosons via BCS-BEC crossover, what is the nature of the fluctuations in the condensate fraction? How many frequencies of oscillation are there?

- Can the dynamical study be used to probe the momentum-space structures of a population-imbalanced two-species Fermi system? Can it be linked to experimental possibilities?

Bibliography

[1] H. K. Onnes, Akad. van Wetenschappen **14**, 818 (1911).

[2] J. F. Allen and A. D. Misener, Nature **141**, 75 (1938).

[3] P. Kapitza, Nature **141**, 74 (1938).

[4] D. D. Osheroff, R. C. Richardson, and D. M. Lee, Phys. Rev. Lett. **28**, 885 (1972).

[5] J. G. Bednorz and K. Mueller, Z. Physik B **64**, 189 (1986).

[6] K. Huang, Statistical Mechanics, (Willy, 1987)

[7] L. N. Cooper, Phys. Rev. **104**, 1189 (1956).

[8] F. London, Superfluids (Wiley, New York, 1950)

[9] R. P. Feynman, Statistical Mechanics: A Set of Lectures (Addison-Wesley, New York, 1988)

[10] D.R. Tilley and J. Tilley, "Superfluidity and Superconductivity, (IOP Publishing Ltd., Bristol, 1990)

[11] James F. Annett: Superconductivity, superfluids, and condensates,(Oxford Univ. Press, Oxford 2005)

[12] C. J. Pethick and H. Smith, Bose-Einstein Condensation in Dilute Gases (Cambridge University Press, Cambridge, England, 2002).

[13] K.B. Davis, M.O. Mewes, M.R. Andrews, N.J. van Druten, D.S. Durfee, D.M. Kurn, and W. Ketterle, Physical Review Letters **75** , 3969 (1995)

[14] C. C. Bradley, C. A. Sackett, J. J. Tollett, and R. G. Hulet, Physical Review Letters **75**, (1995)

[15] S. Inouye, M. R. Andrews, J. Stenger, H.-J. Miesner, D. M. Stamper-Kurn, and W. Ketterle, Nature, **392**, 151 (1998).

[16] J. L. Roberts, N. R. Claussen, J. P. Burke, Jr., C. H. Greene, E. A. Cornell, and C. E. Wieman, Phys. Rev. Lett. **81**, 5109 (1998).

[17] M. Greiner, O. Mandel, T. Esslinger, T. W. Hnsch, and I. Bloch, Nature **415**, 39 (2002).

[18] B. DeMarco and D. S. Jin, Science **285**, 1703 (1999)

[19] A. G. Truscott, K. E. Strecker, W. I. McAlexander, G. B. Partridge, and R. G. Hulet, Science **291**, 2570 (2001).

[20] F. Schreck, L. Khaykovich, K. L. Corwin, G. Ferrari, T. Bourdel, J. Cubi- zolles, and C. Salomon, Phys. Rev. Lett. **87**, 080403 (2001).

[21] G. Roati, F. Riboli, G. Modugno, and M. Inguscio, Phys. Rev. Lett. **89**, 1804 (2002).

[22] S. R. Granade, M. E. Gehm, K. M. O Hara, and J. E. Thomas, Phys. Rev. Lett. **88**, 120405 (2002).

[23] H. T. C. Stoof, M. Houbiers, C. A. Sackett, and R. G. Hulet, Phys. Rev. Lett. **76**, 10 (1996).

[24] P. Fulde, R. A. Ferrel, Phys. Rev. A, **135**, 550, (1964).

[25] A. I. Larkin, Yu. N. Ovchinnikov, Sov. Phys. JETP **20**, (1965).

[26] G.Sarma, J.Phys.Chem.Solid 24,1029(1963).

[27] D. T. Son and M. A. Stephanov, Phys. Rev. A **74** 013614 (2006).

[28] W. V. Liu and F. Wilczek, Phys. Rev. Lett. **90**, 047002 (2003).

[29] C. H. Pao et al., Phys. Rev. B **73**, 132506 (2006).

[30] M.M.Forbes, E.Gubankova, W.V.Liu and F.Wilczek, Phys. Rev. Lett.**94**, 017001(2005).

[31] H.Hu and X.Liu,. , Phys. Rev. A ,73, 051603(R)(2006).

[32] M.Mannarelli, G. Nardulli and M. Ruggieri, Phys. Rev. A.74, 033606(2006)

[33] Lianyi He et al., Phys. Rev. B 79, 024511 (2009).

[34] A.J. Leggett, in Modern Trends in the Theory of Condensed Condensed Matter, edited by A. Pekalski and R. Przystawa (Springer- Verlag, Berlin, 1980).

[35] P. Nozieres and S. Schmitt-Rink, J. Low Temp. Phys. **59**, 195 (1985).

[36] M. Randeria in Bose-Einstein Condensation, edited by A. Griffin, D. Snoke, and S. Stringari, Cambridge University Press, Cambridge, England, 1994.

[37] M. Randeria, J. M. Duan, and L. Y. Shieh, Phys. Rev. Lett. **62**,1989.

[38] C. A. Regal , M. Greiner and D.S. Jin , Phys. Rev. Lett. **92**, (2004) 040403.

[39] M. W. Zwierlein, C. A. Stan, C. H. Schunck, S. M. F. Raupach, A. J. Kerman, and W. Ketterle, Phys. Rev. Lett. **92**, 120403 (2004).

[40] M. W. Zwierlein, C.H. Schunck, A. Schirotzek, and W. Ketterle, Nature(London) **442**, 54 (2006)

[41] E. Timmermans, K. Furuya, P. W. Milonni, and A. K. Kerman, Phys. Lett. A **285**, 228 (2001).

[42] Y. Ohashi and A. Griffin, Physics Review Letter, **89**,130402 (2002).

[43] Q. Chen, J. Stajic, S. Tan, and K. Levin, Phys. Rep. **412**, 1 (2005).

[44] D.M Eagles, Phys. Rev. **186**, 456 (1969).

[45] S. Nascimbe‘ne, N. Navon, K. J. Jiang, L. Tarruell, M. Teichmann, J. McKeever, F. Chevy, and C. Salomon, Phys. Rev. Lett. **103**, 170402 (2009).

[46] S. Giorgini, L. Pitaevskii, and S. Stringari, Rev. Mod. Phys. **80**, 1215 (2008).

[47] F. Chevy, K.W. Madison, and J. Dalibard, Phys. Rev. Lett. **85**, 2223 (2000).

Chapter 2

BCS-BEC Crossover in the Presence of Three-body Interactions

2.1 BCS-BEC Crossover

In the introductory part, we had briefly talked about BCS-BEC crossover. Although the idea is an old one, [1–4], it is still very much relevant and has inspired many experimental endeavours [5–7]. Recent experiments have successfully explored the crossover regime by means of studying the cloud size [8], expansion energy [9], resonance condensation [5, 10] and condensed nature of the fermionic atom pairs [6, 7]. From the theoretical standpoint, the pioneering works by Eagles [11], Leggett [1], Nozieres and Schmitt-Rink [2] and M. Randeria [3, 4] have found many successors [12–22].

2.2 Three-body Scattering Processes

Almost all the works have addressed the crossover phenomenon as a two-body scattering problem, where the interaction between two fermions has played the pivotal role. As the interaction between them is increased gradually, the fermion pairs form boson molecules, and the crossover is driven by the two-body interaction only. However, as Milstein et al. pointed out [23], it would be interesting to extend this approach to incorporate the effect of higher order interactions in the crossover region. In fact, higher order scatterings and nonlinear interactions are being investigated in other domains of ultracold atom physics as well, starting from cubic interactions in BEC [24–27], to atom-dimer scattering in fermi systems [28–30] and induced interactions in three-component Fermi gases [31]. All these

studies have brought out interesting new features of the systems. BCS-BEC crossover, too, should not be an exception.

The simplest form of higher order many-body interactions would be a three-fermion scattering. It has been argued by Holland et al. [15] that its effect will not be a prominent one, because in such a three-body interaction, the s-wave state is forbidden. The only three-body scattering could come from p waves, which have very little contribution at sufficiently low temperatures. We, too, neglect these interactions for the time being. Instead, we shift our focus [1]to a situation when, along the crossover path, some atom pairs have formed composite molecules, while some other pairs are yet to do so (they are still in the Cooper pair state). The newly formed bosons would scatter the pre-formed bosons (or, Cooper pairs). It is basically a three-body scattering. This interaction should be important near the resonance point. Each of the two-body and three-body interactions can be either attractive or repulsive. We take a variational mean field approach, and discuss the effect of this additional term for all the above four cases.

2.3 Model Hamiltonian and Ground State

Here we start with a two-species fermionic system. In addition to the fermion-fermion interaction (denoted by g_1), and an additional interaction (g_2) of the Feshbach variety which couples a fermion of type a with a b fermion to form a bosonic molecule B, we also take into account the scattering of pre-formed bosons or Cooper pairs by freshly formed bosons. Strength of the interaction is given by g_3. The system is described by the Hamiltonian:

$$\begin{aligned} H = \sum (2\nu - \mu_B) B_0^\dagger B_0 + \sum_{\mathbf{p}} \tilde{\epsilon}_{\mathbf{p}}^a a_{\mathbf{p}}^\dagger a_{\mathbf{p}} + \sum \tilde{\epsilon}_{\mathbf{p}}^b b_{\mathbf{p}}^\dagger b_{\mathbf{p}} - g_1 \sum a_{\mathbf{p}'}^\dagger b_{-\mathbf{p}'}^\dagger b_{-\mathbf{p}} a_{\mathbf{p}} \\ + g_2 \sum [B_0^\dagger a_{\mathbf{p}} b_{-\mathbf{p}} + a_{\mathbf{p}}^\dagger b_{-\mathbf{p}}^\dagger B_0] + g_3 \sum B_{0'}^\dagger a_{\mathbf{p}'}^\dagger b_{-\mathbf{p}'}^\dagger b_{-\mathbf{p}} a_{\mathbf{p}} B_0 \end{aligned} \tag{2.1}$$

The ground state of the system is consequently given by [14,32] a product wavefunction of the BCS ground state, and the ground state for the condensate part of the boson

[1]The work reported here is based on the paper " Effects of three-body scattering processes on BCS-BEC crossover", Raka Dasgupta, Phys. Rev. A, **82**, 063607, 2010

subsystem.

$$|\Psi\rangle = \prod (U_{\mathbf{p}} + V_{\mathbf{p}} a^{\dagger}_{\mathbf{p}} b^{\dagger}_{-\mathbf{p}})|0\rangle \otimes \exp(-\alpha^2/2 + \alpha B^{\dagger})|0\rangle \tag{2.2}$$

where $\alpha = \sqrt{N_B}$, N_B being the expectation value of the total number of bosons in the condensed state.

2.4 Effective Coupling

From the Hamiltonian (2.1) and the ground state wave function (2.2), the ground state energy of the system would be

$$\begin{aligned} E = \sum (\tilde{\epsilon}^a_{\mathbf{p}} + \tilde{\epsilon}^b_{\mathbf{p}}) V^2_{\mathbf{p}} + g_1 \sum_{\mathbf{p},\mathbf{p}'} U_{\mathbf{p}} V_{\mathbf{p}} U_{\mathbf{p}'} V_{\mathbf{p}'} + (2\nu - \mu_B)\alpha^2 \\ + 2g_2 \alpha \sum_{\mathbf{p}} U_{\mathbf{p}} V_{\mathbf{p}} + g_3 \alpha^2 \sum_{\mathbf{p},\mathbf{p}'} U_{\mathbf{p}} V_{\mathbf{p}} U_{\mathbf{p}'} V_{\mathbf{p}'} \end{aligned} \tag{2.3}$$

Differentiating E with respect to $V_{\mathbf{p}}$

$$\begin{aligned} 4\epsilon^{+}_{\mathbf{p}} V_{\mathbf{p}} + 2g_1 \sum_{\mathbf{p},\mathbf{p}'} U_{\mathbf{p}'} V_{\mathbf{p}'} (U_{\mathbf{p}} - V^2_{\mathbf{p}}/U_{\mathbf{p}}) + 2g_2 \alpha (U_{\mathbf{p}} - V^2_{\mathbf{p}}/U_{\mathbf{p}}) \\ + 2\alpha^2 g_3 \sum_{\mathbf{p},\mathbf{p}'} U_{\mathbf{p}'} V_{\mathbf{p}'} (U_{\mathbf{p}} - V^2_{\mathbf{p}}/U_{\mathbf{p}}) = 0 \end{aligned} \tag{2.4}$$

We assume that in the mean field framework, instead of couplings g_1, g_2 and g_3, this equation can be written in terms of an effective two-body coupling g_{eff}. This is in conformity with what Mora et al. [30] found out for a confined three-body problem : that it can be completely expressed in terms of two-body quantities. Equation (2.4) now takes the form -

$$4\epsilon^{+}_{\mathbf{p}} V_{\mathbf{p}} + 2g_{eff} \sum_{\mathbf{p},\mathbf{p}'} U_{\mathbf{p}'} V_{\mathbf{p}'} (U_{\mathbf{p}} - V^2_{\mathbf{p}}/U_{\mathbf{p}}) = 0 \tag{2.5}$$

The exact form of g_{eff} is to be determined later. Drawing an analogy with the standard BCS treatment, we can write $-g_{\text{eff}} \sum_{\mathbf{p}} U_{\mathbf{p}} V_{\mathbf{p}} = \Delta$, where Δ is the gap in the excitation spectrum [33].

Next, differentiating E with respect to α, we obtain

$$2\alpha(2\nu - \mu_B) + 2g_2 \sum_{\mathbf{p}} U_{\mathbf{p}} V_{\mathbf{p}} + 2\alpha g_3 \sum_{\mathbf{p},\mathbf{p}'} U_{\mathbf{p}} V_{\mathbf{p}} U_{\mathbf{p}'} V_{\mathbf{p}'} = 0 \tag{2.6}$$

. Or,

$$\alpha = -\frac{g_2 \sum_{\mathbf{p}} U_{\mathbf{p}} V_{\mathbf{p}}}{(2\nu - \mu_B + g_3 \sum_{\mathbf{p},\mathbf{p}'} U_{\mathbf{p}} V_{\mathbf{p}} U_{\mathbf{p}'} V_{\mathbf{p}'})} \tag{2.7}$$

Putting $-g_{\text{eff}} \sum_{\mathbf{p}} U_{\mathbf{p}} V_{\mathbf{p}} = \Delta$ as mentioned before,

$$\alpha = \frac{g_2 \frac{\Delta}{g_e ff}}{(2\nu - \mu_B + g_3 \frac{\Delta^2}{{g_{eff}}^2})} \tag{2.8}$$

Using this in equation (4), we get

$$\begin{aligned} g_{eff} &= g_1 + g_3 \alpha^2 - \frac{g_2^2}{(2\nu - \mu_B + g_3 \frac{\Delta^2}{{g_{eff}}^2})} \\ &= g_1 - \frac{g_2^2}{(2\nu - \mu_B + g_3 \frac{\Delta^2}{{g_{eff}}^2})} + \frac{g_3 g_2^2 \frac{\Delta^2}{{g_{eff}}^2}}{(2\nu - \mu_B + g_3 \frac{\Delta^2}{{g_{eff}}^2})^2} \end{aligned} \tag{2.9}$$

In the BCS limit, Δ goes as $e^{-\frac{1}{a_s}}$ [1]. Therefore, as $a_s \to 0$, Δ goes to zero much faster than g_{eff} (which is proportional to a_s). Hence $\frac{\Delta^2}{g_{eff}^2} \to 0$ in this limit.

We therefore have

$$g_{eff} = g_1 - \frac{g_2^2}{(2\nu - \mu_B)} \tag{2.10}$$

If g_1, i.e., the two-fermion coupling is attractive, then this becomes $|g_{eff}| = |g_1| + \frac{g_2^2}{(2\nu - \mu_B)}$, a result analogous to the effective coupling in a standard two-species fermionic system, where only the fermion-fermion scattering is taken into account [16, 19, 32]. This is consistent with the fact that in the extreme BCS limit, there are almost no composite bosons at all. Therefore, the boson-fermion scattering should not have any effect on the coupling parameter.

On the other hand, in the extreme BEC limit, Δ goes as $a_s^{-\frac{1}{2}}$ [34]. Therefore, $\frac{\Delta^2}{g_{eff}^2} \approx \frac{1}{g_{eff}^3}$. Equation (2.9) thus becomes:

$$\begin{aligned} g_{eff} &= g_1 - \frac{g_2^2}{(2\nu - \mu_B + \frac{g_3}{{g_{eff}}^3})} + \frac{g_3 g_2^2}{{g_{eff}}^3(2\nu - \mu_B + \frac{g_3}{{g_{eff}}^3})^2} \\ &= g_1 - \frac{g_2^2}{(2\nu - \mu_B + \frac{g_3}{{g_{eff}}^3})}\Big(1 - \frac{\frac{g_3}{{g_{eff}}^3}}{2\nu - \mu_B + \frac{g_3}{{g_{eff}}^3}}\Big) \\ &= g_1 - \frac{g_2^2(2\nu - \mu_B)}{(2\nu - \mu_B + \frac{g_3}{{g_{eff}}^3})^2} \end{aligned} \tag{2.11}$$

This is essentially a polynomial in degree 7, its real roots being the solutions for effective coupling.

We approximate the effective coupling in BCS side by equation (2.10) and that of the BEC side by equation (2.11) and study the crossover for various combinations of 2-body coupling (g_1) and 3-body coupling (g_3). At resonance, it is known that Δ is proportinal to Fermi energy only [35]. So very near resonance, we treat Δ as a constant.

In the conventional BCS-BEC crossover picture, the two-body coupling (and thus, the scattering length, too) is positive in the BEC side, and it goes to ∞ at resonance. It assumes a negative value in the BCS side, and near resonance, goes to $-\infty$.

In order to study the effects of three-body processes, here we assign some arbitrary values to g_1, g_2 and g_3 (all the couplings are scaled by the Fermi energy), and calculate the effective two-body couplings. g_{eff} is plotted against the detuning $2\nu - \mu_B$ to obtain the crossover picture. We note that even if the magnitudes of g_1, g_2 and g_3 are changed, the general qualitative trend of the coupling vs. detuning curve remains the same.

2.5 Crossover When Two-body Interaction is Attractive, Three-body Interaction is Repulsive

Here we choose $g_1 = -1$, $g_2 = 10$ and $g_3 = 0.1$

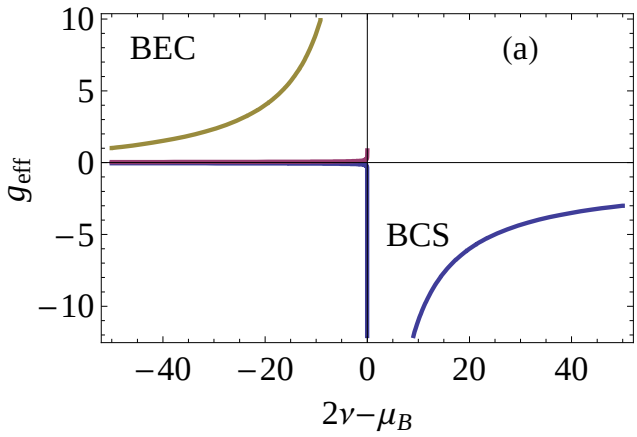

Figure 2.1: Crossover paths near resonance when the two body interaction is attractive, and the three-body one repulsive.

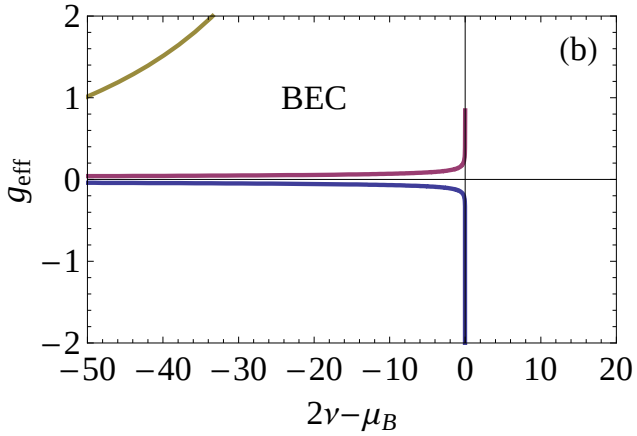

Figure 2.2: A closer view of the multiple roots of Fig. 2.1 at the resonance region.

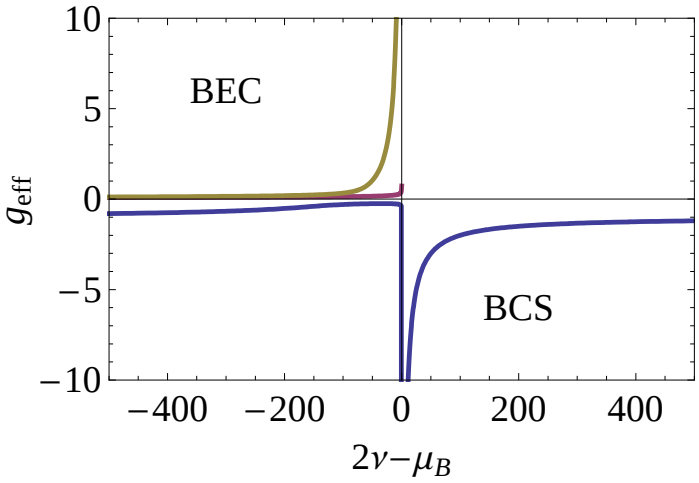

Figure 2.3: Crossover paths for a longer detuning range when the two body interaction is attractive, and the three-body one is repulsive.

The g_{eff} vs. $2\nu - \mu_B$ curve is plotted in Figs. 2.1, 2.2 and 2.3 for two different ranges. As shown in Figs. 2.1and 2.2, when we approach $2\nu = \mu_B$, i.e., the resonance condition from the BEC side, we find there are two additional roots in addition to the $g_{eff} = \infty$ root. Therefore, when we move away slightly from the resonance towards the BEC region, there are three roots : one that corresponds to g_{eff} in the absence of any g_3 (and goes to ∞ at resonance), a negative root that goes almost linearly and reaches g_1 at resonance as evident from equation(2.11), and a positive root that also varies almost in a linear fashion. All the three roots survive even when the system lies deeper at the BEC domain.

In the BCS side, there is a single root which is identical to the effective coupling of the system in that region when there was no g_3. It goes to $-\infty$ at resonance.

Therefore, if starting from the BCS side, one tries to achieve the crossover, right after crossing the $2\nu = \mu_B$ point, one encounters three possible paths (Fig. 2.3) – one coming from $+\infty$, and the other two from finite values of g_{eff}. If the system takes either of the two lower paths, the system actually bypasses the unitarity region (where the scattering length diverges) in the BEC side. In such cases, although a region of unitarity will be present in the BCS side, its BEC side counterpart would be absent.

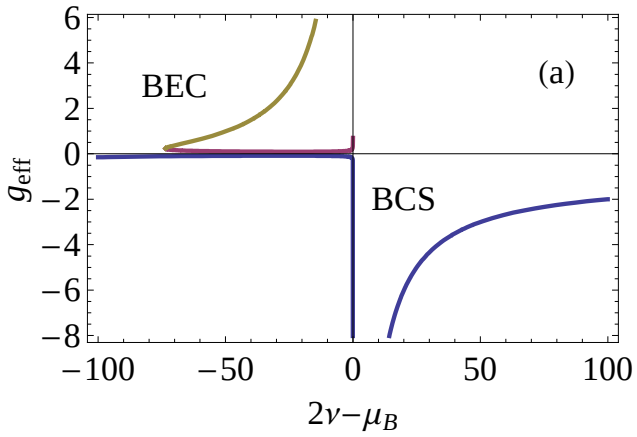

Figure 2.4: Crossover paths near resonance when both the two body and three-body interactions are attractive.

2.6 Crossover When Two-body and Three-body Interactions are Both Attractive:

Here we choose $g_1 = -1$, $g_2 = 10$ and $-g_3 = 0.1$. As before, the g_{eff} vs. $2\nu - \mu_B$ curve is plotted. Here also, we observe the trend to be similar to the previous case. As shown in Figs. 2.4 2.5, we have three real roots in the BEC side and a single real root in the BCS side.

In the BEC side, therefore, the system has the option to take any of the routes : one of them resembles the case of $g_3 = 0$, and unitarity regions are there at both sides of the resonance. However, the other two branches can lead to a crossover scenario where again the unitarity is avoided in the BEC region.

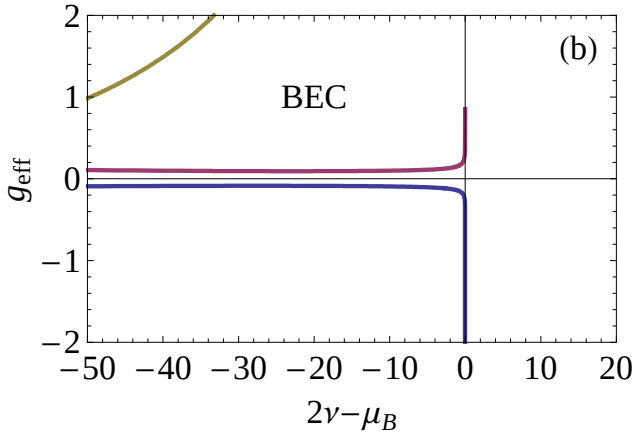

Figure 2.5: A closer view of the multiple roots of Fig. 2.4 at the resonance region.

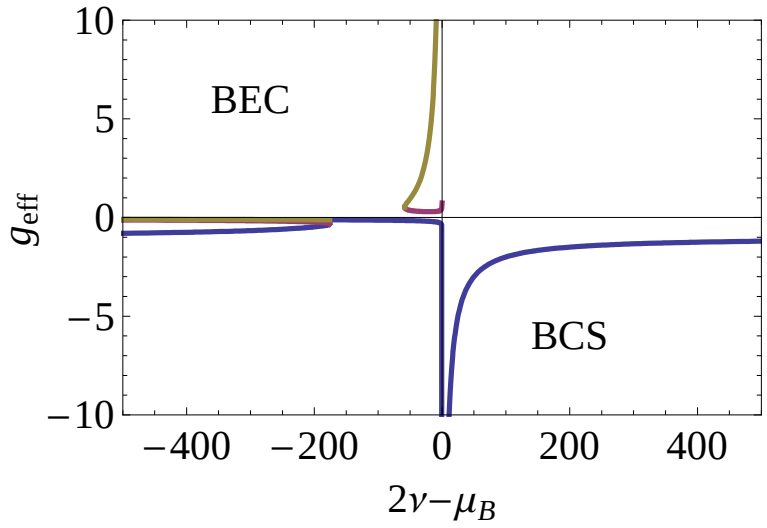

Figure 2.6: Crossover paths for a longer detuning range when both the two body and three-body interactions are attractive.

We observe from Figs.2.4 and 2.6 that that the upper two branches (including the traditional branch that we have for $g_3 = 0$) have a region of discontinuity, while the lowermost route is a continuous one.

2.7 Crossover When Two-body and Three-body Interactions are Both Repulsive

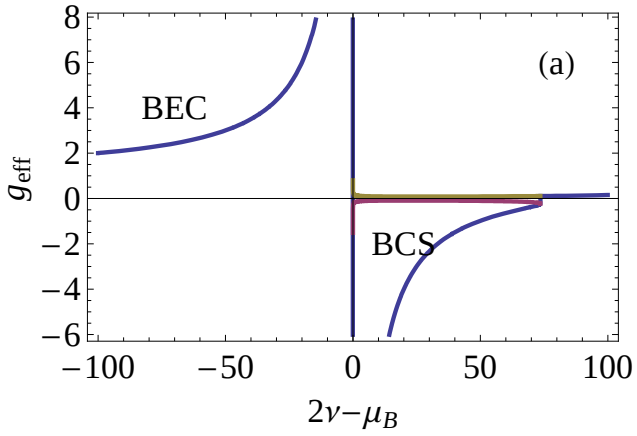

Figure 2.7: Crossover paths near resonance when both the two body and three-body interactions are repulsive.

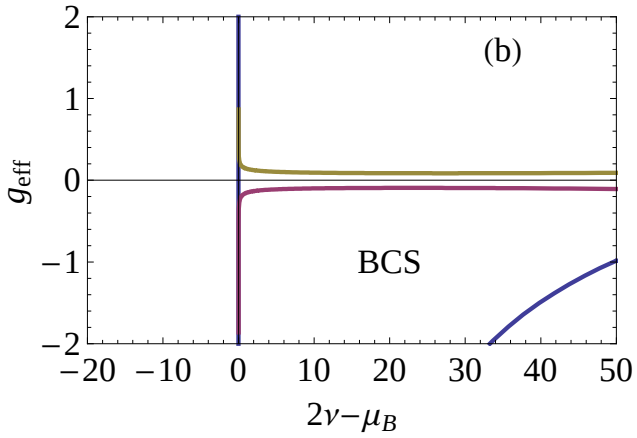

Figure 2.8: A closer view of the multiple roots of Fig. 2.7 at the resonance region.

We choose $g_1 = 1$, $g_2 = 10$ and $g_3 = 0.1$. Here, as shown in Figs. 2.7 and 2.8, there are three real roots in the BCS side, and one single root in the BEC region.

2.8 Crossover When Two-body Interaction is Repulsive, Three-body Interaction is Attractive

Here we choose $g_1 = 1$, $g_2 = 10$ and $g_3 = -0.1$.

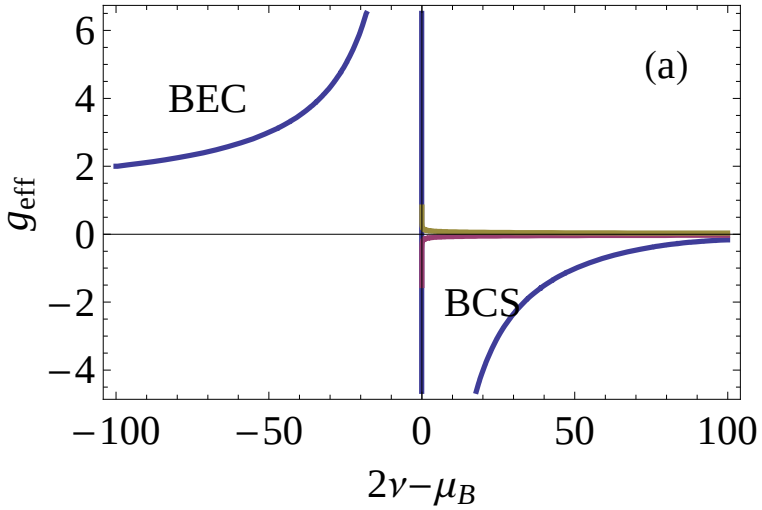

Figure 2.9: Crossover paths near resonance when the two body interaction is repulsive, and the three-body one is attractive.

In this case, as seen from Figs. 2.9 and 2.10 the crossover picture closely resembles the earlier case, i.e., there are three possible routes in the BCS side, while a single route is available in the BEC side.

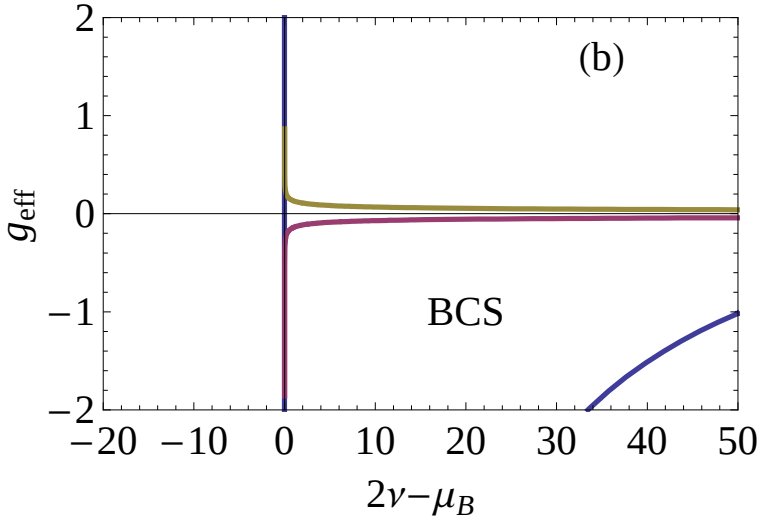

Figure 2.10: A closer view of the multiple roots at the resonance region.

2.9 Which Path is More Favourable? Energy Considerations:

Let E be the total energy of the system minus kinetic energy of the fermions. Now, if we compute and compare E for all three branches, the branch corresponding to the minimum energy should be the one that the system favours. At resonance we can treat Δ as constant. Using this, we plot E with $2\nu - \mu_B$ and g_{eff} (Fig. 2.11). In the BEC side, the lowermost branch corresponds to the minimum energy. Now, since this branch is associated with an attractive effective interaction, the BEC state should either collapse, or be a metastable one. Here we would get the latter, as the attraction is very weak.

Thus, we have a striking property of the BCS-BEC crossover : If we start from a stable BEC state, we can achieve the BCS domain via Feshbach resonance; but if we start from the BCS side instead, we reach at a metastable BEC state. Thus the process is not totally reversible.

In the BCS side, as apparent from the Fig 2.12, the branch closer to $g_{eff} = 0$ should be the favoured one. But in that case, the scattering length does not go to negative infinity, and the system cannot achieve the crossover. This is in contradiction with the well-established theoretical and experimental results [1, 3, 6, 7].

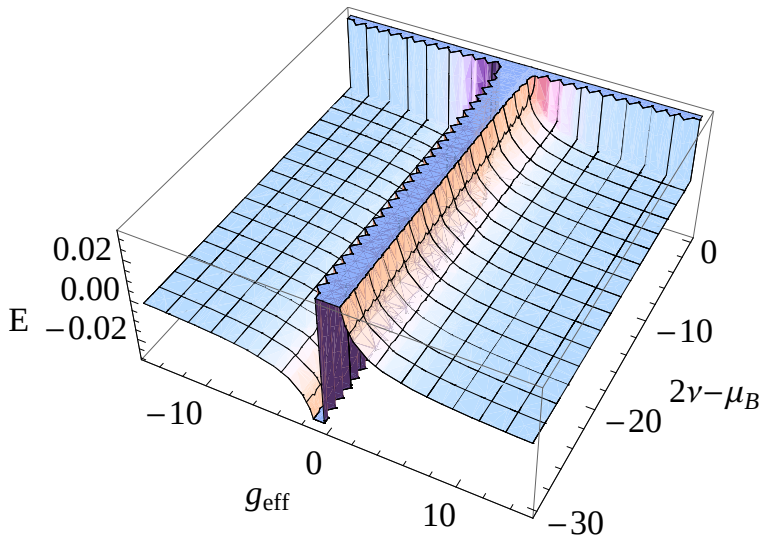

Figure 2.11: Variation in energy in the BEC side with effective coupling and detuning

So we modify Δ using the form of the gap for weak coupling BCS [36] :

$$\Delta_0 = 2\omega_c \exp(-\frac{1}{\rho(0) g_{eff}}) \tag{2.12}$$

here $\rho(0)$ is the density of states in the Fermi level, and ω_c is the cutoff frequency for BCS model. Thus we no longer treat the gap as a constant, and incorporate the coupling-dependence in it. This is justified, since the upper two branches are at the weak coupling domain, so the corresponding Δ should follow the expression for the BCS gap. Now the energy surface takes the form of Fig. 2.13. It shows that in the negative g_{eff} side, the energy is less as one goes away from $g_{eff} = 0$. Therefore, the lowermost branch in the BCS side in Fig. 2.13 will be the favoured one.

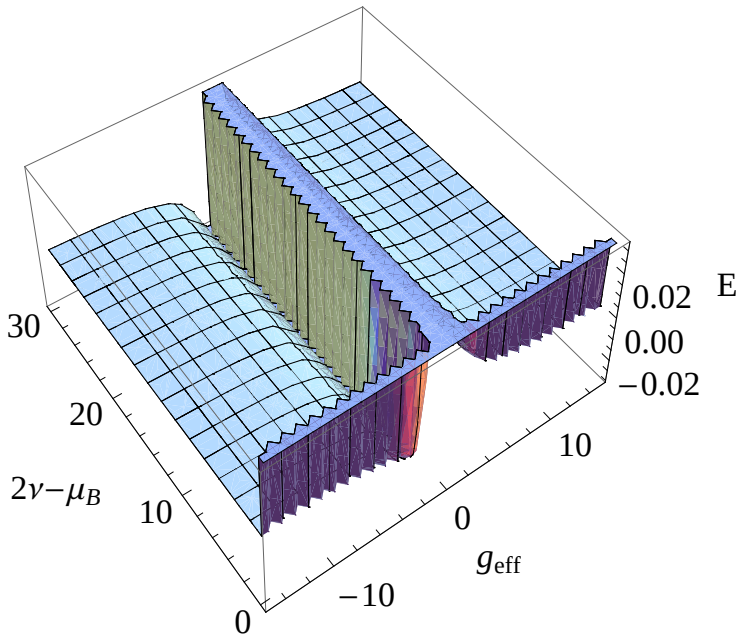

Figure 2.12: Variation in energy in the BCS side with effective coupling and detuning : gap is taken to be constant

2.10 Summary and Discussion

Here we have studied the BCS-BEC crossover in the presence of an additional three-body interaction term : the scattering of a Cooper pair by a newly formed boson near the resonance point. This has led to alternative crossover routes, and hence, brought out interesting properties of the crossover phenomenon. Most noteworthy of them is the non-reversibility of the process. If the two-body interaction is attractive (irrespective of whether the three-body interaction is attractive or repulsive),then starting from a stable BEC system the BCS state can be reached via Feshbach resonance, but the path cannot be reversed : a start from the BCS side can only end up in a metastable BEC state (and not the stable one). This, we believe is an important finding and it reconfirms the need of more theoretical and experimental investigations along this line.

BEC-BCS crossover has been experimentally investigated so far in ^{6}Li and ^{40}K systems. In most cases [6–9] the system is first prepared in the BEC state, and the magnetic field is varied to obtain the BCS. This is completely in agreement with our results. In contrast,

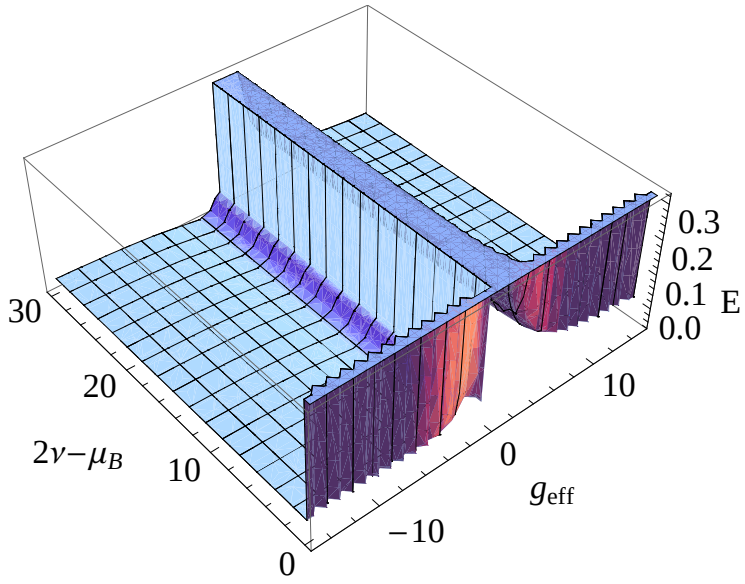

Figure 2.13: Variation in energy in the BCS side with effective coupling and detuning : gap is coupling dependent

in the experiment by C.A. Regal et al. [5], the ultracold ^{40}K system went through the crossover in the opposite direction, i.e., it was a BCS-BEC crossover, and not a BEC-BCS one. Whether the final state here is a stable BEC or a metastable one with a weak attractive interaction (as predicted by our calculations) can be ascertained only after a study of the long-time response of the system. Moreover, in this experiment they first lowered the magnetic field slowly $(10ms/G)^{-1}$ to bring it near resonance, and then rapidly changed it $(50\mu s/G)^{-1}$ to lower it further and obtain the BEC. Thus, although the crossover from the BCS to the resonance is an adiabatic one, it is a fast quench which takes the system from resonance to the BEC domain. So the mechanism may not have followed the dynamics of a smooth crossover, and that could have resulted in a different final state (a stable BEC state, for example). An experiment which probes the crossover starting from the BCS side, and changes the magnetic field adiabatically all through, might clarify this point. The final BEC state should also be studied carefully for a longer time so that the distinction between a metastable and a stable state can be easily made.

Bibliography

[1] A.J. Leggett, in Modern Trends in the Theory of Condensed Matter, edited by A. Pekalski and R. Przystawa (Springer- Verlag, Berlin, 1980).

[2] P. Nozires and S. Schmitt-Rink, J. Low Temp. Phys. **59**, 195 (1985).

[3] M. Randeria in Bose-Einstein Condensation, edited by A. Griffin, D. Snoke, and S. Stringari, Cambridge University Press, Cambridge, England, 1994.

[4] M. Randeria, J. M. Duan, and L. Y. Shieh, Phys. Rev. Lett. **62**, 981 (1989); and Phys. Rev. B **41**, 327 (1990).

[5] C. A. Regal , M. Greiner and D.S. Jin , Phys. Rev. Lett. **92**, (2004) 040403.

[6] M. W. Zwierlein, C. A. Stan, C. H. Schunck, S. M. F. Raupach, A. J. Kerman, and W. Ketterle, Phys. Rev. Lett. **92**, 120403 (2004).

[7] M. W. Zwierlein, C.H. Schunck, A. Schirotzek, and W. Ketterle, Nature(London) **442**, 54 (2006).

[8] M. Bartenstein, A. Altmeyer, S. Riedl, S. Jochim, C. Chin, J. Hecker Denschlag, and R. Grimm, Phys. Rev. Lett. **92**, 120401 (2004).

[9] T. Bourdel, L. Khaykovich, J. Cubizolles, J. Zhang, F. Chevy, M. Teichmann, L. Tarruell, S. J. J. M. F. Kokkelmans, and C. Salomon, Phys. Rev. Lett. **93**, 050401 (2004).

[10] M. Greiner, C.A. Regal, and D.S. Jin, Nature **426**, 537 (2003).

[11] D.M Eagles, Phys. Rev. **186**, 456 (1969).

[12] J.R. Engelbrecht, M. Randeria, and C.A.R. Sade Melo, Phys. Rev.B **55**, 15153 (1997).

[13] C. A. R. Sade Melo, M. Randeria, and J. R. Engelbrecht, Phys. Rev. Lett. **71**, 3202 (1993); J. R. Engelbrecht, M. Randeria, and C. A. R. Sade Melo, Phys. Rev. B **55**, 15153 (1997).

[14] T. Kostyrko and J. Ranninger, Phys. Rev. B **54**, 13105 (1996).

[15] M. Holland, S.J.J.M.F. Kokkelmans, M.L. Chiofalo, R. Walser, Phys. Rev. Lett.**87**, 120406 (2001).

[16] Y. Ohashi and A. Griffin, Physics Review Letter, **89**,130402 (2002).

[17] J. N. Fuchs, A. Recati, and W. Zwerger, Phys. Rev. L **93**,090408 (2004).

[18] N Manini, L Salasnich, Physical Review A **71**, 033625 (2005).

[19] Q. J. Chen, J. Stajic, S. N. Tan, and K. Levin, Phys. Rep. **412**, 1 (2005).

[20] K. Levin and Q. Chen, in Ultra-cold Fermi Gases, edited by M. Inguscio, W. Ketterle, and C. Salomon (Italian physical society, 2007), p. 751.

[21] A. Perali, P. Pieri, G. C. Strinati, and C. Castellani, Phys. Rev. B **66**, 024510 (2002).

[22] D. E. Sheehy and L. Radzihovsky, Ann. Phys. **322**, 1790 (2007).

[23] J.N. Milstein, S.J.J.M.F Kokkelmans, M.J. Holland , Physical Review A **66**, 043604 (2002).

[24] A Gammal, T Frederico, Lauro Tomio and Ph Chomaz, Journal of Physics B - At. Mol. Opt. **33**, 4053 (2000).

[25] L. D. Carr, J. N. Kutz, and W. P. Reinhardt, Phys. Rev. E **63**, 066604 (2001).

[26] Yong Wen-Mei, Wei Xiu-Fang,Zhou Xiao-Yan and Xue Ju-Kui1,Commun. Theor. Phys. **51**, 433 (2009).

[27] Priyam Das, Manan Vyas and Prasanta K Panigrahi, J. Phys. B: At. Mol. Opt. Phys. **42**, 245304 (2009).

[28] M. Iskin Physical Review A **81**, 043634 (2010).

[29] J. Levinsen, T. G. Tiecke, J. T. M. Walraven, and D. S. Petrov, Phys. Rev. Lett. **103**, 153202 (2009).

[30] C. Mora, R. Egger, A. O. Gogolin and A. Komnik, Phys. Rev. Lett. **93**, 170403 (2004).

[31] J.-P. Martikainen, J. J. Kinnunen, P. Torma, C. J. Pethick, Phys. Rev. Lett. **103**, 260403 (2009).

[32] R. Dasgupta, Phys. Rev. A **80**, 063623 (2009).

[33] R. P. Feynman, Statistical Mechanics: A Set of Lectures (Addison-Wesley, New York, 1988).

[34] A. J. Leggett, Quantum Liquids, Bose Condensation and Cooper Pairing in Condensed-Matter System (Oxford University Press, Oxford, 2006).

[35] C. Chin, M. Bartenstein, A. Altmeyer, S. Riedl, S. Jochim, J.H. Denschlag, and R. Grimm, Science **305**, 1128-1130 (2004).

[36] C. J. Pethick and H. Smith, Bose-Einstein Condensation in Dilute Gases (Cambridge University Press, Cambridge, England, 2002).

Chapter 3

Stability of the Breached Pair State for a Population-Imbalanced Fermionic System

In Bardeen-Cooper-Schrieffer (BCS) theory, the phenomenon of superconductivity in fermionic systems is attributed to the formation of Cooper pairs between particles with opposite spins and equal but opposite momenta. In ultracold atom systems, too, there is a parallel in the form of superfluidity, where a pairing takes place between two species of fermions. The fact that each fermion has a partner to pair with ensures that the system is a superfluid all the way. In such a system, there is a single Fermi surface. When the fermion-fermion interaction is tuned, and the system is taken from the weak coupling regime to the strong coupling one, there would be a smooth crossover from a superfluid with loosely bound Cooper pairs to the condensation of tightly bound bosonic molecules.

Figure 3.1: Cooper pairing

However, when there is an asymmetry/ population imbalance introduced in the system, i.e., the number of atoms belonging to the first species is not equal to the number of atoms of the second species, the physics of pairing no longer remains the same. With this imbalance in population, it is not possible anymore to pair all the fermions in the BCS fashion. The problem now is to decide how the excess unpaired fermions will be

accommodated in the system, and whether the system would remain a superfluid at all.

The problem with unequal population arises in many important fields of physics. It appears in the study of superfluidity of quarks in the dense matter of the early universe, in the form of imbalanced quark densities. In superconducting materials, the application of an external magnetic field serves the same purpose : it creates an imbalance in the densities of spin up and spin down electrons.

In ultracold atoms, fermionic pairing and superfluidity with mismatched Fermi surfaces have been widely investigated in recent years. Theoretical studies have zoomed in on thermodynamic and superfluid properties of these systems. [1–14]. Population imbalance in cold atom systems have been realized in experiments [15–17], and the signature of superfluidity was obtained.

A mismatch in Fermi surfaces can be easily realized in a two-species fermionic system where the pairing species have unequal populations or different masses/ chemical potentials. Typically, such a system would consist of two different fermionic atoms (e.g., ^{6}Li and ^{40}K) or alternatively, two hyperfine states of the same atom (e.g., states $|F = 1/2, m_F = 1/2\rangle$ and $|F = 1/2, m_F = -1/2\rangle$ of ^{6}Li atoms).

Several phases have been proposed to describe the possible ground state of such a system. The list includes the FFLO phase [18–20](pairing with non-zero centre-of-mass momentum, where the order parameter shows a spatial variation), the gapless BP (breached pair) or interior-gap phase [1–4] (pairing with zero centre-of mass momentum: where the order parameter is nonzero but the excitation energy becomes zero), and the inhomogeneous phase-separated state [8,9], where any two pure states coexist. Some of these novel states have been discussed in the introductory chapter of this thesis.

In this chapter [1], our focus is on the homogeneous and gapless breached pair state, also known as the Sarma state. Sarma [21], in the early theoretical studies of superconductivity, predicted a spatially isotropic, homogeneous and uniform state with gapless excitation modes in the presence of a magnetic field. However, for weak coupling BCS

[1]The work reported here is based on the papers " Stability of the breached pair state for a two-species fermionic system in the presence of Feshbach resonance", Raka Dasgupta, Phys. Rev. A, **80**, 063623, (2009) and "Stability of a gapless state for population-imbalanced fermionic systems", Raka Dasgupta, Physics Teacher (Quarterly Journal of Indian Physical Society) **51**, numbers 3-4, (2009)

theory, it was found that this gapless breached pair state marks the maximum of the thermodynamic potential, and thus, cannot be the stable ground state of the system. This is the well-known Sarma instability. In the last few years, several prescriptions were put forward to avoid this instability. According to Forbes et.al. [22], a stable Sarma state is possible in a model with finite range interaction where the momentum dependence of the pairing gap cures the instability. It has also been proposed by a number of workers [7, 20, 23, 24]that the breached pair state becomes stable in the deep BEC regime, if the BCS-BEC crossover picture is taken into account. He et al.,in a very recent work [25] has argued that the breached pair state can be a possible ground state in the weak coupling region for a two-band Fermi system.

3.1 Model Hamiltonian

To study the breached pair state, we start with a two-species fermionic system. In addition to the weak BCS attraction (denoted by $-g_1$), we consider a strong interaction (g_2) of the Feshbach variety which couples a fermion of type a with a b fermion to form a bosonic molecule B. Our model resembles the one used in [26, 27], but we extend it to cover the two-species case. The system is described by the Hamiltonian:

$$\begin{aligned}\hat{H} = \sum (E_{\mathbf{q}} + 2\nu) B^{\dagger}_{\mathbf{q}} B_{\mathbf{q}} + \sum \epsilon^{a}_{\mathbf{p}} a^{\dagger}_{\mathbf{p}} a_{\mathbf{p}} + \sum \epsilon^{b}_{\mathbf{p}} b^{\dagger}_{\mathbf{p}} b_{-\mathbf{p}} - g_1 \sum a^{\dagger}_{\mathbf{p}'} b^{\dagger}_{-\mathbf{p}'} b_{-\mathbf{p}} a_{\mathbf{p}} \\ + g_2 \sum [B^{\dagger}_{\mathbf{q}} a_{\mathbf{q}/2+\mathbf{p}} b_{\mathbf{q}/2-\mathbf{p}} + B_{\mathbf{q}} a^{\dagger}_{\mathbf{q}/2+p} b^{\dagger}_{\mathbf{q}/2-p}]\end{aligned} \tag{3.1}$$

Here $a_{\mathbf{p}}$, $a^{\dagger}_{\mathbf{p}}$ are the creation and annihilation operators of atom a, while $b_{\mathbf{p}}$, $b^{\dagger}_{\mathbf{p}}$ are the corresponding operators for atom b. The kinetic energies of species a and b are $\epsilon^{a}_{\mathbf{p}}$, $\epsilon^{b}_{\mathbf{p}}$. The annihilation and creation operators for the composite boson B formed out of a and b are $B_{\mathbf{q}}$ and $B^{\dagger}_{\mathbf{q}}$ respectively. The kinetic energy of the bosons is $E_{\mathbf{q}}$ and the threshold energy of the composite bose particle energy band is 2ν.

We have a constraint: the total number of bare fermi atoms must be conserved:

$$\langle \hat{N} \rangle = \langle \Sigma a^{\dagger}_{\mathbf{p}} a_{\mathbf{p}} \rangle + \langle \Sigma b^{\dagger}_{\mathbf{p}} b_{\mathbf{p}} \rangle + 2 \langle \Sigma B^{\dagger}_{\mathbf{q}} B_{\mathbf{q}} \rangle \tag{3.2}$$

Replacing $\hat{H}$ with the grand canonical Hamiltonian $H = \hat{H} - \mu\hat{N}$

$$H = \sum (E_{\mathbf{q}} + 2\nu - \mu_B) B^\dagger_{\mathbf{q}} B_{\mathbf{q}} + \sum \tilde{\epsilon}^a_{\mathbf{p}} a^\dagger_{\mathbf{p}} a_p + \sum \tilde{\epsilon}^b_{\mathbf{p}} b^\dagger_{\mathbf{p}} b_{\mathbf{p}} - g_1 \sum a^\dagger_{\mathbf{p}'} b^\dagger_{-\mathbf{p}'} b_{-\mathbf{p}} a_{\mathbf{p}} + g_2 \sum [B^\dagger_{\mathbf{q}} a_{\mathbf{q}/2+\mathbf{p}} b_{\mathbf{q}/2-\mathbf{p}} + B_{\mathbf{q}} a^\dagger_{\mathbf{q}/2+\mathbf{p}} b^\dagger_{\mathbf{q}/2-\mathbf{p}}] \tag{3.3}$$

In the above Hamiltonian, $\tilde{\epsilon}^a_{\mathbf{p}} = \epsilon^a_{\mathbf{p}} - \mu_a$ and $\tilde{\epsilon}^b_{\mathbf{p}} = \epsilon^b_{\mathbf{p}} - \mu_b$, while μ_a, μ_b, μ_B are the chemical potentials for the fermion species and the composite boson respectively.

We now restrict ourselves to the case where only zero-momentum bosons are formed. i.e., $\mathbf{q} = 0$, $E_{\mathbf{q}} = 0$. Therefore,

$$H = \sum (2\nu - \mu_B) B^\dagger_0 B_0 + \sum \tilde{\epsilon}^a_{\mathbf{p}} a^\dagger_{\mathbf{p}} a_{\mathbf{p}} + \sum \tilde{\epsilon}^b_{\mathbf{p}} b^\dagger_{\mathbf{p}} b_{\mathbf{p}} - g_1 \sum a^\dagger_{\mathbf{p}'} b^\dagger_{-\mathbf{p}'} b_{-\mathbf{p}} a_{\mathbf{p}} + g_2 \sum [B^\dagger_0 a_{\mathbf{p}} b_{-\mathbf{p}} + B_0 a^\dagger_{\mathbf{p}} b^\dagger_{-\mathbf{p}}] \tag{3.4}$$

Using this Hamiltonian, we study the effect of the Feshbach parameters first on the gapped BCS superfluid state, and then on the gapless Sarma state, taking a variational approach. The stability of such a gapless state is analysed using the concept of Meissner mass [28, 29]. Considering the BCS-BEC crossover picture, we show that the breached pair state is stable only in a narrow region in the BEC side, bounded by two magnetic field values.

3.2 Effective Coupling and Gap Equation

We want to study the ground state of the two-fermion system by a variational method. We take $|\Psi\rangle = |F\rangle \otimes |B\rangle$ as the trial form of the ground state of the system. Here $|F\rangle$ $= |BCS\rangle = \prod (U_p + V_p a^\dagger_{\mathbf{p}} b^\dagger_{-\mathbf{p}})|0\rangle$, i.e., the probability of the pair $(a_{\mathbf{p}\uparrow}, b_{-\mathbf{p}\downarrow})$being occupied is $|V_{\mathbf{p}}|^2$, and the probability that it is unoccupied is $|U_{\mathbf{p}}|^2 = 1 - |V_{\mathbf{p}}|^2$, while $|B\rangle$ is the ground state for the condensate part of the boson subsystem.

Our variational prescription is that $|B\rangle$ has to be chosen in such a manner that it is an eigenstate of the annihilation operator B, which would make it a coherent state.

$|B\rangle = \Sigma C_n |n\rangle$. Since $|B\rangle$ is an eigenstate of B, $B|B\rangle = \alpha|B\rangle$ where α is a number.

This leads to $C_n = \alpha^n C_0/(n!)^{1/2}$.

Normalization condition gives $\langle B|B\rangle = 1$, gives $C_0 = \exp(-\alpha^2/2)$.

This yields $|B\rangle = \exp(-\alpha^2/2)\Sigma\alpha^n/(\sqrt{n!})|n\rangle$.

Noting $|n\rangle = (B^\dagger)^n/\sqrt{n!}|0\rangle$, we write $|B\rangle = \exp(-\alpha^2/2)\exp(\alpha B^\dagger)|0\rangle$.

To determine α, we note that $\langle B|B^\dagger B|B\rangle = \alpha^2$.But $\langle B|B^\dagger B|B\rangle = N_B$, the expectation value of the total no. of bosons in the ground state. So $\alpha = \sqrt{N_B}$ Therefore, the ground state of the system can be written as

$$|\Psi\rangle = \prod (U_p + V_p a_p^\dagger b_{-p}^\dagger)|0\rangle \otimes \exp(-\alpha^2/2 + \alpha B^\dagger)|0\rangle \tag{3.5}$$

From the Hamiltonian (3.4) and the ground state wave function (3.5), the ground state energy of the system would be

$$E = \sum (\tilde{\epsilon}_{\mathbf{p}}^a + \tilde{\epsilon}_{\mathbf{p}}^b) V_{\mathbf{p}}^2 - g_1 \sum_{\mathbf{p},\mathbf{p}'} U_{\mathbf{p}} V_{\mathbf{p}} U_{\mathbf{p}'} V_{\mathbf{p}'} + (2\nu - \mu_B)\alpha^2 + 2g_2\alpha \sum_{\mathbf{p}} U_{\mathbf{p}} V_{\mathbf{p}} \tag{3.6}$$

Minimizing E with respect to $V_{\mathbf{p}}$ and α we get

$$4\epsilon_{\mathbf{p}}^+ V_{\mathbf{p}} - 2g_{eff} \sum_{\mathbf{p},\mathbf{p}'} U_{\mathbf{p}'} V_{\mathbf{p}'} (U_{\mathbf{p}} - V_{\mathbf{p}}^2/U_{\mathbf{p}}) = 0 \tag{3.7}$$

where $\epsilon_{\mathbf{p}}^+ = (\tilde{\epsilon}_{\mathbf{p}}^a + \tilde{\epsilon}_{\mathbf{p}}^b)/2$.
g_{eff} is defined by the relation

$$g_{eff} = g_1 + g_2^2/(2\nu - \mu_B) \tag{3.8}$$

We note that this expression matches with the one obtained by Ohashi et al [26] using diagrammatic methods.

Now, if we choose $g_{eff} \sum_{\mathbf{p}'} U_{\mathbf{p}'} V_{\mathbf{p}'} = \Delta$, the usual form of the gap equation follows, and we can identify Δ as the gap in the excitation spectrum. A similar relation is obtained in finite temperature systems as well, if we incorporate the appropriate Fermi distribution functions in the expression of the free energy.

3.3 Temperature Dependence

At finite temperatures, let $f_{\mathbf{p}}$ be the probability of an a particle being excited with momentum $\mathbf{p}$, and $g_{\mathbf{p}}$ be the probability of a b particle being excited with momentum $-\mathbf{p}$. Then the entropy of the system is given by $\sum_{\mathbf{p}} f_{\mathbf{p}} \ln f_{\mathbf{p}} + \sum_{\mathbf{p}} g_{\mathbf{p}} \ln g_{\mathbf{p}} + \sum_{\mathbf{p}} (1-f_{\mathbf{p}}) \ln(1-f_{\mathbf{p}}) + \sum_{\mathbf{p}} (1-g_{\mathbf{p}}) \ln(1-g_{\mathbf{p}})$ [5, 30]. And the Helmholtz free energy $\Omega = E - TS$ becomes

$$\begin{aligned}\Omega = &\sum_{p} \tilde{\epsilon}^a_{\mathbf{p}}[(1-f_{\mathbf{p}}-g_{\mathbf{p}})V^2_{\mathbf{p}} + f_{\mathbf{p}}] + \sum_{\mathbf{p}} \tilde{\epsilon}^b_{\mathbf{p}}[(1-f_{\mathbf{p}}-g_{\mathbf{p}})V^2_{\mathbf{p}} + g_{\mathbf{p}}] + (2\nu - \mu_B)\alpha^2 \\ &-g_1 \sum_{\mathbf{p},\mathbf{p}'} U_{\mathbf{p}'} V_{\mathbf{p}'} U_{\mathbf{p}} V_{\mathbf{p}} (1-f_{\mathbf{p}}-g_{\mathbf{p}})(1-f_{\mathbf{p}'}-g_{\mathbf{p}'}) + 2g_2\alpha[(1-f_{\mathbf{p}}-g_{\mathbf{p}})U_{\mathbf{p}}V_{\mathbf{p}}] \\ &-\beta^{-1}[f_{\mathbf{p}}\ln f_{\mathbf{p}} + g_{\mathbf{p}}\ln g_{\mathbf{p}} + (1-f_{\mathbf{p}})\ln(1-f_{\mathbf{p}}) + (1-g_{\mathbf{p}})\ln(1-g_{\mathbf{p}})]\end{aligned} \tag{3.9}$$

Proceeding as before, and using the conditions for minimum, we observe that

$$\alpha = -g_2 \sum_{\mathbf{p}} U_{\mathbf{p}} V_{\mathbf{p}} (1-f_{\mathbf{p}}-g_{\mathbf{p}})/(2\nu - \mu_B) \tag{3.10}$$

It follows that just like the zero temperature case, here, too, the system can be treated in the standard BCS framework, provided we use $g_{eff} = g_1 + g_2^2/(2\nu - \mu_B)$ as the coupling.

In a two-species fermionic system, had there been only BCS attraction, and no Feshbach-related term, the gap equation would be [5, 31]

$$\Delta = g_1 \sum_{\mathbf{p}} U_{\mathbf{p}} V_{\mathbf{p}} (1-f_{\mathbf{p}}-g_{\mathbf{p}}) \tag{3.11}$$

The critical temperature (temperature at which the gap vanishes) is given by

$$T_C = \frac{\sigma \Delta_0}{2\pi} \exp[-\frac{1}{2}F(a_c)] \tag{3.12}$$

where

$$\sigma = \sqrt{m_a m_b}/(m_a + m_b) \tag{3.13a}$$

$$F(a_c) = \Psi(\frac{1}{2} + \frac{ia}{\pi}) + \Psi(\frac{1}{2} - \frac{ia}{\pi}) \tag{3.13b}$$

$$a = \frac{\beta}{2}(m_b\mu_b - m_a\mu_a)/(m_a + m_b) \tag{3.13c}$$

Ψ being the digamma function. m_a and m_b are the masses of fermions a and b respectively. Δ_0 is the BCS gap in the weak coupling limit, which is given by

$$\Delta_0 = 2\frac{8}{e^2}\epsilon_F \exp(-\frac{1}{\rho(0)g_{eff}}) \tag{3.14}$$

Here $\rho(0)$ is the density of states in the Fermi level, e is the base of natural logarithms, and ϵ_F is the Fermi energy.Thus the value of T_c can be raised or lowered by adjusting 2ν, the tunable parameter depending on the Feshbach resonance process.

In our system, all these relations hold good, provided g_1 is replaced by g_{eff}. Now, if $\mu_B < 2\nu$, we have $g_{eff} > g_1$ from relation (3.8). Thus, we have a greater value of Δ_0, and T_c is, therefore, higher than what it was when there was no possibility for molecule formation. On the other hand, if $\mu_B > 2\nu$, we have $g_{eff} < g_1$, and we get a lower value of T_c. Thus the value of T_c can be raised or lowered by adjusting g_2 and ν, since both of them are tunable parameters depending on the Feshbach resonance process.

3.4 Gapless Excitations

Next we study gapless excitations.The quasiparticle dispersions as obtained from standard BCS-like treatment is of the form [31]:

$$E^{a,b}_{\mathbf{p}} = \pm\frac{\tilde{\epsilon}^a_{\mathbf{p}} - \tilde{\epsilon}^b_{\mathbf{p}}}{2} + \sqrt{(\frac{\tilde{\epsilon}^a_{\mathbf{p}} + \tilde{\epsilon}^b_{\mathbf{p}}}{2})^2 + \Delta^2} \tag{3.15}$$

Depending on the values of particle masses and corresponding chemical potentials, these quasiparticle excitations can be negative, thus paving the way for having gapless excitations. This is possible only if the magnitude of Δ is less than a critical value Δ_c [3, 31].

$$\Delta_c = \frac{|m_b\mu_b - m_a\mu_a|}{2\sqrt{m_a m_b}} \tag{3.16}$$

When $|\Delta| > \Delta_c$, both E^a_p and E^b_p remain positive for all values of p. This corresponds to usual BCS pairing. When $|\Delta| < \Delta_c$, either E^a_p or E^b_p crosses zero at the points:

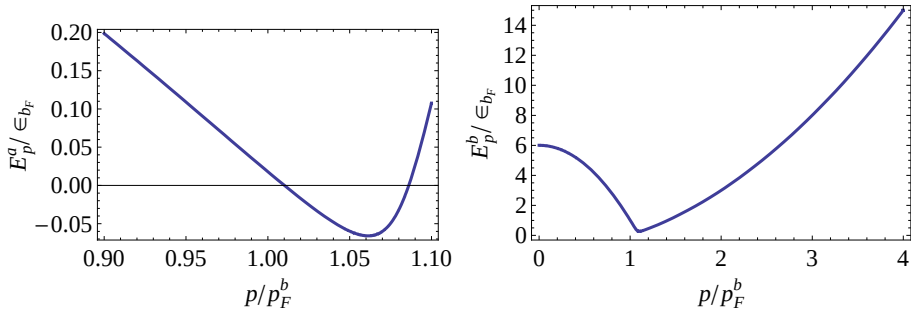

Figure 3.2: $(\varepsilon_p^{a,b}$-$p)$ curve when the Feshbach term is absent

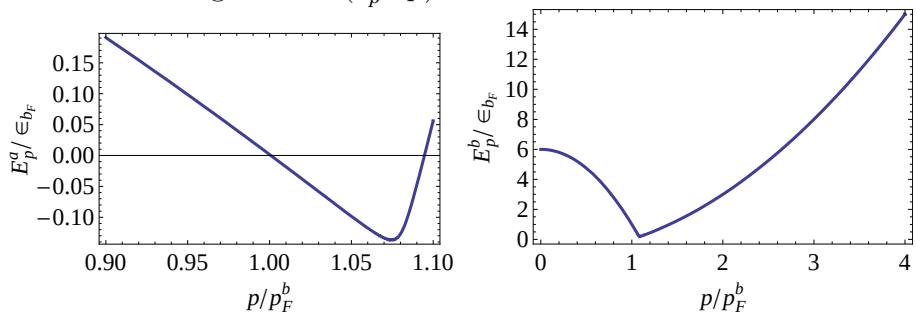

Figure 3.3: $(\varepsilon_p^{a,b}$-$p)$ curve for $\mu_B - 2\nu = .5$, $g_2 = .6$

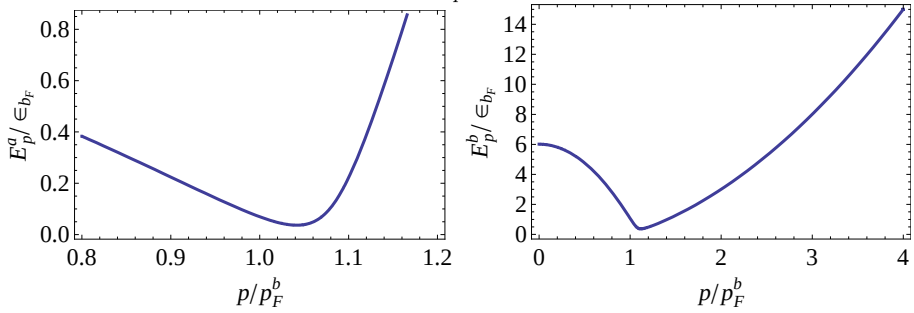

Figure 3.4: $(E_p^{a,b}$-$p)$ curve for $\mu_B - 2\nu = -.5$, $g_2 = .6$

$$p_{1,2}^2 = (m_b\mu_b + m_a\mu_a) \mp [(m_b\mu_b - m_a\mu_a)^2 - 4m_a m_b\Delta^2]^{1/2} \tag{3.17}$$

The difference between p_1 and p_2 gives the span over which we get a gapless region in the parameter space. The state with gapless excitations marks the coexistence of the superfluid and normal components at zero temperature, and is called the Sarma phase, or the Breached Pair state. When we include the Feshbach term in the Hamiltonian, we have a control over this Sarma phase as well.

In Figs. 3.3, 3.3 and 3.4, we plot the *E-p* curve for a two-species system. Here we scale all energies by ϵ_{b_F} (Fermi energy of species b) and all momenta by p_{b_F} (Fermi momentum of species b). It is evident that in this convention, $m_b = .5$ and $\mu_b = 1$(in the BCS limit). We choose $m_a = .1$, $\mu_a = 6$ and multiply quantities g_1, g_2, $(2\nu - \mu_B)$ and g_{eff} by $\rho(0)$, the density of states at the Fermi level to get dimensionless quantities $\tilde{g_1}$, $\tilde{g_2}$, $(2\tilde{\nu} - \tilde{\mu_B})$ and $\tilde{g_{eff}}$. Let $\tilde{g_1} = 0.3$. Had there been no Feshbach coupling g_2, we would get a gapless region from p=1.01 to p=1.85 (in units of p_{b_F}) as seen from Fig. 3.3.

If $\tilde{g_2} = .2$ is introduced in the system, and we choose ν in such a way that $(\tilde{\mu_B} - 2\tilde{\nu}) = 0.5$, we get the Sarma phase for a wider region, from p=1.00 to p=1.95 (in units of p_{b_F}) as seen from Fig.3.3

If, on the other hand, $(\tilde{\mu_B} - 2\tilde{\nu}) = -.5$, the gapless phase vanishes entirely as shown in Fig. 3.4.

3.5 Stability Analysis

The stability of such a superfluid phase has been studied in different ways like demanding positivity of the superfluid density [23], ensuring non-negative eigenvalues of the number susceptibility matrix of the system [23, 32], minimization of thermodynamic potential [9, 33] etc.

Here we adopt the first criterion and demand that the superfluid density n_s must be positive. If the fermions are charged, this is equivalent to saying that the Meissner mass-squared must be positive [32], since n_s, the superfluid density, and M^2, the Meissner mass squared obey the relation : $M^2 = \frac{n_s q^2}{m^2}$ [28], q being the electronic charge and m, the mass

of the particle. In our treatment, we work with the superfluid density directly, since we are talking of a charge neutral Fermi system. However, the term "Meissner mass" can still be used just to continue the analogy with superconductors, as it only serves to express the superfluid density to within a multiplicative constant.

For convenience, we assume that the two species have equal masses. Therefore, equation (3.17) takes a simpler form:

$$p_{1,2} = 2m[\bar{\mu} \pm \sqrt{\delta\mu^2 - \Delta^2}]^{\frac{1}{2}} \tag{3.18}$$

where $\bar{\mu} = (\mu_a + \mu_b)/2$ and $\delta\mu = (\mu_a - \mu_b)/2$. Thus, $\Delta_c = \delta\mu$ here.

He et al [28,29] have shown that when the two species have equal masses, the superfluid density can be expressed as

$$n_s = mn\left(1 - \frac{\eta\delta\mu\theta(\delta\mu - \Delta)}{\sqrt{\delta\mu^2 - \Delta^2}}\right) \tag{3.19}$$

where $\eta = \dfrac{p_1^3 + p_2^3}{6\pi^2 n}$. We note that here n marks the bare fermion density or the density of the atoms that have not been part of the condensate yet (i.e., unpaired fermions, fermions forming the Cooper pair and fermions that constitute the non-condensate bosons all are counted in n). Since the total number of bare Fermi atoms is conserved, so $n+2N_B=$ constant, N_B being the expectation value of the total number of bosons in the condensate. If $\Delta < \Delta_c$, for n_s is to be positive, $\dfrac{\eta\delta\mu}{\sqrt{\delta\mu^2 - \Delta^2}}$ has to be less than 1, which is satisfied if $\eta < 1$, and $|\eta^2 - 1| > \dfrac{\Delta^2}{\delta\mu^2}$.

Now when both p_1 and p_2 are real and there is a breached pair phase between them (this state has sometimes been termed as BP2 state in the literature [34,35]), the bare fermion density can be written as:

$$n = \frac{1}{2\pi^2}\int_{p_1}^{p_2} \mathbf{p}^2\, d\mathbf{p} + \frac{1}{\pi^2}\left[\int_0^{p_1} V_{\mathbf{p}}^2 \mathbf{p}^2\, dp + \int_{p_2}^{\infty} V_{\mathbf{p}}^2 \mathbf{p}^2\, d\mathbf{p}\right] \tag{3.20}$$

Here the first term denotes the contribution from the gapless region between p_1 and p_2, i.e., the normal component. The next two integrals take care of the contributions from the gapped superfluid regimes, one from momenta 0 to p_1 and the other from p_2 to infinity.

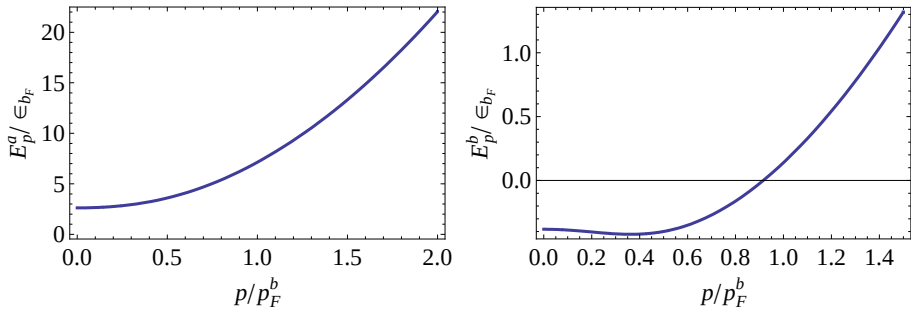

Figure 3.5: ($\varepsilon_p^{a,b}$-p) curve when p_1 is imaginary

The terms, when rearranged, gives

$$n = \frac{p_1^3 + p_2^3}{6\pi^2} + \frac{1}{\pi^2}(-\int_0^{p_1} \mathbf{p}^2 U_{\mathbf{p}}^2 \, d\mathbf{p} + \int_{p_2}^{\infty} \mathbf{p}^2 V_{\mathbf{p}}^2 \, d\mathbf{p}) \tag{3.21}$$

In the weak coupling limit, the last two integrals are very small, and hence, can be neglected. Therefore, η=1, and n_s is negative. Thus, the Sarma state is unstable here.

We shift our focus to a special case, where only one of p_1 and p_2 is real (in the literature, this is called the BP1 state [34, 35]). In this case the ε-p curve resembles Fig. 3.5, and the fermion density is

$$n = \frac{p_2^3}{6\pi^2} + \frac{1}{\pi^2}\int_{p_2}^{0} \mathbf{p}^2 V_{\mathbf{p}}^2 \, d\mathbf{p} \tag{3.22}$$

This yields $\eta < 1$, and thus the stability criterion is fulfilled. Now, from equation(3.18), p_1 is imaginary if $\sqrt{\delta\mu^2 - \Delta^2} > \bar{\mu}$, i.e., $-\mu_a\mu_b > \Delta^2$. So, Sarma phase is stable only in a region where the chemical potential of one species is positive, and the other, negative, provided the magnitude of their product is greater than Δ^2.

Leggett has shown [36] that in the BCS-BEC crossover picture, the chemical potential can be determined by solving the gap and the number equations.

$$\sum_{\mathbf{p}} (\frac{1}{\epsilon_{\mathbf{p}}} - \frac{1}{E_{\mathbf{p}}}) = \frac{m}{2\pi\hbar^2 a_s} \tag{3.23a}$$

$$\sum_{\mathbf{p}} (1 - \frac{\epsilon_{\mathbf{p}} - \bar{\mu}}{E_{\mathbf{p}}}) = 2\frac{k^3}{3\pi^2} \tag{3.23b}$$

Here a_s is the $a-b$ scattering length and k is the Fermi wave number.

Extending these equations to the two species case, we get

$$\sum_{|\mathbf{p}|=0}^{\infty}\left(\frac{1}{\epsilon_{\mathbf{p}}}-\frac{1}{\sqrt{{\epsilon_{\mathbf{p}}}^2+\Delta^2}}\right)=\frac{m}{2\pi\hbar^2 a_s} \tag{3.24a}$$

$$\sum_{|\mathbf{p}|=p_2}^{\infty}\left(1-\frac{\epsilon_{\mathbf{p}}-\bar{\mu}}{\sqrt{{\epsilon_{\mathbf{p}}}^2+\Delta^2}}\right)=2\frac{k_{b_F}^3}{3\pi^2} \tag{3.24b}$$

$$\sum_{|\mathbf{p}|=0}^{\infty}\left(1-\frac{\epsilon_p-\bar{\mu}}{\sqrt{{\epsilon_p}^2+\Delta^2}}\right)+\sum_{|\mathbf{p}|=0}^{p_2}\left(1+\frac{\epsilon_p-\bar{\mu}}{\sqrt{{\epsilon_p}^2+\Delta^2}}\right)=2\frac{k_{a_F}^3}{3\pi^2} \tag{3.24c}$$

Where k_{a_F} and k_{b_F} corresponds to the Fermi wave number of the more populated species, and the less populated species respectively. Let k' denote the wave number corresponding to the breaching point for the BP1 state, i.e., $p_2=\hbar k'$. Converting the sums into integrals, we obtain that in the weak coupling limit, $\bar{\mu}=(\epsilon_{a_F}+\epsilon_{b_F})/2=\hbar^2(k_{a_F}^2+k_{b_F}^2)/4m$, as expected. In contrast, in the strong coupling limit,

$$\bar{\mu}=-\frac{\hbar^2}{2ma_s^2}+\frac{2\epsilon_{b_F}(k_{b_F}a_s)}{3\pi}\left(1+\frac{2k'^3a_s^3}{\pi}\right) \tag{3.25}$$

provided $k' << \bar{\mu}$ (a condition which is satisfied if the population imbalance is small compared to the total population). In this case $\bar{\mu}$ asymptotically approaches $-\hbar^2/2ma_s^2$, i.e., half the binding energy of the molecule.

If we think of μ_a and μ_b separately, the first one differs from the other by the Fermi energy of the excess fermions. Moreover, in the presence of a magnetic field H, there is an asymmetry between the chemical potentials given by m_BH, m_B being the fermion magneton. So we have

$$\delta\mu=\frac{1}{2}\left(\frac{\hbar^2k'^2}{2m}+m_BH\right) \tag{3.26}$$

$$\mu_{a,b}=\bar{\mu}\pm\delta\mu=-\frac{\hbar^2}{2ma_s^2}+\frac{2\epsilon_{b_F}(k_{b_F}a_s)}{3\pi}\left(1+\frac{2k'^3a_s^3}{\pi}\right)\pm\left(\frac{\hbar^2k'^2}{4m}+\frac{m_BH}{2}\right) \tag{3.27}$$

Our domain of interest is when μ_a is positive, and μ_b is negative, i.e., while approaching the BEC side, μ_b has already crossed zero but μ_a has not. Now, μ_a and μ_b becomes zero at magnetic field values H_1 and H_2 respectively, where

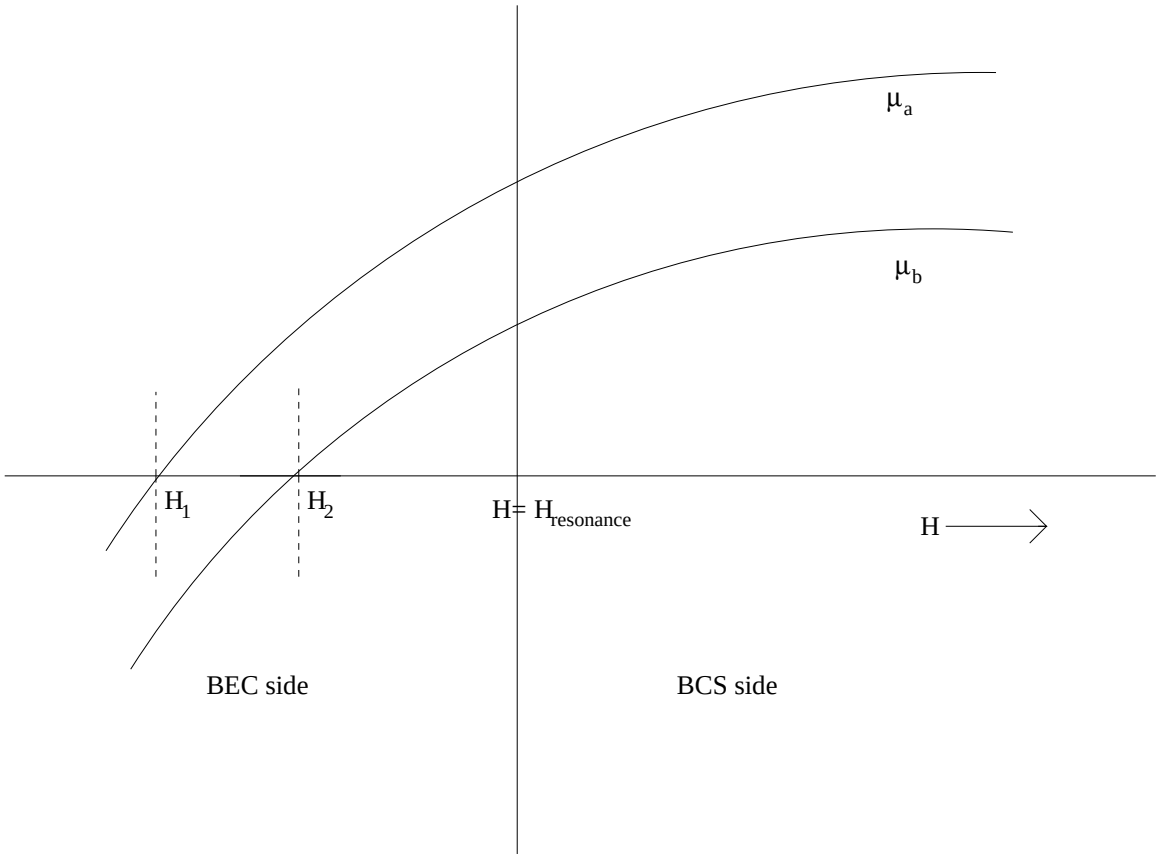

Figure 3.6: Behaviour of μ_a and μ_b in the crossover picture

$$H_1 = (2/m_B)\left[\frac{\hbar^2}{2ma_{s1}^2} - \frac{2\epsilon_{b_F}(k_{b_F}a_{s1})}{3\pi}\left(1 + \frac{2k'^3a_{s1}^3}{\pi}\right) - \frac{\hbar^2k'^2}{4m}\right] \tag{3.28a}$$

$$H_2 = (2/m_B)\left[-\frac{\hbar^2}{2ma_{s2}^2} + \frac{2\epsilon_{b_F}(k_{b_F}a_{s2})}{3\pi}\left(1 + \frac{2k'^3a_{s2}^3}{\pi}\right) - \frac{\hbar^2k'^2}{4m}\right] \tag{3.28b}$$

Here a_{s1}, a_{s2} are the respective values of the scattering length at H_1 and H_2. Between these two magnetic field values, the Sarma state becomes stable.

3.6 Estimates of H_1 AND H_2

Experiments with population-imbalanced fermionic systems have been done by Zwierlein et al. [15, 16] and Patridge et al [17]. They obtained the signature of superfluidity in an unequal mixture of two spin states of ^{6}Li atoms, and a quantum phase transition between the superfluid state and the normal state was observed at a critical polarization. Another method for experimental detection of the breached pair phase has been suggested by Yi et al. [34]. However, no clear signature of this gapless phase has been obtained till date.

We now use the data obtained from these experiments on population-imbalanced gas of ^{6}Li atoms [15, 16] to make an estimate of the magnetic field values corresponding to the breached pair Sarma state. To be able to use the expressions (3.28a,3.28b), we need to know the scattering length as a function of the magnetic field. This is provided by $a_s = a_0\left(1 - \frac{\Gamma}{H - H_0}\right)$, where a_0 is the background background scattering length, Γ is the width of the resonance, and H_0 is the position of the resonance peak.

We use this expression for scattering length, and put $a_o = 45.5r_0$ (r_0=Bohr radius), which is the singlet scattering length for ^{6}Li. We also take $n_a = 1.8 \times 10^7$, $n_b = 2.6 \times 10^6$ as population of the two species, H_0= 834 G, Γ= 300G (These values correspond to experimental data for Feshbach resonances in ^{6}Li as reported in [15, 16, 37].) We now solve equations (3.28a,3.28b) explicitly to find H_1 to be 832.40 G and H_2 to be 833.95 G. It would be interesting to speculate that the superfluid observed by Zwierlein et al. in this range is of the BP1 variety.

This estimate of H_1 and H_2 is not a highly accurate one. In fact, the range of the breached pair state should get shifted a bit towards lower values of the magnetic field.

Actually, for deriving equations (3.28a,3.28b), we had assumed the magnitudes of the chemical potentials to be very large compared to Δ and k_1, an assumption which does not hold at points where μ_a and μ_b become zero. However, the values are not unreasonable in view of the fact that in the BCS-BEC crossover picture, the chemical potential falls quite sharply after crossing zero and quickly becomes a large negative quantity.

3.7 Summary and Discussion

Here we have studied a two-species fermionic system in the presence of Feshbach resonance, taking a variational route with an explicit construct of the ground state. It was observed how the critical temperature as well as the BCS gap behaves in the positive and the negative detuning regions respectively. Furthermore, the gapless breached pair state was discussed, and its stability was analysed using the concept of Meissner mass. We showed that a breached pair state with two Fermi surfaces is always unstable, while its single Fermi-surface counterpart is stable when the chemical potential of the two pairing species bear opposite signs.

The stability of the breached pair state is indeed a widely debated issue. Although it has often been suggested that the BP1 state might be stable in deep BEC region, nothing, to the best of our knowledge, was said anything about how 'deep' that really is. In this note, however, we observe that, the requirement that μ_a and μ_b should be of opposite signs, automatically puts two bounds in terms of the Feshbach magnetic fields, between which the gapless state is stable. Moreover, this stable breached pair state is obtained not in deep BEC, but near the vicinity of the point when the average chemical potential crosses zero, i.e., right after the onset of condensation.

Gubankova et al [32], while discussing the stability of breached pair states by analysing the number susceptibility, commented that stable gapless states with a single Fermi surface exist for negative average chemical potential. In a recent paper, A. Mishra et al [33] reached the same conclusion by comparing the thermodynamic potentials of the condensed phase and the normal phase. Although the criterion they arrive at (the negativity of the average chemical potential) does not fully match with ours (the chemical potential of the two species to have opposite signs), there is definitely a region of overlap.

In their experiment, Zwierlein et al. observed that superfluidity breaks down when the pairing gap Δ becomes small compared to the chemical potential difference $\mu_a - \mu_b$. We note that this matches with the stability criterion for the BP2 state, since, if $\Delta < \delta\mu$ and $\eta = 1$, the state becomes unstable, as seen from equation (3.19).

As for the BP1 state, we have shown that this state is stable in a region where μ_a and μ_b have opposite signs, which can be achieved by keeping the system between two specific magnetic field values. For simplicity we took the two species to have same masses in our calculation, but the treatment should be extendable to a situation where the fermion species are of different masses, as for example in a ^{6}Li-^{40}K system.

Bibliography

[1] W. V. Liu and F. Wilczek, Phys. Rev. Lett. **90**, 047002 (2003).

[2] P. F. Bedaque, H. Caldas, and G. Rupak, Phys. Rev. Lett. **91**, 247002 (2003).

[3] S-T. Wu and S. Yip, Phys. Rev. A **67**, 053603 (2003).

[4] Bimalendu Deb, Amruta Mishra, Hiranmaya Mishra, and Prasanta K. Panigrahi, Phys. Rev. A **70**, 011604(R)

[5] H. Caldas, C.W. Morais and A.L. Mota, Phys. Rev. D **72**, 045008 (2005).

[6] J. Carlson and S. Reddy, Phys. Rev. Lett. **95**, 060401 (2005).

[7] D. T. Son and M. A. Stephanov, Phys. Rev. A **74** 013614 (2006).

[8] D. E. Sheehy and L. Radzihovsky, Phys. Rev. Lett. **96**, 060401 (2006).

[9] D. E. Sheehy and L. Radzihovsky, Annals of Physics **322**, 1790 (2007).

[10] C. C. Chien, Q. Chen, Y. He and K. Levin, Phys Rev Lett. **98**, 110404, (2007).

[11] Q. Chen, Y. He, C. C. Chien and K. Levin, Phys Rev B **75**, 014521, (2007).

[12] T. Koponen, J. Kinnunen, J.P. Martikainen, L.M. Jensen, P. Torma, New Journal of Physics B **8**, 179 (2006).

[13] M. Iskin and C. A. R. Sa de Melo, Phys. Rev. Lett. **97**, 100404 (2006).

[14] K. B. Gubbels, M. W. J. Romans, and H. T. C. Stoof, Phys. Rev. Lett. **97**, 210402 (2006).

[15] M. W. Zwierlein, A. Schirotzek, C. H. Schunck and W. Ketterle, Science **311**, 492 (2006).

[16] M. W. Zwierlein, C.H. Schunck, A. Schirotzek, and W. Ketterle, Nature(London) **442**, 54 (2006).

[17] G.B. Patridge, W. Li, R. I. Kamar, Y. A. Liao, and R. G. Hulet, Science **311**, 503 (2006).

[18] A. I. Larkin, Yu. N. Ovchinnikov, Sov. Phys. JETP **20**, (1965).

[19] P. Fulde, R. A. Ferrel, Phys. Rev. A, **135**, 550, (1964).

[20] M. Mannarelli, G. Nardulli and M. Ruggieri, Phys. Rev. A.74, 033606(2006).

[21] G.Sarma, J.Phys.Chem.Solid 24,1029(1963).

[22] M. M. Forbes, E. Gubankova, W. V. Liu and F. Wilczek, Phys. Rev. Lett.**94**, 017001(2005).

[23] C.-H. Pao, S.-T. Wu, and S.-K. Yip, Phys. Rev. B **73**, 132506 (2006).

[24] H.Hu and X.Liu, Phys. Rev. A ,73, 051603(R)(2006).

[25] L. He and P. Zhuang , Phys. Rev. B **79**, 024511 (2009).

[26] Y. Ohashi and A. Griffin, Phys. Rev. Lett. **89**, 130402 (2002).

[27] M. Holland et al., Phys. Rev. Lett.**87**, 120406 (2001).

[28] L. He, M. Jin, P. Zhuang, Phys. Rev. B **73**, 214527 (2006).

[29] L. He, M. Jin, P. Zhuang, Phys. Rev. B **73**,024511 (2006).

[30] R.P. Feynman, Statistical Mechanics, A Set of Lectures, Addison-Wesley, New York, 1988.

[31] Pairing in Fermionic Systems, edited by A. Sedrakian, J. W. Clark, and M. Alford, World Scientific Publishing Co, Singapore, 2006.

[32] E. Gubankova, A. Schmitt, F. Wilczek, Phys. Rev. B **74**, 064505 (2006).

[33] A. Mishra and H. Mishra The Eur. Phys. J. D., **53**,75,(2009).

[34] W. Yi and L.-M. Duan, Phys. Rev. Lett. **97**, 120401 (2006).

[35] H. Caldas and A.L. Mota, J Stat. Mech, P08013 (2008).

[36] A.J. Leggett, Quantum Liquids,Bose Condensation and Cooper pairing in condensed-matter systems, Oxford University Press, Oxford, 2006.

[37] C. H. Schunck, M. W. Zwierlein, C. A. Stan, S. M. F. Raupach, and W. Ketterle, PRA **71**, 045601(2005).

Chapter 4

Quench Dynamics in a BCS-like Fermi Superfluid System

4.1 Introduction

In the last few decades, quench dynamics has been a subject of intense theoretical research [1–4]. In the last few years it has become all the more important because of the high tunability associated with cold atom experiments. In these experiments, although it is possible to have an excellent control over the system parameters, it is not always feasible to vary them in a perfectly adiabatic way. Moreover, the ability to rapidly change parameters enables one to study the quantum evolution that follows. Abrupt changes in the parameter value often leads to newer properties of the system, and demands for a thorough investigation of the nonadiabatic "fast quench" dynamics. Superfluid-to-Mott insulator transition, BCS-BEC crossover are some of the phenomena for which nonadiabatic dynamics has been studied in the recent past [5–8].

In quench studies, the system parameters are changed very fast. It is assumed that the system is prepared in the ground state of an initial Hamiltonian and then the subsequent evolution is controlled by the final Hamiltonian. However, it has been found that the long time steady state still retains information of the initial state [9–13] .

For sudden quench, the final state of the system is not the same as the ground state of the final Hamiltonian. Thus, defects are produced [14, 15] .

4.2 Quench Dynamics and Scaling Laws

Quench Dynamics is extremely important in the context of quantum phase transitions (QPT). Unlike usual classical phase transitions, quantum phase transitions are entirely driven by quantum fluctuations and not by thermal ones. So they can take place in zero temperature as well. However, quite often the quantum phase transitions can be linked with analogous thermal transitions, and QPT in a d-dimensional system can be mapped into thermal transition in a d+z dimensional system. Here z is the dynamical critical exponent [16, 17]. A significant attribute of QPTs (and second order classical transitions as well) is the universality of the low energy properties of the system, and the transition is characterized by diverging length and time scales near the quantum critical point. Low-energy properties of the system can be described by parameters like correlation length or energy gap, and they show power-law scaling behaviours with respect to the tuning parameter [16].

In our work we first study the scaling behaviour of the response of an ultracold quantum system to sudden quenches. The dynamics will be universal if it is dominated by the low energy excitations . The system that we consider here is a BCS-like ultracold superfluid system. We treat the coupling as the driving parameter through which the quench can be achieved. However, there is no actual phase transition here. So it is not a quantum phase transition that we talk about, but a rapid change in the superfluid state as the BCS-coupling strength is changed suddenly. We wish to probe if scaling laws still hold for parameters like defect density and quasiparticle excitation energy.

The correlation length ξ which defines the length scale separating qualitatively different behaviour of the order parameter, diverges with the tuning parameter λ as [17]

$$\xi \sim \frac{1}{|\lambda - \lambda_c|^{\nu}}.$$

In quantum systems a divergent time scale is characterized by a vanishing energy scale

$$\Delta \sim \frac{1}{\xi^z} \sim |\lambda - \lambda_c|^{z\nu},$$

where z is dynamical exponent. The energy scale Δ represent a gap in the spectrum or some crossover energy scale which separates region with different dispersion relations.

Another important quantity that becomes important in the study of quench dynamics is susceptibility. In case of QPT, susceptibilities usually have singular non-analytic behaviour characterized by there own critical exponent near quantum critical point. It was realized recently that fidelity susceptibility (FS) is a very useful measure to analyze quantum evolutions. If $|\psi_n(\lambda)\rangle$ denotes the instantaneous eigenstates of the Hamiltonian $H(\lambda)$ and $E_n(\lambda)$ are the instantaneous energies then FS is the leading order of expansion of the overlap of the ground state functions $|\langle\psi_0(\lambda+\delta\lambda)|\psi_0(\lambda)\rangle|^2$ in power of $\delta\lambda$.

$$|\langle\psi_0(\lambda+\delta\lambda)|\psi_0(\lambda)\rangle|^2 \approx 1-\delta\lambda^2\chi_F(\lambda) \tag{4.1}$$

Again, we emphasize that here we are not dealing with quantum critical systems, but a quantum system which has been changed drastically as the coupling is altered via Feshbach resonance. Our aim is to study the scaling behaviour of the response of the system, and whether the dynamics will be universal in the low-energy spectrum.

We assume the system is initially prepared in the ground state of some Hamiltonian H_0. We then suddenly apply perturbation λV , where λ is a small parameter and V is some operator independent of λ. The scaling of various quantities for a quantum phase transition using ordinary perturbation theory has been discussed in Ref. [16]. For example fidelity ($f(\lambda)$) scales as

$$f(\lambda) = |\lambda|^{d\nu}. \tag{4.2}$$

Likewise heat density which is defined as the difference between the energy after the quench and the ground state energy, scales as

$$Q(\lambda) \sim |\lambda|^{(d+z)\nu} \tag{4.3}$$

The scaling of the density of quasi particle excitations is given by

$$n_{ex} \sim |\lambda|^{d\nu} \tag{4.4}$$

We want to probe if exponents can be calculated in a similar fashion and linked to each other for our system also.

4.3 Model Hamiltonian and Sudden Quenches

[1] In this article we consider a superfluid BCS-like system undergoing sudden quenches. Now, the grand-canonical Hamiltonian for a weakly interacting Fermi gas with repulsion between the particles is given by,

$$H = \sum_{\mathbf{p}} \xi_{\mathbf{p}} \psi^{\dagger}_{\mathbf{p}} \psi_{\mathbf{p}} - g \sum_{\mathbf{p}',\mathbf{p}} \psi^{\dagger}_{\uparrow \mathbf{p}'} a^{\dagger}_{\downarrow -\mathbf{p}'} \psi_{\downarrow -\mathbf{p}} \psi_{\uparrow \mathbf{p}} \tag{4.5}$$

The first term denotes the kinetic energy of the fermions and the second term represents the four-fermion interaction. Here $g = 4\pi\hbar^2 a/m < 0$ in the BCS-coupling whose sign is positive if the interaction is attractive. , Also, $\epsilon_p = -[\mathrm{cos}p_x + \mathrm{cos}p_y]$ is the band energy spectrum for the fermions. $\xi_p = \varepsilon_p - \mu$, and μ is the chemical potential.

The gap parameter $\Delta(p)$ is dependent on the pairing symmetry.

For the s-wave pairing,$\Delta(p)$ is a constant, i.e.,

$$\Delta(p) = \Delta_0 \tag{4.6}$$

For the d-wave pairing,

$$\Delta(p) = \Delta_0(\mathrm{cos}p_x - \mathrm{cos}p_y) \tag{4.7}$$

It can be written in terms of θ using $p_x = p\mathrm{cos}\theta$ and $p_y = p\mathrm{sin}\theta$.

Here we consider g as the driving parameter. Before the quench the Superfluid ground state is given by:

$$|\psi_0(g)\rangle = \prod_{\mathbf{p}} (U_{\mathbf{p}} + V_{\mathbf{p}}\ \psi^{\dagger}_{\mathbf{p}\uparrow} \psi^{\dagger}_{-\mathbf{p}\downarrow})|0\rangle \tag{4.8}$$

where

$$U^2_{\mathbf{p}} = \frac{1}{2}(1 + \frac{\xi_{\mathbf{p}}}{E_{\mathbf{p}}}) \tag{4.9}$$

$$V^2_{\mathbf{p}} = \frac{1}{2}(1 - \frac{\xi_{\mathbf{p}}}{E_{\mathbf{p}}}) \tag{4.10}$$

[1]The work reported here is in collaboration with Sanhita Modak and K. Sengupta

with $E_p = \sqrt{\Delta^2 + \xi_p^2}$ and

$$\Delta = -g \sum_{\mathbf{p}} \langle \psi_{-p\downarrow} \psi_{p\uparrow} \rangle \tag{4.11}$$

$$= -g \sum_{\mathbf{p}} U_{\mathbf{p}} V_{\mathbf{p}} (1 - 2N_{\mathbf{p}}) \tag{4.12}$$

$$N_{\mathbf{p}} = \frac{1}{\exp\beta\epsilon_{\mathbf{p}} + 1} \tag{4.13}$$

4.4 Fidelity and Defect Density after Sudden Quench

We now suddenly change the parameter g to $g + \delta g$ and after the quench the superfluid ground state is given by,

$$|\psi_0(g + \delta g)\rangle = \prod_{\mathbf{p}} (\widetilde{U}_{\mathbf{p}} + \widetilde{V}_{\mathbf{p}} \psi^\dagger_{\mathbf{p}\uparrow} \psi^\dagger_{-\mathbf{p}\downarrow}) |0\rangle \tag{4.14}$$

Therefore the overlap between the two ground states at g and $g + \delta g$ can be defined as,

$$F(g, g + \delta g) = \langle \psi_0(g) | \psi_0(g + \delta g) \rangle. \tag{4.15}$$

This overlap marks the "fidelity" of the system, a quantity that represents the similarity/ difference between two states. We define

$$f(g, g + \delta g) = 1 - |F(g, g + \delta g)|^2 \tag{4.16}$$

$$= 1 - \prod_{\mathbf{p}} [U_{\mathbf{p}} \widetilde{U}_{\mathbf{p}} + V_{\mathbf{p}} \widetilde{V}_{\mathbf{p}}] \tag{4.17}$$

as a measure for this fidelity.

We plot $f(g) \equiv f(g, g + \delta g) = 1 - |F(g, g + \delta g)|^2$ vs. δg, the change in the coupling. To see whether the system shows any power-law behaviour, we make a log-log plot as well. For both the s-wave and d-wave pairing, the slope comes as 2.032 from the log-log graph which is nearly equal to 2. Therefore, the scaling exponent can be considered to be 2.

We define the number operator as

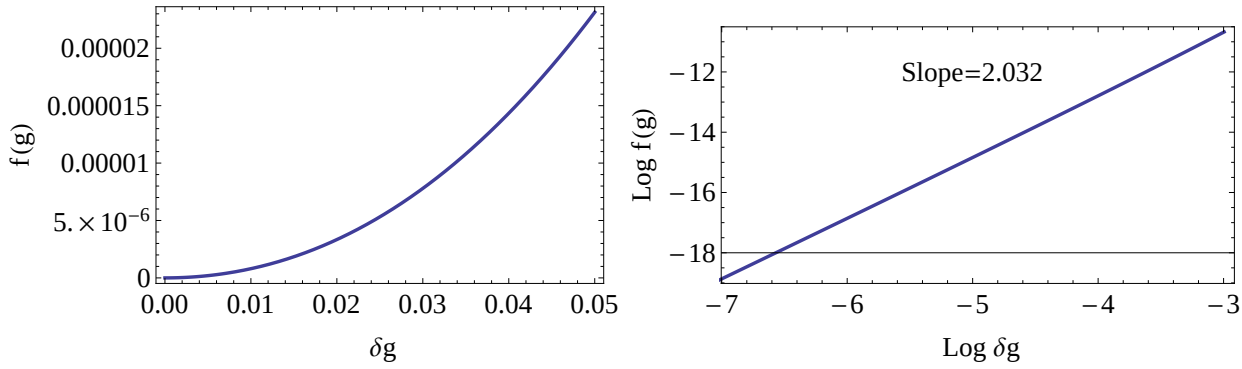

Figure 4.1: (a) $f(g)$ vs. δg plot for s-wave pairing (b) The log-log plot gives the scaling exponent.

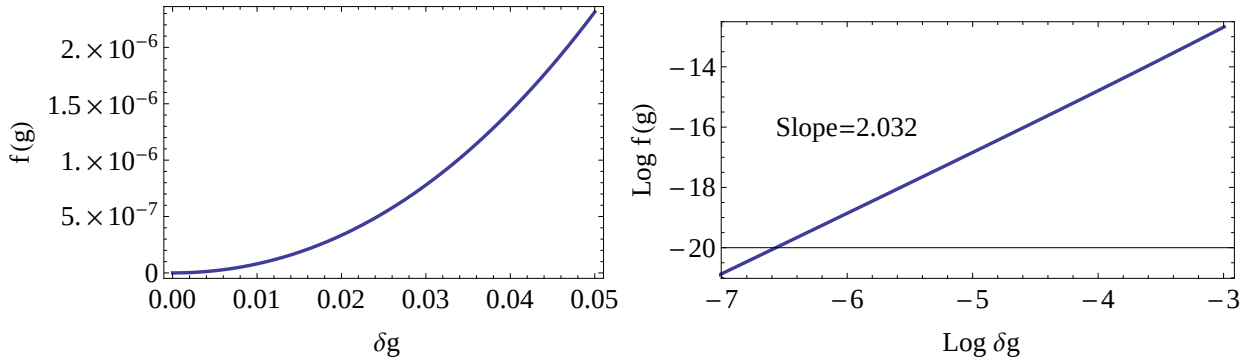

Figure 4.2: (a) $f(g)$ vs. δg plot for d-wave pairing (b) The log-log plot gives the scaling exponent.

$$\hat{N} = \sum_{\mathbf{p}} [\psi^{\dagger}_{\mathbf{p}\uparrow}\psi_{\mathbf{p}\uparrow} + \psi^{\dagger}_{-\mathbf{p}\downarrow}\psi_{-\mathbf{p}\downarrow}] \tag{4.18}$$

So the density of quasi particle excitation is given by:

$$n_{ex} = \langle\psi^f|\hat{N}|\psi^f\rangle - \langle\psi^f_G|\hat{N}|\psi^f_G\rangle \tag{4.19}$$

Now for sudden quench $|\psi^f\rangle = |\psi^i_G\rangle$, where $|\psi^{f(i)}_G\rangle$ is the ground state after (before) the quench and $|\psi^f\rangle$ is the final state after quench. Therefore

$$n_{ex} = \langle\psi^i_G|\hat{N}|\psi^i_G\rangle - \langle\psi^f_G|\hat{N}|\psi^f_G\rangle \tag{4.20}$$

$$= \sum_p 2[V_p^2 - \widetilde{V}_p^2] \tag{4.21}$$

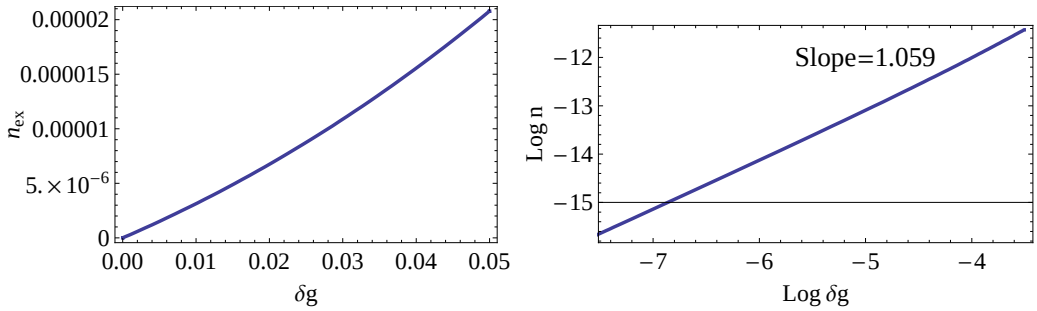

Figure 4.3: (a) Quasiparticle excitation vs. δg plot for s-wave pairing (b) The log-log plot gives the scaling exponent.

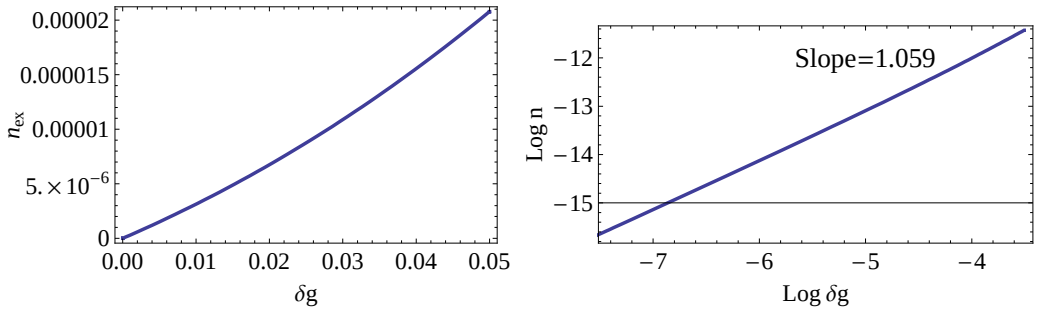

Figure 4.4: (a) Quasiparticle excitation vs. δg plot for d-wave pairing (b) The log-log plot gives the scaling exponent.

We find that the slope for quasiparticle excitation density graph comes as 1.059, which is essentially equal to 1. The same scaling exponent is found for quasiparticle excitation energy as well.

4.5 Periodically Driven BCS Systems

[2] Next we study the effect of periodically driven quenches in BCS superfluid systems . In the last few years, periodically driven quantum systems have generated a lot of research interests and activities, especially from the theoretical stand-point [18–21]

It has been observed that coherent periodic driving in a class of integrable quantum many-body systems can result in exotic quantum phenomena like dynamical many-body freezing. Highly non-monotonic freezing behaviour is observed in these cases with respect to the driving frequency [21, 22]. In the high driving frequency limit, all the many-body modes remain maximally frozen for all time for certain combination of the driving parameters, while in the low-frequency limit, universal behaviour of the response is observed since only the excitations of the low-lying critical modes of the system [23] is relevant.

The experimental realization of periodically driven quantum systems was achieved in the 90s by F. L. Moore et al. [24] when they devised a quantum delta-kicked rotor in the form of ultracold sodium atoms in a periodic standing wave pulsed on periodically in time. Later C. Ryu et al. [25] observed high-order resonances in a quantum delta-kicked rotor of Bose-condensed Na atoms.

This connection between cold atoms and quantum rotors suggests that periodic drives can be applied to other cold-atom experiments, and can be studied in the context of both BEC and BCS superfluidity, which are connected by a crossover via Feshbach resonance [26–31]. Driven BEC [32]and superfluid-Mott transition in the presence of an oscillatory force in a Bose-Hubbard model [33] have been studied theoretically.

In our work, we focus on the other side of the spectrum, i.e., on ultracold BCS superfluids. We drive the system by varying the chemical potential sinusoidally in time and observe the non-adiabatic dynamics. A large driving frequency ensures a fast quench while a small ω corresponds to slow quenching dynamics. We restrict our study only in the low driving frequency and amplitude regime.

[2]This section and the following sections are results of a collaborative project. Ref: "Periodic Dynamics of Fermi superfluids in the BCS regime", Analabha Roy, Raka Dasgupta, Sanhita Modak, Arnab Das and K. Sengupta, to be submitted soon.

4.6 The Model for Periodic Driving

In this part, we study the response of a fermionic superfluid in the BCS regime under the influence of a periodic drive. The periodicity is introduced in the chemical potential $\mu(t)$ which is the time-dependent parameter here that causes the quench. At equilibrium, μ_0 is the chemical potential that fixes the particle number, and $\mu(t)$ is chosen to be $\mu_0 + \mu_a \sin \omega t$.

The Hamiltonian is given by

$$H = \sum_{\mathbf{p}} (\epsilon_{\mathbf{p}} - \mu(t)) \psi^{\dagger}_{\mathbf{p}} \psi_{\mathbf{p}} - g \sum_{\mathbf{p}',\mathbf{p}} \psi^{\dagger}_{\uparrow \mathbf{p}'} \psi^{\dagger}_{\downarrow -\mathbf{p}'} \psi_{\downarrow -\mathbf{p}} \psi_{\uparrow \mathbf{p}} \tag{4.22}$$

Here, $\psi^{\dagger}_{\mathbf{p}}$ represents the creation operator and $\psi_{\mathbf{p}}$ represents the annihilation operator for Fermions of momentum $\mathbf{p}$.

The time-dependent Bogoliubov de-Gennes Hamiltonian for the same system is given by

$$H(t) = \sum_{\mathbf{p}} h_{\mathbf{p}}(t) \tag{4.23}$$

$$h_{\mathbf{p}}(t) = \begin{pmatrix} \epsilon_{\mathbf{p}} - \mu(t) & \Delta \\ \Delta^* & -(\epsilon_{\mathbf{p}} - \mu(t)) \end{pmatrix}$$
$$= (\epsilon_{\mathbf{p}}(t) - \mu(t))\sigma_z + \frac{1}{2}(\Delta(t)\sigma_+ + \Delta^*(t)\sigma_-)$$

If $\Delta = \Delta^*$,

$H = (\epsilon_{\mathbf{p}} - \mu(t))\sigma_z + \Delta\sigma_x$

in terms of the Pauli matrices $\sigma_{x,y}$. $\sigma_{\pm} = \frac{1}{2}(\sigma_x \pm i\sigma_y$)are the usual ladder operators. Δ and ϵ_p are determined by the system properties and the chemical potential μ is the tunable control parameter.

4.7 Rotating Wave Approximation

We split the Hamiltonian into two parts $H_0 = \Delta\sigma_x$ and $v(t) = (\epsilon_p - \mu(t))\sigma_z$

We make a transformation to a rotating frame with the operator W.

$$\begin{aligned} W(t) &= \exp(-i\int v(t)dt) \\ &= \exp[-i((\epsilon_p - \mu_0)t + \frac{\mu_a \cos\omega t}{\omega})\sigma_z] \\ &= \exp(-i\frac{\eta(t)}{2}\sigma_z) \end{aligned} \tag{4.24}$$

Here $\eta(t) = 2(\epsilon_p - \mu_0)t + \dfrac{2\mu_0 \cos\omega t}{\omega}$

Therefore,

$$\begin{aligned} H' = W^\dagger H_0 W &= \Delta\exp(i\frac{\eta(t)}{2}\sigma_z)\sigma_x\exp(-i\frac{\eta(t)}{2}\sigma_z) \\ &= \Delta(e^{i\eta}\sigma_+ + e^{-i\eta}\sigma_-) \end{aligned} \tag{4.25}$$

Now,

$$e^{ix\cos\theta} = \sum i^n J_n(x)e^{in\theta} \tag{4.26}$$

$$\begin{aligned} & e^{i\eta(t)} \\ &= e^{i(2(\epsilon_p-\mu_0)t+\frac{2\mu_0 cos\omega t}{\omega})} \\ &= e^{i(2(\epsilon_p-\mu_0)t}\sum i^n J_n(2\mu_0/\omega)e^{in\omega t} \\ &= \sum i^n J_n(2\mu_0/\omega)e^{i(n\omega+2(\epsilon_p-\mu_0))t} \end{aligned} \tag{4.27}$$

We know,

$$\sigma_+ = \begin{pmatrix} 0 & 1 \\ 0 & 0 \end{pmatrix}$$

and

$$\sigma_- = \begin{pmatrix} 0 & 0 \\ 1 & 0 \end{pmatrix}$$

Thus the matrix is off-diagonalised. We have,

$$H'(t) = \Delta \begin{pmatrix} 0 & \sum i^n J_n(\frac{2\mu_0}{\omega}) e^{i(n\omega+2f_p)t} \\ \sum i^n J_n(\frac{2\mu_0}{\omega}) e^{-i(n\omega+2f_p)t} & 0 \end{pmatrix}$$

Let $(\epsilon_p - \mu_0) = f_p$. We ignore all the faster oscillating terms in the off-diagonal sum in $H(t)$ except for the resonant term $n = n_r$, for which the effective frequency $(n\omega + 2(\epsilon_p - \mu_0)$is the smallest. In the high frequency limit $n_r = 0$.

Therefore,

$$H'(t) = \Delta \begin{pmatrix} 0 & J_0(\frac{2\mu_0}{\omega}) e^{2if_pt} \\ J_0(\frac{2\mu_0}{\omega}) e^{-2if_pt} & 0 \end{pmatrix}$$

$$i\hbar \frac{\partial}{\partial t} \begin{pmatrix} u_p \\ v_p \end{pmatrix} = \Delta \begin{pmatrix} 0 & J_0(\frac{2\mu_0}{\omega}) e^{2if_pt} \\ J_0(\frac{2\mu_0}{\omega}) e^{-2if_pt} & 0 \end{pmatrix} \begin{pmatrix} u_p \\ v_p \end{pmatrix}$$

Putting $\hbar = 1$

$$\frac{\partial u_p}{\partial t} = -i\Delta J_0(\frac{2\mu_0}{\omega}) e^{2if_pt} v_p$$
$$\frac{\partial v_p}{\partial t} = -i\Delta J_0(\frac{2\mu_0}{\omega}) e^{-2if_pt} u_p$$

Solving for $v(t)$ and $u(t)$,

$$v_p(t) = -2ie^{-if_pt}[\frac{J_0(\frac{2\mu_0}{\omega})\Delta}{2\phi_p}\sin(\phi_p t)]u_p(0) + e^{-if_pt}[\cos(\phi_p t) + i\frac{f_p}{\phi_p}\sin(\phi_p t)]v_p(0)$$

$$u_p(t) = -2ie^{if_pt}[\frac{J_0(\frac{2\mu_0}{\omega})\Delta}{2\phi_p}\sin(\phi_p t)]v_p(0) + e^{if_pt}[\cos(\phi_p t) - i\frac{f_p}{\phi_p}\sin(\phi_p t)]u_p(0)$$

Here $\phi_p = \sqrt{J_0^2(\frac{2\mu_0}{\omega})\Delta_p^2 + f_p^2}$

We see that for $p = \pi/2$ and $p = \pi$, $|v_p(t)|^2$ oscillates with a diminishing amplitude, i.e.,

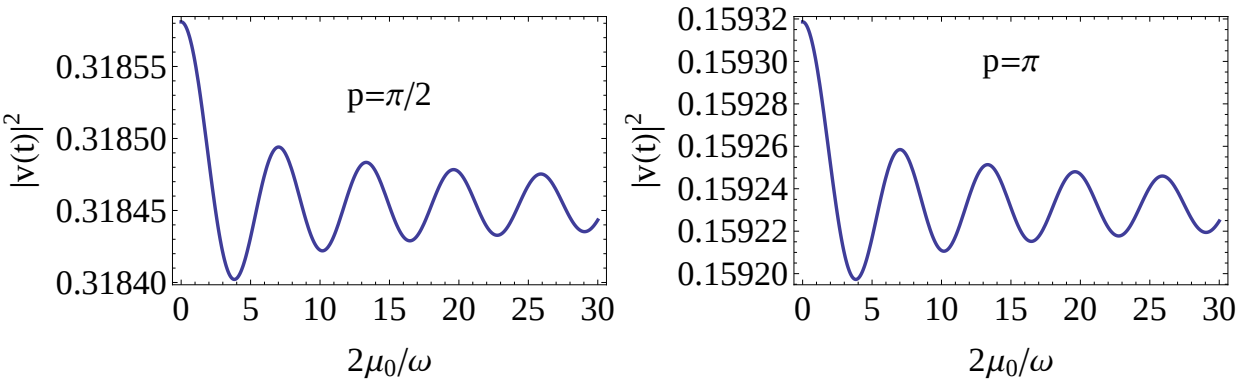

Figure 4.5: $|v_p(t)|^2$ vs $(\frac{2\mu_0}{\omega})$ for various p's

there is a freezing. Here all energies are scaled by E_F, and h_0 is taken as 1.

In case of Ising systems, nonmonotonic behaviour of the response with respect to ω showing peak and valley structures has been termed as "freezing"', can contrasted with the expected monotonic behaviour manifested in periodic driving in classical systems [21]. Here also, the oscillation is indicative of some freezing. Non-monotonic freezing comes from the non-monotonicity of $J_0(\frac{2\mu_0}{\omega})$, as the peaks in $|v_p(t)|^2$ corrrespond to the dips of the Bessel function, and vice versa.

For d-wave pairing, where there is a directional dependence of the gap parameter, we observe similar features, i.e., oscillation with a decaying amplitude. These plots are for μ_0=25.

In the above plots, self-consistency of Δ has not been taken into account explicitly.

4.8 Magnetization and Defect Production in the Periodic Quench

To study the effect of periodic quench, we choose a few observable quantities. The first amongst them is the effective magnetization $m(t)$. It is defined as

$$\begin{aligned} m_{\mathbf{p}}(t) &= \langle\psi_{\mathbf{p}}(t)|\sigma_z|\psi_{\mathbf{p}}(t)\rangle, \\ m(t) &= \sum_{\mathbf{p}} m_{\mathbf{p}}(t) = \sum_{\mathbf{p}}[1-2|v_{\mathbf{p}}(t)|^2] \end{aligned} \tag{4.28}$$

where σ_z is the Pauli matrix. Here $m(t)$ plays a similar role as that of magnetization of the Ising model, only, the self-consistency condition is not there in the Ising case. $m(t)$ will be equal to $m(0)$, the initial value of the magnetization after a full drive cycle, i.e., at $T = 2\pi/\omega$. This is true for both in the impulse (where the wavefunction does not have time to adjust itself in accordance with the drive) and adiabatic limit.

The long time average of $m(t)$ is defined as :

$$Q \equiv \lim_{n\to\infty} \frac{1}{nT} \int_0^{nT} \mathrm{d}t \times m(t) \tag{4.29}$$

The second quantity which is relevant here is the wavefunction overlap. Let us first define the amplitudes $u_{\mathbf{p}}^{\mathrm{ad}}(t)$ and $v_{\mathbf{p}}^{\mathrm{ad}}(t)$ which correspond to the values of $u_{\mathbf{p}}$ and v_{p} at time t for adiabatic evolution. The ground state of H with $\mu = \mu(t)$ can be written in terms of these quantities as

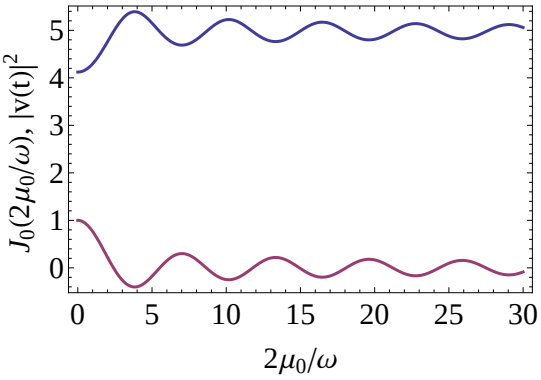

Figure 4.6: Blue line: $|v_p(t)|^2$ and Red line :$J_0(\frac{2\mu_0}{\omega})$ plotted against $(\frac{2\mu_0}{\omega})$

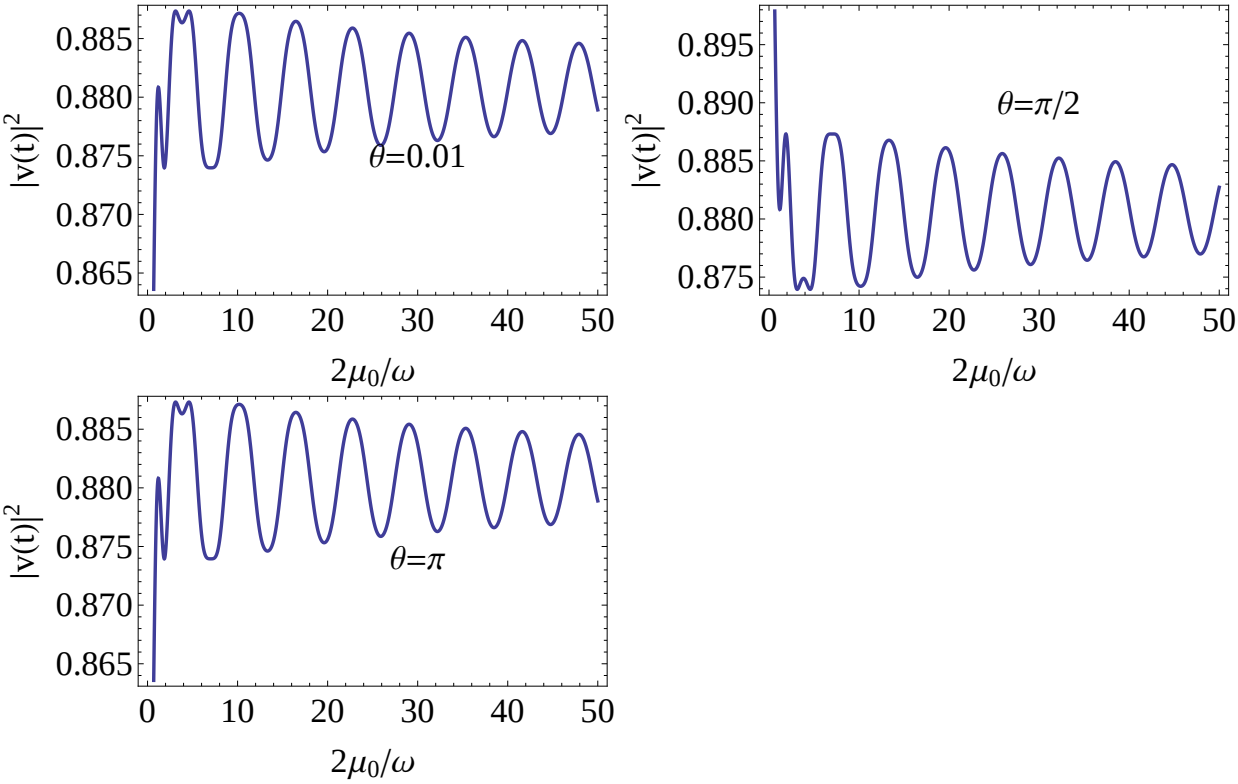

Figure 4.7: $|v_p(t)|^2$ vs $(\frac{2\mu_0}{\omega})$ for various θ' s

$$
\begin{aligned}
|\psi^{\mathrm{ad}}(t)\rangle &= \prod_{\mathbf{p}} \left(u^{\mathrm{ad}}_{\mathbf{p}}(t) + v^{\mathrm{ad}}_{\mathbf{p}}(t) \psi^{\dagger}_{\mathbf{p}} \psi^{\dagger}_{-\mathbf{p}} \right) |0\rangle \\
u^{\mathrm{ad}}_{\mathbf{p}}(t) &= \frac{1}{\sqrt{2}} \left(1 + \frac{[\epsilon_{\mathbf{p}} - \mu(t)]}{E(\mathbf{p};t)} \right)^{1/2} \\
v^{\mathrm{ad}}_{\mathbf{p}}(t) &= \frac{1}{\sqrt{2}} \left(1 - \frac{[\epsilon_{\mathbf{p}} - \mu(t)]}{E(\mathbf{p};t)} \right)^{1/2}
\end{aligned}
\tag{4.30}
$$

Here $E_p(t) = \sqrt{[\epsilon_{\mathbf{p}} - \mu(t)]^2 + \Delta^2(t)}$.

Since we are talking of a periodic drive, $|\psi^{\mathrm{ad}}(t_f)\rangle = |\psi\rangle$. Let

$$
|\psi(t)\rangle \;=\; \prod_{\mathbf{p}} \left(u_{\mathbf{p}}(t) + v_{\mathbf{p}}(t) \psi^{\dagger}_{\mathbf{p}} \psi^{\dagger}_{-\mathbf{p}} \right) |0\rangle, \tag{4.31}
$$

We define the wavefunction overlap F as

$$\begin{aligned} F &= |\langle\psi^{\rm ad}(t)|\psi(t)\rangle|^2 \\ &= \prod_{\mathbf{p}} F_{\mathbf{p}} = \prod_{\mathbf{p}} |u^{\rm ad*}_{\mathbf{p}}(t)u_{\mathbf{p}}(t) + v^{\rm ad*}_{\mathbf{p}}(t)v_{\mathbf{p}}(t)|^2 \end{aligned} \tag{4.32}$$

The dynamical fidelity of the system is an important parameter to study periodic quench. It is the overlap between the evolving wave-function and the instantaneous adiabatic state.Instead of the standard definition of fidelity where the overlap between the wavefunction with the initial state is measured, here the overlap between the evolving wave-function and the corresponding adiabatic state at that particular instant becomes the relevant parameter. It is a measure of the deviation of the wave function from the instantaneous adiabatic state, and hence represents the non-adiabaticity caused by the periodic drive.

The defect density or the density of excitations generated due the dynamics at any instant of time can be written in terms of F as

$$\begin{aligned} \rho_d &= \sum_{\mathbf{p}} \rho_d(\mathbf{p}) \\ \rho_d(\mathbf{p}) &= 1 - F_{\mathbf{p}} = |u^{\rm ad*}_{\mathbf{p}}(t)v_{\mathbf{p}}(t) - v^{\rm ad*}_{\mathbf{p}}(t)u_{\mathbf{p}}(t)|^2 \end{aligned} \tag{4.33}$$

The defect density identically vanishes for adiabatic dynamics and thus provides a suitable measure for deviation from adiabaticity.

We also compute the residual energy which is defined as the additional energy put in the system due to the drive. This is the difference between the energy of the system at time t from the instantaneous ground state energy and can be written as

$$\begin{aligned} E_r(t) &= \sum_{\mathbf{p}} \left[\langle\psi_{\mathbf{p}}(t)|h_{\mathbf{p}}(t)|\psi_{\mathbf{p}}(t)\rangle - \langle\psi^{\rm ad}_{\mathbf{p}}(t)|h_{\mathbf{p}}(t)|\psi^{\rm ad}_{\mathbf{p}}(t)\rangle\right], \\ &= \frac{1}{g}\left[\Delta^2(t) + \Delta^{*2}(t) - 2\Delta_0^2\right] \\ &\quad - \sum_{\mathbf{p}} \left[\epsilon_{\mathbf{p}} - \mu(t)\right]\left[m_{\mathbf{p}}(t) - m^{\rm ad}_{\mathbf{p}}(t)\right], \end{aligned} \tag{4.34}$$

where $m^{\rm ad}_{\mathbf{p}} = 1 - 2|v^{\rm ad}_{\mathbf{p}}|^2$. Note that the residual energy also vanishes for adiabatic dynamics.

4.9 Numerical Results

In this section, the self-consistent numerical evaluation of the Bogoliubov de-Gennes equation and subsequent computation of $m(t)$, Q, ρ_d, and E_r is reported. The equilibrium gap and chemical potential has been taken to be $\Delta_0 = 0.1$ and $\mu_0 = 0.01$ respectively. The periodic drive term has been taken to be of the form $\mu_a \sin\omega t$ with $\mu_a = 0.1$.

Next, we plot the effective magnetization $m(t)$ as a function of time t and its time average Q as a function of the drive frequency ω. We find that for $\omega \geq \Delta_0$, Q deviates from its equilibrium value and never returns to m_0 as ω is increased. This behaviour is to be contrasted with the non-self-consistent dynamics shown in the left panel of Fig. 4.9, where $Q = m(0)$ for some special values of ω. This phenomenon was termed as exotic freezing in [21] in the context of one-dimensional Ising model. The self-consistent dynamics, as appropriate for the current non-integrable system of BCS fermions, seems to destroy such phenomenon. Next, we consider the behaviour of $m(t)$. We find that for $\omega \ll \Delta_0$, $m(t)$ displays oscillatory behaviour as shown in the right panel of Fig. 4.8. Such an oscillatory behaviour is seen for all drive frequencies $\omega \leq 2\Delta_0$ for the non-self-consistent dynamics as shown in right panel of Fig. 4.9 and is characteristic of dynamics of an integrable system. However, for the self-consistent dynamics appropriate for fermions in the BCS regime, we find that the oscillatory behaviour is replaced by realization of the steady state at long times $\omega t/(2\pi) \geq 1$ and for $\omega \simeq \Delta_0$.

Finally, we consider the behaviour of defect density ρ_d as shown in Fig. 4.10. Here, as expected, that the defect density becomes non-zero only for $\omega \geq \Delta_0$. The plot of the self-consistent defect dynamics shown in the left panel of Fig. 4.10 demonstrates that the defect density is an oscillatory function of ω. The time-averaged defect density is plotted in the right panel of Fig. 4.10 for the self-consistent dynamics shows that these quantities display qualitatively similar behaviour.

4.10 Summary and Discussion

The response of a BCS-paired fermionic superfluid has been studied both for a sudden linear quench and a periodic drive. In our model, the sudden quench has been achieved by

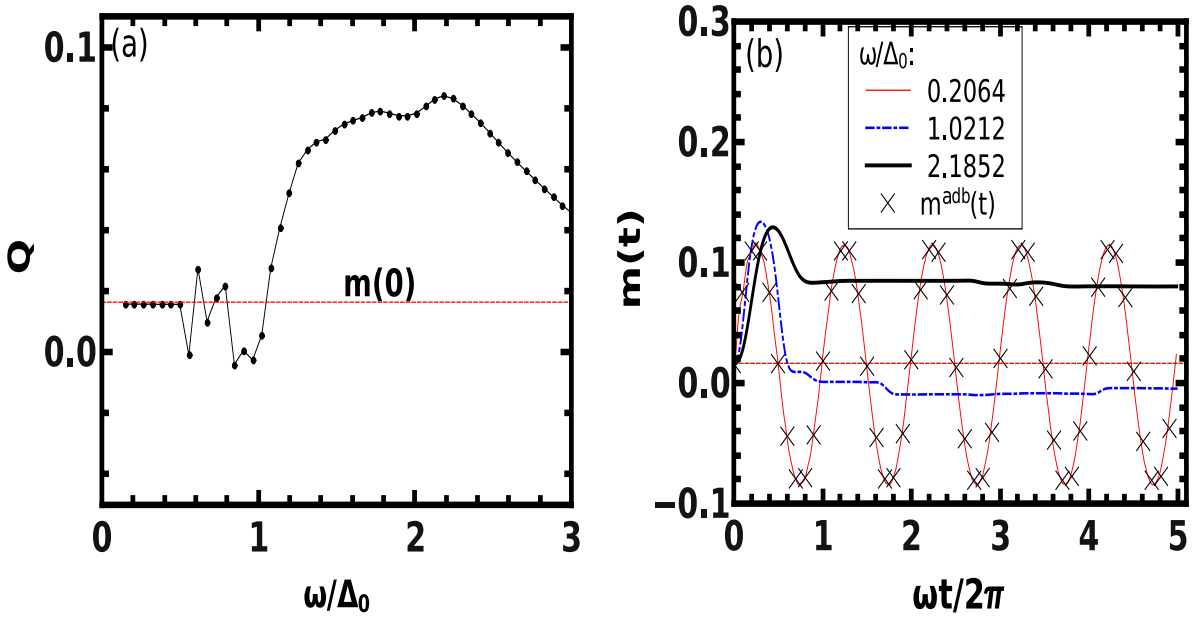

Figure 4.8: Left Panel: Plot of Q as a function of ω with averaging carried over 10 drive cycles. Right panel: Plot of $m(t)$ as a function of $\omega t/2\pi$.

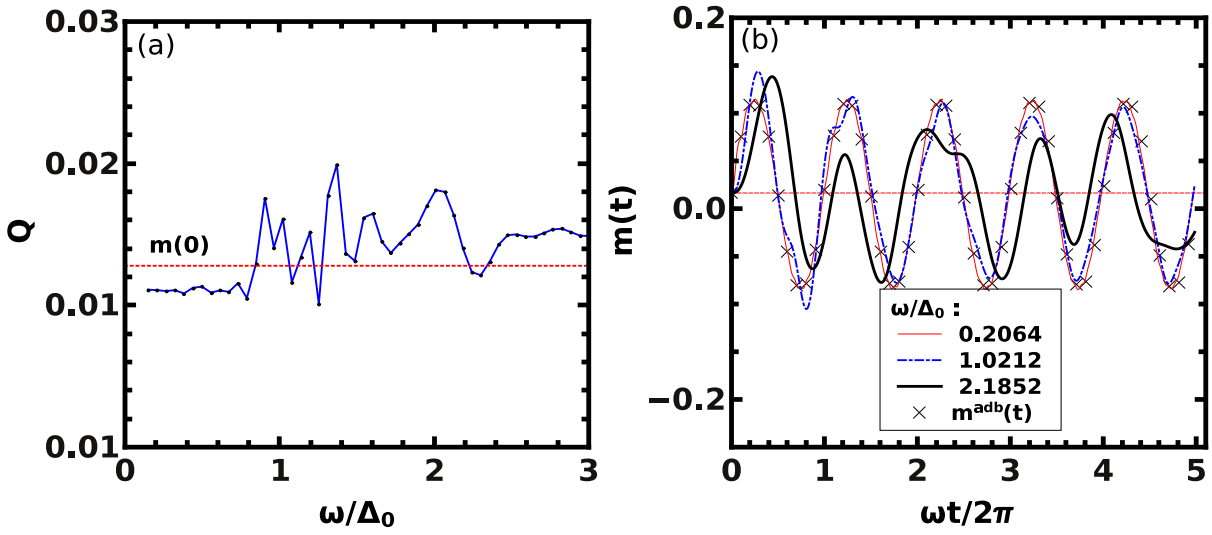

Figure 4.9: Same as in Fig. 4.8 but for the non-self-consistent dynamics.

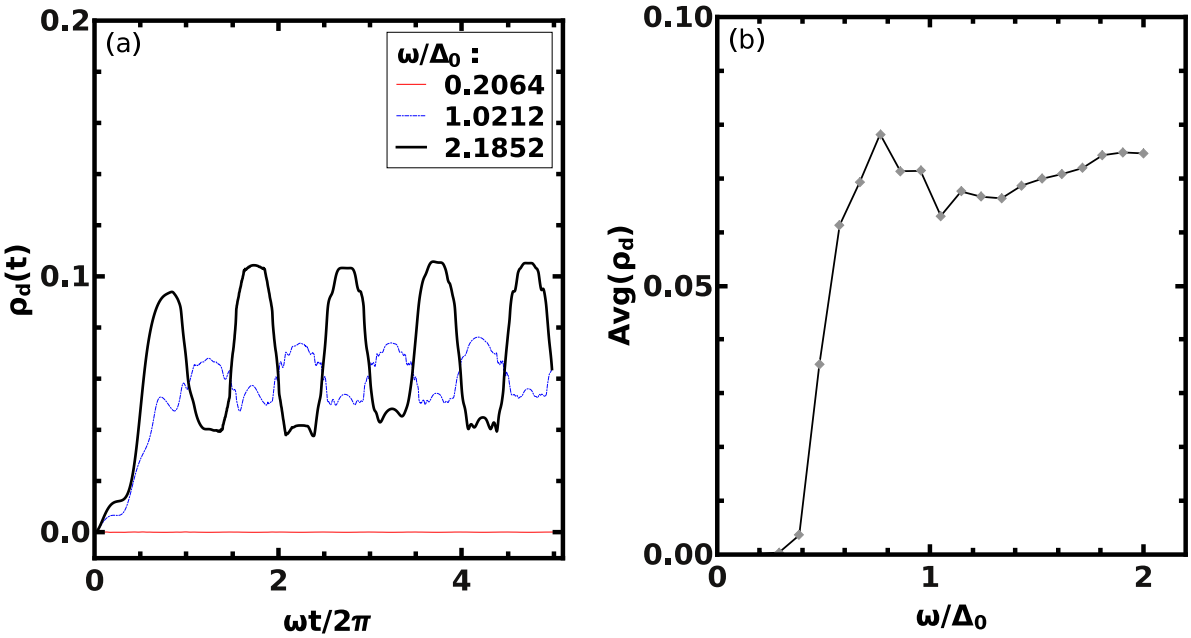

Figure 4.10: Plots of the instantaneous and long time averages of the defect density evaluated BCS fermions in an optical lattice for the self-consistent case.

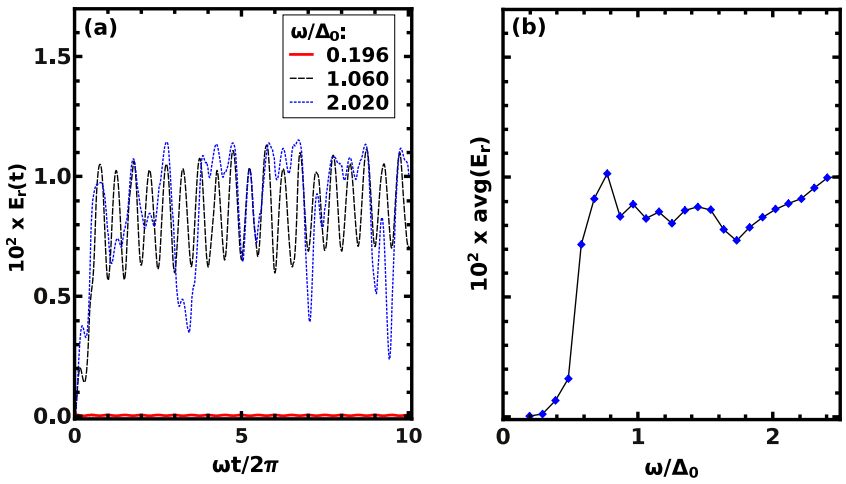

Figure 4.11: Same as fig 4.10 but for the residual energy.

abruptly changing the fermion-fermion coupling by means of Feshbach magnetic field. We observed that just like systems undergoing quantum phase transition (QPT), here also quantities like the fidelity and defect density follow power law equations when plotted against the change in the coupling amplitude.

The periodic quench has been introduced by adding a time-dependent sinusoidal component in the chemical potential. If the self consistency condition in terms of the gap parameter is not used, system responses show an oscillatory nature. However, the condition for self-consistency of the gap parameter introduces a non-linearity in the system, and causes a rapid decay of the response to a stabilized well-defined mean value with very small oscillations around that point. This is true for quantities such as the effective magnetization and defect density. The self-consistency also leads to a time-dependence of Δ. Thus the system remarkably deviates from integrable systems (e.g, Kitaev model, Ising model) which can be described solely by Bogoliubov like Hamiltonians and the self-consistency condition is not needed.

If the time dependence of Δ is ignored or rendered negligible, then the system resembles a decoupled two-level systems (TLS) in momentum space with constant gap for sufficiently low ω. The corresponding dynamics can be described by Landau-Zener-Stückelberg theory. The fact that self-consistency plays a significant role in our model can thus open the door to a modified theory of Landau-Zener tunneling and the Stückelberg phase.

Bibliography

[1] Anatoli Polkovnikov , Phys. Rev. B **72**, 161201(R) (2005).

[2] Diptiman Sen, K. Sengupta, Shreyoshi Mondal, Phys. Rev. Lett. **101**, 016806 (2008).

[3] Shreyoshi Mondal, Diptiman Sen, and K. Sengupta, Phys. Rev. B **78**, 045101 (2008).

[4] A. Polkovnikov, K. Sengupta, A. Silva and M. Vengalat- tore, Rev. Mod. Phys. 83 863 (2011).

[5] M. Greiner, et al., Nature **415**, 39 (2002).

[6] M. Greiner, et al., Nature **419**, 51 (2002).

[7] M. Greiner, et al., Phys. Rev. Lett. **94**, 070403 (2005).

[8] M.W. Zwierlein, et al., Phys. Rev. Lett. **94**, 180401 (2005).

[9] F. Igloi and H. Rieger, Phys. Rev. Lett. **85**, 3233 (2000).

[10] K. Sengupta, et al., Phys. Rev. A **69**, 053616 (2004).

[11] R. W. Cherng and L. S. Levitov, Phys. Rev. A **73**, 043614 (2006).

[12] P. Calabrese and J. Cardy, Phys. Rev. Lett. **96**, 136801 (2006).

[13] M. Rigol, et al., Phys. Rev. Lett. **98**, 050405 (2007).

[14] T. W. B. Kibble, J. Phys. A *9*, 1387 (1976); W. H. Zurek, Nature (London) **317**, 505 (1985).

[15] B. Damski, Phys. Rev. Lett. **95**, 035701 (2005).

[16] Vladimir Gritsev and Anatoli Polkovnikov, arXiv:0910.3692v3

[17] Subir Sachdev,Quantum Phase Transitions, Cambridge University Press,cambridge,1999.

[18] Peter Hnggi in Quantum Transport and Dissipation, edited by Thomas Dittrich et al., Wiley-VCH, Germany, England, 1998.

[19] G. Behinaein, V. Ramareddy, P. Ahmadi, and G.S. Summy, Phys. Rev. Lett. **97**, 244101 (2006).

[20] S. Denisov, L. Morales-Molina, S. Flach, and P. Hnggi, Phys. Rev. A **75**, 063424 (2007).

[21] A. Das, Phys. Rev. B, **82**, 172402 (2010).

[22] S. Bhattacharyya, A. Das and S. Dasgupta, arXiv:1112.6171v1 [quant-phys] (2011).

[23] A. Russomanno, A. Das, A. Silva and G. E. Santoro (in prereration).

[24] F. L. Moore, J. C. Robinson, C. F. Bharucha, Bala Sundaram, and M. G. Raizen, Phys. Rev. Lett. **75**, 4598 (1995).

[25] C. Ryu, M. F. Andersen, A. Vaziri, M. B. d'Arcy, J. M. Grossman, K. Helmerson, and W. D. Phillips, Phys. Rev. Lett. **96**, 160403(2006).)

[26] A.J. Leggett, in Modern Trends in the Theory of Condensed Matter, edited by A. Pekalski and R. Przystawa (Springer- Verlag, Berlin, 1980).

[27] D.M Eagles, Phys. Rev. **186**, 456 (1969).

[28] P. Nozires and S. Schmitt-Rink, J. Low Temp. Phys. **59**, 195 (1985).

[29] M. Randeria in Bose-Einstein Condensation, edited by A. Griffin, D. Snoke, and S. Stringari, Cambridge University Press, Cambridge, England, 1994.

[30] M. W. Zwierlein, C. A. Stan, C. H. Schunck, S. M. F. Raupach, A. J. Kerman, and W. Ketterle, Phys. Rev. Lett. **92**, 120403 (2004).

[31] M. W. Zwierlein, C.H. Schunck, A. Schirotzek, and W. Ketterle, Nature(London) **442**, 54 (2006).

[32] T P Billam and S A Gardiner New J. Phys. **14** 013038 (2012).

[33] Andr Eckardt, Christoph Weiss, and Martin Holthaus, Phys. Rev. Lett.**95**, 260404 (2005).

Chapter 5

Can Dynamics be Used to Probe Population-Imbalanced Fermionic System?

In chapters 1 and 3, we have talked about population imbalanced fermionic systems. In chapter 1, we briefly introduced exotic superfluid phases that result from population imbalance/ asymmetry amongst the two components of a two-species fermionic gas. In chapter 3, we focused on one such particular phase : the 'breached pair state' and discussed its stability criteria.

However, in those chapters, we have only dealt with the static properties of the cold fermionic system. We, of course, had a variable parameter in the form of the Feshbach magnetic field, which allowed the system to shuttle between Bose Einstein condensate and fermionic Cooper pairs. Still, if the magnetic field was kept fixed at a certain value, the system remained at equilibrium. Our analytical treatment never went beyond that.

Dynamical properties are very important aspects of an ultracold atom system. The study of natural and driven dynamics can indeed unveil newer features of a cold quantum gas, and even throw light to some of its static properties as well. Therefore, many physicists chose to study the cold atom systems from the perspective of dynamics. R.A. Barankov et al. discussed the collective nonlinear evolution of BCS state when the pairing interaction is turned on instantaneously [1]. V. A Andreev et al. showed that if the position of the Feshbach resonance is suddenly changed , the superfluid undergoes a coherent BEC-to-BCS oscillation [2]. M. H. Szyman'ska et al. [3] addressed the situation when the Feshbach magnetic field is shifted abruptly. They studied the short time dynamics that followed – damped oscillations with an amplitude depending on the initial conditions. In

this context, they also argued that atom-molecule oscillations are negligibly small and can be ruled out for all practical purposes.

In this chapter, [1] we aim at studying the dynamical properties of a population-imbalanced Fermi gas. Instead of introducing a sudden change in Feshbach magnetic field, we focus on the natural dynamics of the system when a natural fluctuation of Bose Einstein condensate occurs along the BCS-BEC crossover path, and the system tries to relax back to the steady state.

Our results show periodic or quasiperiodic oscillations in the condensate fraction. We find that it is the strength of the Feshbach term that determines whether the oscillation will be periodic or quasi periodic. Moreover, these frequencies of oscillations are found to depend on the nature of pairing in the momentum space. We propose that using this method, the momentum-space structure of the novel pairing states can be mapped. This is very important since such a study turns out to be an efficient handle on the experimental probe of the exotic pairing states.

5.1 Model Hamiltonian and Equations of Motion

Our model resembles the one in chapter 3 and the Hamiltonian is identical to the on used in 3.1. Only, this time we are not considering two arbitrary fermionic atoms, bur either two hyperfine states of the same atom (so that their masses are equal), or two fermions with the same mass. This is for calculational simplicity only.

Our Hamiltonian is :

$$\begin{aligned} H = \sum_{p} \epsilon_{\mathbf{p}} (\psi_{\mathbf{p}\uparrow}^{\dagger}\psi_{\mathbf{p}\uparrow} + \psi_{\text{-}\mathbf{p}\downarrow}^{\dagger}\psi_{\text{-}\mathbf{p}\downarrow}) + g \sum_{\mathbf{p},\mathbf{p}',\mathbf{q}} \psi_{\mathbf{p}+\frac{\mathbf{q}}{2}\uparrow}^{\dagger}\psi_{\text{-}\mathbf{p}+\frac{\mathbf{q}}{2}\downarrow}^{\dagger}\psi_{\text{-}\mathbf{p}'+\frac{\mathbf{q}}{2}\downarrow}\psi_{\mathbf{p}'+\frac{\mathbf{q}}{2}\uparrow} \\ + g_2 \sum_{\mathbf{p},\mathbf{q}} (\psi_{\mathbf{p}+\frac{\mathbf{q}}{2}\uparrow}\psi_{\text{-}\mathbf{p}+\frac{\mathbf{q}}{2}\downarrow}\phi_{\mathbf{q}}^{\dagger} + \psi_{\mathbf{p}+\frac{\mathbf{q}}{2}\uparrow}^{\dagger}\psi_{\text{-}\mathbf{p}+\frac{\mathbf{q}}{2}\downarrow}^{\dagger}\phi_{\mathbf{q}}) + \sum_{\mathbf{q}} (E_{\mathbf{q}} + 2\nu - \mu_B)\phi_{\mathbf{q}}^{\dagger}\phi_{\mathbf{q}} \end{aligned} \tag{5.1}$$

We work in the mean-field framework, and restrict ourselves to the case where only zero-momentum bosons are there. This is because we assume that all the bosons are

[1] The work reported here is based on the paper "Dynamics as a probe for population-imbalanced fermionic systems", Raka Dasgupta and J. K. Bhattacharjee, arXiv:1110.4092v1

formed out of BCS-paired fermions, i.e., the resultant momentum is zero. Later we shall also discuss the effect of having non-zero momentum pairing. With the zero-momentum pairing the Hamiltonian becomes -

$$\begin{aligned} H = \sum_{\mathbf{p}} \epsilon_{\mathbf{p}} (\psi_{\mathbf{p}\uparrow}^{\dagger} \psi_{\mathbf{p}\uparrow} + \psi_{\text{-}\mathbf{p}\downarrow}^{\dagger} \psi_{\text{-}\mathbf{p}\downarrow}) + g \sum_{\mathbf{p},\mathbf{p}'} \psi_{\mathbf{p}'\uparrow}^{\dagger} \psi_{\text{-}\mathbf{p}\downarrow}^{\dagger} \psi_{\text{-}\mathbf{p}'\downarrow} \psi_{\mathbf{p}'\uparrow} \\ + g_2 \sum_{\mathbf{p}} (\psi_{\mathbf{p}\uparrow} \psi_{\text{-}\mathbf{p}\downarrow} \phi^{\dagger} + \psi_{\mathbf{p}'\uparrow}^{\dagger} \psi_{\text{-}\mathbf{p}\downarrow}^{\dagger} \phi) + (2\nu - \mu_B) \phi^{\dagger} \phi \end{aligned} \tag{5.2}$$

For convenience, we split the Hamiltonian into four parts :

$$H_{BCS} = g \sum_{\mathbf{p},\mathbf{p}'} (\langle \psi_{\mathbf{p}'\uparrow}^{\dagger} \psi_{-\mathbf{p}\downarrow}^{\dagger} \rangle \psi_{-\mathbf{p}'\downarrow} \psi_{\mathbf{p}'\uparrow} + \psi_{\mathbf{p}'\uparrow}^{\dagger} \psi_{-\mathbf{p}\downarrow}^{\dagger} \langle \psi_{-\mathbf{p}'\downarrow} \psi_{\mathbf{p}'\uparrow} \rangle) \tag{5.3}$$

$$H_{kin} = \sum_{\mathbf{p}} \epsilon_{\mathbf{p}} (\psi_{\mathbf{p}\uparrow}^{\dagger} \psi_{\mathbf{p}\uparrow} + \psi_{-\mathbf{p}\downarrow}^{\dagger} \psi_{-\mathbf{p}\downarrow}) \tag{5.4}$$

$$H_{\phi\psi} = g_2 \sum_{\mathbf{p}} (\psi_{\mathbf{p}\uparrow} \psi_{-\mathbf{p}\downarrow} \phi^{\dagger} + \psi_{\mathbf{p}'\uparrow}^{\dagger} \psi_{-\mathbf{p}\downarrow}^{\dagger} \phi) \tag{5.5}$$

and

$$H_{\phi} = (2\nu - \mu_B) \phi^{\dagger} \phi \tag{5.6}$$

Next we calculate the commutation relations in order to arrive at the equations of motion. This is in accordance with the Ehrenfest Theorem, which relates the time derivative of the expectation value for a quantum mechanical operator to the commutator of that operator with the Hamiltonian of the system.

$$\begin{aligned} [\psi_{\mathbf{p}\uparrow}, H_{BCS}] = g(- \sum_{\mathbf{p}'} \langle \psi_{\mathbf{p}'\uparrow}^{\dagger} \psi_{-\mathbf{p}'\downarrow}^{\dagger} \rangle \psi_{-\mathbf{p}\downarrow} \psi_{\mathbf{p}\uparrow} \psi_{\mathbf{p}\uparrow} \\ - \sum_{\mathbf{p}'} \langle \psi_{\mathbf{p}'\uparrow}^{\dagger} \psi_{-\mathbf{p}'\downarrow}^{\dagger} \rangle \psi_{-\mathbf{p}\downarrow} \psi_{\mathbf{p}\uparrow} \psi_{\mathbf{p}\uparrow} \\ + \psi_{\mathbf{p}\uparrow} \psi_{\mathbf{p}'\uparrow}^{\dagger} \psi_{-\mathbf{p}\downarrow}^{\dagger} \sum_{\mathbf{p}'} \langle \psi_{-\mathbf{p}'\downarrow} \psi_{\mathbf{p}'\uparrow} \rangle) \\ - \psi_{\mathbf{p}'\uparrow}^{\dagger} \psi_{-\mathbf{p}\downarrow}^{\dagger} \psi_{\mathbf{p}\uparrow} \sum_{\mathbf{p}'} \langle \psi_{-\mathbf{p}'\downarrow} \psi_{\mathbf{p}'\uparrow} \rangle) \\ = g \psi_{-\mathbf{p}\downarrow}^{\dagger} \sum_{\mathbf{p}} \langle \psi_{-\mathbf{p}\downarrow} \psi_{\mathbf{p}\uparrow} \rangle \end{aligned} \tag{5.7}$$

$$\begin{aligned}[\psi_{\mathbf{p}\uparrow}, H_{kin}] &= \epsilon_{\mathbf{p}}(\psi_{\mathbf{p}\uparrow}{\psi_{\mathbf{p}}}^{\dagger}{}_{\uparrow}\psi_{\mathbf{p}\uparrow} - {\psi_{\mathbf{p}}}^{\dagger}{}_{\uparrow}\psi_{p\uparrow}\psi_{p\uparrow}) \\ &= \epsilon_{\mathbf{p}}\psi_{\mathbf{p}\uparrow}\end{aligned} \tag{5.8}$$

$$\begin{aligned}[\psi_{\mathbf{p}\uparrow}, H_{\phi\psi}] &= g_2[\psi_{\mathbf{p}\uparrow}, {\psi_{\mathbf{p}}}^{\dagger}{}_{\uparrow}\psi^{\dagger}_{-\mathbf{p}\downarrow}\phi] \\ &= g_2\psi^{\dagger}_{-\mathbf{p}\downarrow}\phi\end{aligned} \tag{5.9}$$

$$[\phi, H] = g_2\sum_{\mathbf{p}}\langle\psi_{-\mathbf{p}\downarrow}\psi_{\mathbf{p}\uparrow}\rangle + (2\nu - \mu_B)\phi \tag{5.10}$$

Heisenberg operators are introduced as :

$\psi_{H\uparrow}(\mathbf{p}, t) = e^{iHt/\hbar}\psi_{\mathbf{p}\uparrow}e^{-iHt/\hbar}$

$\psi^{\dagger}_{H\downarrow}(-\mathbf{p}, t) = e^{iHt/\hbar}\psi^{\dagger}_{-\mathbf{p}\downarrow}e^{-iHt/\hbar}$

The equations of motion are :

$$\begin{aligned}i\hbar\frac{\partial}{\partial t}\psi_{H\uparrow}(\mathbf{p}, t) &= e^{iHt/\hbar}[\psi_{\mathbf{p}\uparrow}, H]e^{-iHt/\hbar} \\ i\hbar\frac{\partial}{\partial t}\psi^{\dagger}_{H\downarrow}(-\mathbf{p}, t) &= e^{iHt/\hbar}[\psi^{\dagger}_{-\mathbf{p}\downarrow}, H]e^{-iHt/\hbar}\end{aligned} \tag{5.11}$$

$$i\hbar\frac{\partial\psi_{H\uparrow}}{\partial t} = \epsilon_{\mathbf{p}}\psi_{H\uparrow} + g\sum_{\mathbf{p}}\langle\psi_{\mathbf{p}\uparrow}\psi_{-\mathbf{p}\downarrow}\rangle{\psi_{H\downarrow}}^{\dagger} + g_2{\psi_{H\downarrow}}^{\dagger}\phi \tag{5.12}$$

$$i\hbar\frac{\partial{\psi_{H\downarrow}}^{\dagger}}{\partial t} = \epsilon_{\mathbf{p}}{\psi_{H\downarrow}}^{\dagger} + g\sum_{\mathbf{p}}\langle{\psi_{\mathbf{p}\downarrow}}^{\dagger}{\psi_{-\mathbf{p}\uparrow}}^{\dagger}\rangle\psi_{H\uparrow} + g_2\psi_{H\uparrow}\phi^{\dagger} \tag{5.13}$$

5.2 Green's Functions and the Effective Coupling

We define single particle Green's functions in the momentum space.

$$\mathcal{G}(\mathbf{p}t, \mathbf{p}'t') = -\langle[\psi_{H\uparrow}(\mathbf{p}t){\psi_{H\uparrow}}^{\dagger}(\mathbf{p}'t')]\rangle \tag{5.14}$$

$$\mathcal{F}(\mathbf{p}t, \mathbf{p}'t') = -\langle[\psi_{H\uparrow}(\mathbf{p}t)\psi_{H\downarrow}(\mathbf{p}'t')]\rangle \tag{5.15}$$

$$\mathcal{F}^{\dagger}(\mathbf{p}t, \mathbf{p}'t') = -\langle[\psi_{H\downarrow}^{\dagger}(\mathbf{p}t)\psi_{H\uparrow}(\mathbf{p}'t')]\rangle \tag{5.16}$$

Therefore,

$$\begin{aligned} i\hbar\frac{\partial}{\partial t}\mathcal{G}(\mathbf{p}t, \mathbf{p}'t') = \\ -i\hbar\delta(t-t')\langle\psi_{H\uparrow}(\mathbf{p}t){\psi_{H\uparrow}}^{\dagger}(\mathbf{p}'t')\rangle - \langle T[i\hbar\frac{\partial\psi_{H\uparrow}(\mathbf{p}t)}{\partial\tau}{\psi_{H\uparrow}}^{\dagger}(\mathbf{p}'t')]\rangle \\ = -i\hbar\delta(\mathbf{p}-\mathbf{p}')\delta(t-t') + \epsilon_{\mathbf{p}}\langle Tr[{\psi_{H\downarrow}}^{\dagger}{\psi_{H\uparrow}}^{\dagger}]\rangle + g\langle\psi_{\mathbf{p}\uparrow}\psi_{\text{-}\mathbf{p}\downarrow}\rangle\langle Tr[{\psi_{H\downarrow}}^{\dagger}{\psi_{H\uparrow}}^{\dagger}]\rangle + g_2\phi\langle Tr[{\psi_{H\downarrow}}^{\dagger}{\psi_{H\uparrow}}^{\dagger}]\rangle \\ = -(i\hbar(\mathbf{p}-\mathbf{p}')\delta(t-t') + \epsilon_{\mathbf{p}}\mathcal{G}(\mathbf{p}t, \mathbf{p}'t') + g_{eff}\langle\psi_{\mathbf{p}\uparrow}\psi_{\text{-}\mathbf{p}\downarrow}\rangle\mathcal{F}^{\dagger}(\mathbf{p}t, \mathbf{p}'t')) \end{aligned} \tag{5.17}$$

This leads to the usual gap equation [4], provided we replace the BCS-coupling g by g_{eff} where

$$g_{eff}\sum_{\mathbf{p}}\langle\psi_{\mathbf{p}\uparrow}\psi_{-\mathbf{p}\downarrow}\rangle = g\sum_{\mathbf{p}}\langle\psi_{\mathbf{p}\uparrow}\psi_{-\mathbf{p}\downarrow}\rangle + g_2\phi \tag{5.18}$$

5.3 Dynamics of Condensate Order Parameter and Pair Wavefunction

Let us now define the pair wavefunction.

$$O_{\mathbf{p}} = \langle \psi_{H\uparrow} \psi_{H\downarrow} \rangle \tag{5.19}$$

$$\begin{aligned} i\hbar \frac{\partial \psi_{H\uparrow}}{\partial t} \psi_{H\downarrow} &= \epsilon_{\mathbf{p}} \langle \psi_{H\uparrow} \psi_{H\downarrow} \rangle + g N_2 \langle \psi_{\mathbf{p}\uparrow} \psi_{-\mathbf{p}\downarrow} \rangle + g_2 \phi N_2 \\ i\hbar \psi_{H\uparrow} \frac{\partial \psi_{H\downarrow}}{\partial t} &= \epsilon_{\mathbf{p}} \langle \psi_{H\uparrow} \psi_{H\downarrow} \rangle + g(1 - N_1) \langle \psi_{\mathbf{p}\uparrow} \psi_{-\mathbf{p}\downarrow} \rangle - g_2 \phi (1 - N_1) \end{aligned} \tag{5.20}$$

$\langle \psi_{H\uparrow} \psi_{H\downarrow} \rangle$ represents the expectation value of the pair wave function in the Heisenberg picture while $\langle \psi_{\mathbf{p}\uparrow} \psi_{-\mathbf{p}\downarrow} \rangle$ is the same quantity in the Schroedinger's picture. Since these are expectation values, they should not depend on the choice of the representation. So we can denote both $\langle \psi_{H\uparrow} \psi_{H\downarrow} \rangle$ and $\langle \psi_{\mathbf{p}\uparrow} \psi_{-\mathbf{p}\downarrow} \rangle$ by $O_{\mathbf{p}}$. Adding up the two parts of equation 5.20),

$$i\hbar \frac{\partial O_{\mathbf{p}}}{\partial t} = 2\epsilon_{\mathbf{p}} O_{\mathbf{p}} + g \sum_{\mathbf{p}} O_{\mathbf{p}} (N_2 + N_1 - 1) + g_2 \phi (N_2 + N_1 - 1) \tag{5.21}$$

$$\text{Here } N_1 = \langle \psi_{H\uparrow}^{\dagger} \psi_{H\uparrow} \rangle$$
$$\text{and}$$
$$N_2 = \langle \psi_{H\downarrow}^{\dagger} \psi_{H\downarrow} \rangle$$

or,

$$i\hbar \frac{\partial O_{\mathbf{p}}}{\partial t} = 2\epsilon_{\mathbf{p}} O_{\mathbf{p}} + g(N_{\mathbf{p}} - 1) \sum_{\mathbf{p}} O_{\mathbf{p}} + g_2 \phi (N_{\mathbf{p}} - 1) \tag{5.22}$$

Here $N_p = N_1 + N_2$, i.e., the total population corresponding to a particular momentum $\mathbf{p}$.

When both the pairing states are occupied, (e.g, in region of BCS pairing, $N_p = 2$)

$$i\hbar \frac{\partial O_{\mathbf{p}}}{\partial t} = 2\epsilon_{\mathbf{p}} O_{\mathbf{p}} + g \sum_{\mathbf{p}} O_{\mathbf{p}} + g_2 \phi \tag{5.23}$$

As for the evolution of ϕ

$$i\hbar\frac{\partial\phi}{\partial t} = g_2\sum_{\mathbf{p}} O_{\mathbf{p}} + (2\nu - \mu_B)\phi \tag{5.24}$$

A quick comparison with the results obtained by Andreev et al. [2] and Burnett et. al [3] shows that our equations are linearized versions of the evolution equations appeared in [2,3]. It is this linearized approximation which is the relevant part for our calculation. The nonlinear terms are essential only for dynamics following a sudden quench.

5.4 System in Equilibrium:

The first test of the new theory is that, whether we can reproduce previously established results as special cases of the new formalism. So we try to go back to the static case using these dynamical equations.

In the static case,

Let the condensate order parameter be a constant, i.e., $\dfrac{\partial\phi}{\partial t} = 0$

From Equation (5.24),

$$g_2\sum_{\mathbf{p}} O_{\mathbf{p}} = -(2\nu - \mu_B)\phi \tag{5.25}$$

but from equation (5.18),

$$g_{eff}\sum_{\mathbf{p}} O_{\mathbf{p}} = g\sum_{\mathbf{p}} O_{\mathbf{p}} + g_2\phi \tag{5.26}$$

Therefore,

$$g_{eff} = g - \frac{g_2^2}{(2\nu - \mu_B)} \tag{5.27}$$

If the fermion-fermion four point interaction is an attractive one (which is indeed the case for a BCS superfluid), then writing $g = -|g_1|$, we arrive at

$$g_{eff} = g_1 + \frac{g_2^2}{(2\nu - \mu_B)} \tag{5.28}$$

The effective interaction g_{eff} is also taken in the attractive sense. And the result matches with Equation (3.8) in Chapter 3. So, we are able to reproduce the results in chapter 3 by writing down the equations of motion and putting $\frac{\partial \phi}{\partial t} = 0$ therein. In Chapter 3, we followed a variational mean field approach, and had to use a trial form of the ground state of the system. This time, howver, there are no such trial solutions. The Ehrenfest theorem and the commutation relations have directly landed us here, and this treatment is certainly more general.

5.5 System out of Equilibrium : Frequencies of Oscillation

Let, $\tilde{O_{\mathbf{p}}}$ be the fluctuation in $O_{\mathbf{p}}$, and $\tilde{\phi}$ be the fluctuation in ϕ,

$$i\hbar \frac{\partial \tilde{O_{\mathbf{p}}}}{\partial t} = 2\epsilon_{\mathbf{p}}\, \tilde{O_{\mathbf{p}}} + g \sum_{\mathbf{p}} \tilde{O_{\mathbf{p}}} + g_2 \tilde{\phi} \tag{5.29}$$

$$i\hbar \frac{\partial \tilde{\phi}}{\partial t} = g_2 \sum_{\mathbf{p}} \tilde{O_{\mathbf{p}}} + (2\nu - \mu_B)\tilde{\phi} \tag{5.30}$$

We take the respective Fourier transforms

$$\begin{aligned} \phi(t) &= \int \tilde{\phi}(\omega) e^{i\omega t} d\omega \\ O_{\mathbf{p}}(t) &= \int \tilde{O_{\mathbf{p}}}(\omega) e^{i\omega t} d\omega \end{aligned} \tag{5.31}$$

Putting these in Equations (5.29) and (5.30),

$$\begin{aligned} i\omega . i\hbar O_{\mathbf{p}}(\omega) &= 2\epsilon_{\mathbf{p}} O_{\mathbf{p}}(\omega) + g \sum_{\mathbf{p}} O_{\mathbf{p}}(\omega) + g_2 \phi(\omega) \\ O_{\mathbf{p}}(\omega)(2\epsilon_{\mathbf{p}} + \omega\hbar) &= -(g_2\phi(\omega) + g \sum_{\mathbf{p}} O_{\mathbf{p}}(\omega)) \\ O_{\mathbf{p}}(\omega) &= -\frac{g_2\phi(\omega) + g\sum_{\mathbf{p}} O_{\mathbf{p}}(\omega)}{2\epsilon_{\mathbf{p}} + \hbar\omega} \end{aligned} \tag{5.32}$$

So far, the treatment has been general, and the population imbalance has not been taken into account. Now we come to the particular situation where there are two different species of Fermions, or, two hyperfine states of the same atom (for simplicity, we have used $\uparrow$ and $\downarrow$ to denote them): but one has a larger population than the other. In the momentum picture, this corresponds to a specific geometry.

The natural choice is that of a three-shell structure [5–8] : a core comprising paired fermions, an annular region hosting the excess unpaired ones, and an outermost shell consisting of the rest of the paired fermions. Another probable option is a two-shell structure: one consisting of the paired atoms, and another occupied by the remaining unpaired fermions. These two topologically distinct cases have been discussed in depth in [9–11]. Further, it is shown that [12] a population-imbalanced Breached Pair state is stable only for a two-tier configuration.

We shall discuss the dynamics of these two structures in details, and show how one differs from the other.

5.6 Dynamics of the Two-shell Structure

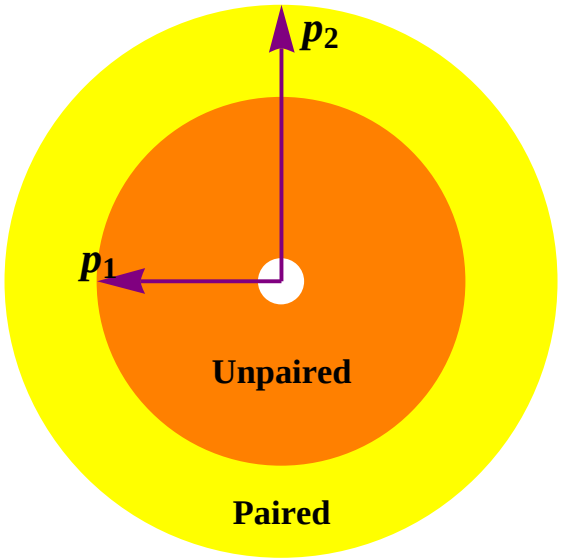

Figure 5.1: Two-shell structure for population-imbalanced fermionic system

In Fig. 5.1, the shell structure in momentum space is depicted. The unpaired majority fermions stay in the core region, which is a normal fluid. The pair superfluid forms the outer shell, from radii p_1 to p_2, where p_1 and p_2 mark the momenta boundaries between which the fermions form BCS-like pairs.

Experimental results obtained by the Ketterle group at MIT [13] is indicative of this structure. They studied a strongly interacting Fermi gas with imbalanced populations, and observed a superfluid region surrounded by a normal gas in the form of a shell structure in the coordinate space. Now, the configuration we described above (unpaired inner region and paired outer shell), when mapped into real space via a Fourier Transformation shows a high density of superfluid in the centre (i.e., the picture obtained by Shin et al. [13]), provided the population imbalance is not too high. Our Fourier space calculation shown that this holds till $p_2 > 1.26p_1$. Now, $\frac{p_1}{p_2}$ is the measure of the population imbalance of the system, and indeed from the experimental results obtained by Shin et al., this core and shell structure survives upto a population imbalance of 75 percent (i.e., when $p_2 > 1.05p_1$). So our calculation matches with their findings within an error margin of 20 percent.

Thus, $O_{\mathbf{p}}(\omega)$ has to be summed over the superfluid region, i.e., over all p from p_1 to p_2.

$$\sum_p O_{\mathbf{p}}(\omega) = -g_2\phi \int_{p_1}^{p_2} \frac{p^2 dp}{(\epsilon_{\mathbf{p}} + \hbar\omega)} - g \sum_{\mathbf{p}} O_{\mathbf{p}}(\omega) \int_{p_1}^{p_2} \frac{p^2 dp}{(\epsilon_p + \hbar\omega)} \tag{5.33}$$

The constant that comes with the density of states is absorbed in g_2 and g. Let p_F be the Fermi momentum of the majority species and M the mass of the atoms.

Let $\int \frac{p^2 dp}{(2\epsilon_p + \hbar\omega)} = u(p)$

Now,

$$\begin{aligned} 2\epsilon_p &= 2(\frac{p^2}{2M} - \frac{{p_F}^2}{2M}) \\ &= ((p_F + (p - p_F))^2 - p_F^2)/M \\ &2\frac{p_F}{M}(p - p_F) \\ &= \frac{2p_F p}{M} - \frac{2p_F^2}{M} \end{aligned} \tag{5.34}$$

Therefore,

$2\epsilon_p + \omega\hbar = ap + b$

where $a = \frac{2p_F}{M}$, $b = -\frac{2p_F^2}{M} + \omega\hbar$

$$\begin{aligned} &\int \frac{p^2 dp}{ap + b} \\ &= \frac{1}{a}\int \frac{p^2 dp}{p + b/a} \\ &= \frac{1}{a}\int \frac{((p + \frac{b}{a})^2 - \frac{b^2}{a^2} - 2p\frac{b}{a})dp}{p + b/a} \\ &= \frac{1}{a}[\int (p + \frac{b}{a})d(p + \frac{b}{a}) - \frac{b^2}{a^2}\int \frac{d(p + \frac{b}{a})}{(p + \frac{b}{a})} - \frac{2b}{a}\int \frac{pd((p + \frac{b}{a})}{(p + \frac{b}{a})}] \\ &= \frac{1}{a}[\frac{(p + \frac{b}{a})^2}{2} - \frac{b^2}{a^2}ln(p + \frac{b}{a}) - \frac{2b}{a}(\int \frac{(p + \frac{b}{a})d(p + \frac{b}{a})}{(p + \frac{b}{a})} - \frac{b}{a}\int \frac{d(p + \frac{b}{a})}{(p + \frac{b}{a})})] \\ &= \frac{1}{a}[\frac{(p + \frac{b}{a})^2}{2} - \frac{b^2}{a^2}ln(p + \frac{b}{a}) - \frac{2b}{a}(p + \frac{b}{a}) + \frac{2b^2}{a^2}ln(p + \frac{b}{a})] \\ &= \frac{1}{a}[\frac{(p + \frac{b}{a})^2}{2} - \frac{2b}{a}(p + \frac{b}{a}) + \frac{b^2}{a^2}ln(p + \frac{b}{a})] \\ &= u(p) \end{aligned} \tag{5.35}$$

Putting in the limits of integration, and using equation (5.31), we have

$\sum_p O_p(\omega) = -g_2\phi(\omega)\frac{u(p_2) - u(p_1)}{1 + g(u(p_2) - u(p_1))}$

Putting back in Eq(5.30), we obtain

$\phi(\omega)[(2\nu - \mu_B) + \hbar\omega - g_2^2 f(p_1, p_2, \omega)] = 0$, where $f(p_1, p_2, \omega) = \frac{u(p_2) - u(p_1)}{1 + g(u(p_2) - u(p_1))}$

Which means, $\phi(\omega)$ is zero if $[(2\nu - \mu_B) + \hbar\omega - g_2^2 f(p_1, p_2, \omega)] \neq 0$. Therefore, in the expansion of $\phi(t)$, only those $\phi(\omega)$s will survive for which

$$(2\nu - \mu_B) + \hbar\omega - g_2^2 f(p_1, p_2, \omega) = 0 \tag{5.36}$$

Therefore, $\phi(t) = \phi_1 e^{i\omega_1 t} + \phi_2 e^{i\omega_2 t} + ...$

Here ω_1, ω_2 .. are the solutions of equation (5.36).

$\omega\hbar = g_2^2(f(p_2) - f(p_1)) - (2\nu - \mu_B)$

To find out whether there exists real values for ω, we take resort to graphical solutions. We are only interested in real ω, because that would give us solutions in the form of $\phi(t) = \phi e^{i\omega t}$, which denotes oscillation. If, on the other hand, we get imaginary solutions for ω, then the solutions are of the form $\phi(t) = \phi e^{\omega t}$ or $\phi(t) = \phi e^{-i\omega t}$. The first one signifies an exponential growth in ϕ and is, therefore, unphysical. The second one marks exponential decay, and its effect should be negligible as time increases. So we look out for real solutions only.

From equation (5.36), the roots of ω are given by $\omega = f1(\omega)$, where $f1(\omega) = g_2^2 f(p_1, p_2, \omega) - (2\nu - \mu_B)$ for a fixed set of p_1 and p_2. So we plot ω along X-axis and both $f1(\omega)$ and ω along Y-axis. The blue lines (curved lines) correspond to $f1(\omega)$ and the red lines (straight lines) mark ω. An intersection of the two lines correspond to a real solution of the equation.

We scale all energies by the Fermi energy E_F, and all momenta by the Fermi momentum p_F of the majority species. Therefore, in this convention, mass of each partcle gets fixed at 0.5.

The BCS pairing takes place near the Fermi surface,within a cut-off region. For standard superconductors, this cut-off is $\hbar\omega_D$, ω_D being the Debye frequency. For Ultracold atoms, the cut-off is $\frac{4}{e^2}E_F$=$0.541E_F$ [14]. Here e is the base of natural logarithms. Since we have scaled all energies by E_F, Fermi level corresponds to 1, and the lower cut-off is at $1 - 0.541 = 0.459$. Thus we have to choose p_1 to lie between 0.459 and 1. We take p_2 to be 1, the Fermi momentum.

Deep inside the Fermi surface the occupation number $v_p^2 = 1$, as shown in Fig. 5.6. The dotted region marks the momentum span over which the unpaired fermions reside.

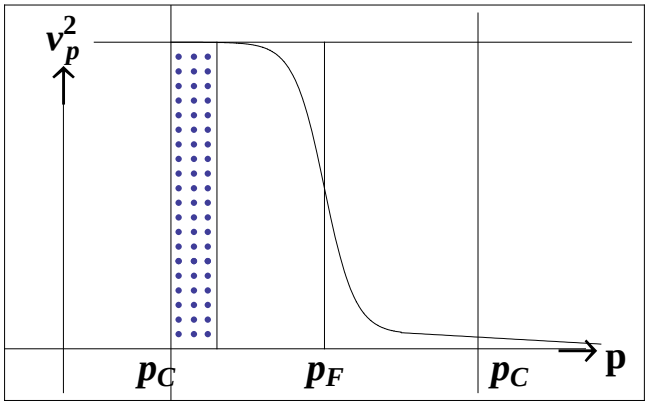

Figure 5.2: Plot of occupation probability $v_{\mathbf{p}}^2$ vs. momentum p for the two-shell structure

Although the outer shell actually extends to infinity, v_p^2 decreases sharply to zero following a power law as a function of momentum p, and its magnitude becomes very small after crossing the Fermi momentum. Therefore, instead of taking p upto infinity with this form of v_p, we can approximate the system by using a cut-off, and taking $v_p^2 = 1$ within it. The justification of such an approximation is evident from the following example: if the superfluid gap $\Delta = 0.4$ (scaled by the Fermi energy) and ${v_p}^2 = \frac{1}{2}(1 - \frac{\epsilon_p}{\sqrt{\epsilon_p^2+\Delta^2}})$ (as in BCS theory) near the Fermi surface (say, from $\epsilon = 0.8$ onwards), then $\int_{0.8}^{\infty} g(\epsilon) v_p^2 d\epsilon$ becomes almost equal to $\int_{0.8}^{1} g(\epsilon) d\epsilon$ where $g(\epsilon)$ is the density of states proportional to $\epsilon^{1/2}$. Therefore, we can safely take the cut-off at the Fermi surface and $v_{\mathbf{p}}^2 = 1$ within it.

Dependence on g_2 when the Imbalance is Fixed:

We take $p_1 = 0.5$, $p_2 = 1$ and $(2\nu - \mu_B)$ at 0.03. From Fig. 5.3, we see that when g_2 is 0.1, there is only one point where $f1(\omega)$ and ω intersect one another, i.e., there exists only one real solution for ω. A single solution exists for $g_2 = 1$ as well. As this coupling is increased slightly, at $g_2 = 1.7$, there appears two such points, i.e., two real ω's. Then, as g_2 goes to higher values, there are always two real solutions for ω .

So we can call $g_2 = 1.7$ a critical coupling. If g_2 is less than this coupling value, there is only one real frequency of oscillation in $\tilde{\phi}(t)$. Beyond it, there are two frequencies.

When g_2 is Fixed and the population imbalance is Varied:

Here, with p_2 fixed at 1, $(2\nu - \mu_B)$ at 0.03, we vary p_1, which measures the amount of imbalance, because it is up to a momentum p_1 that the majority fermions remain

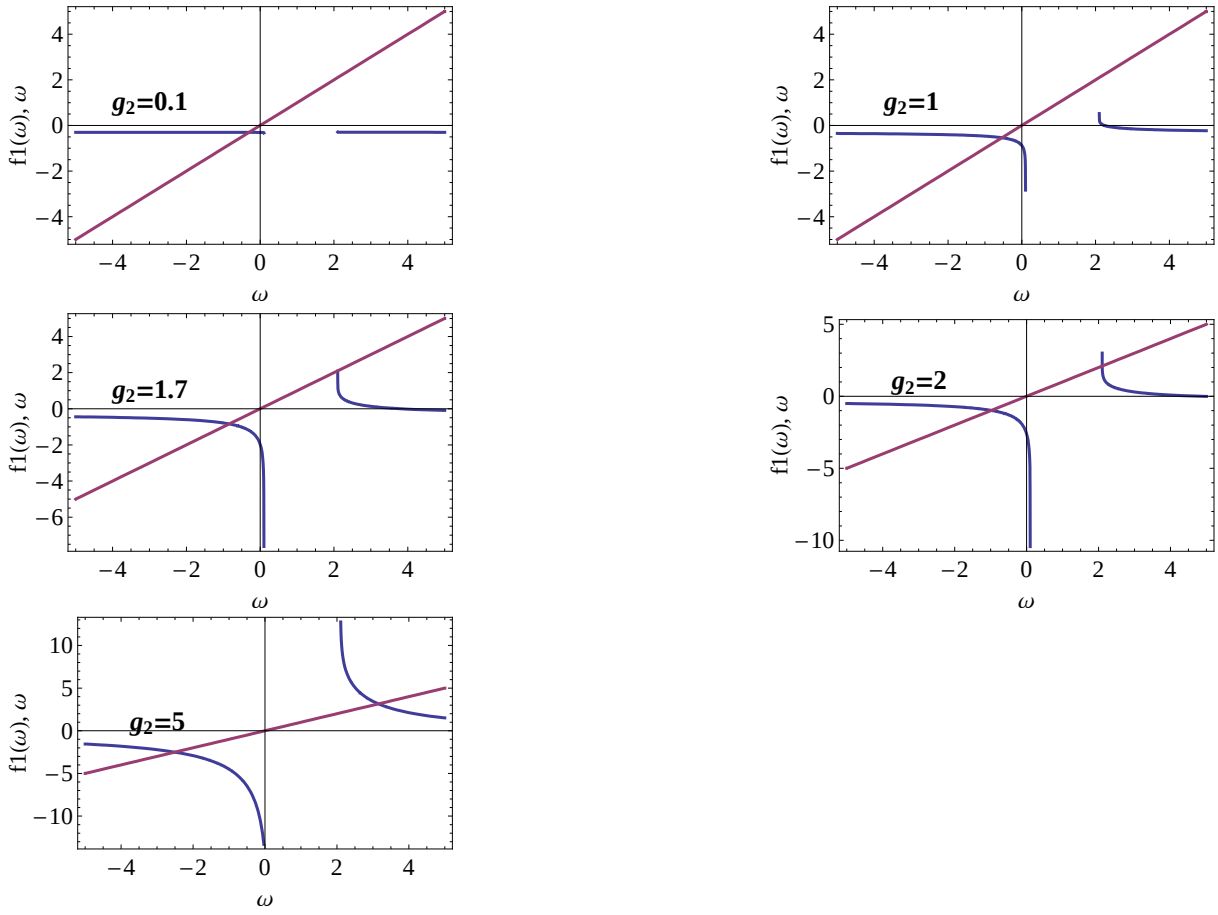

Figure 5.3: Variation of $f1(\omega)$ with ω and solutions for $f1(\omega) = \omega$ for different values of g_2

unpaired.

In Fig. 5.4 we observe that when the population imbalance is very low (p_1 is 0.5, i.e., a value slightly higher than the lower cut-off for pairing), the double frequency region appears at $g_2 = 1.7$. As the imbalance is increased gradually, the value of the critical coupling decreases.

Thus, the fluctuation in ϕ can undergo oscillations with one or two frequencies, depending on the value of g_2.

In Case 1, $\tilde{\phi}(t) = \phi_1 e^{i\omega_1 t}$, or, $\phi(t) = \phi_0 + \phi_1 e^{i\omega_1 t}$

In Case 2, $\tilde{\phi}(t) = \phi_1 e^{i\omega_1 t} + \phi_2 e^{i\omega_2 t}$, or, $\phi(t) = \phi_0 + \phi_1 e^{i\omega_1 t} + \phi_2 e^{i\omega_2 t}$

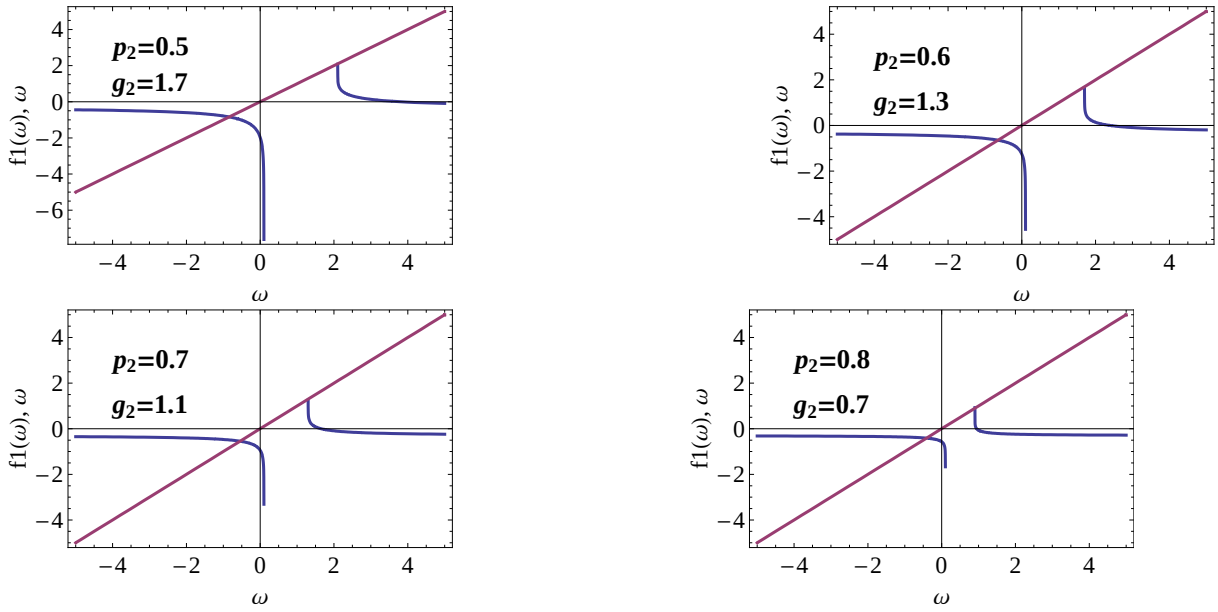

Figure 5.4: Variation of $f1(\omega)$ with ω and critical coupling for different values of population imbalance.

5.7 Dynamics of the Three-shell Structure

Here the pairing takes place in two regions: from p_1 to p_2 and from p_3 to p_4. We take $p_1 = .46$ (the lower cut-off), $p_2 = .80$, $p_3 = .84$ and $p_4 = 1$ (Fermi momentum). The pairing is breached between p_2 and p_3 and this annular region hosts the unpaired fermions.

As before, we plot ω along X-axis and both $f1(\omega)$ and ω along Y-axis to get the real solutions. In this case, $f1(\omega) = g_2^2(f'(p_3, p_4, \omega)) + f'(p_1, p_2, \omega)) - (2\nu - \mu_B)$ for a definite set of p_1, p_2, p_3 and p_4.

Fig. 5.6 shows the behaviour of occupation number $v_{\mathbf{p}}^2$. In this case, too, we can approximate the system by considering the pairing to take place strictly within the cut-off, and taking $v_{\mathbf{p}}^2 = 1$. The dotted area represents the region containing excess majority fermions.

We find, as before, that when the value of g_2 is small, there is a single frequency of oscillation. At some higher value of g_2, there are two frequencies. And beyond a certain coupling, the system oscillates with three frequencies.

Thus, for a particular system, whether the actual structure is a two-shell or a three-

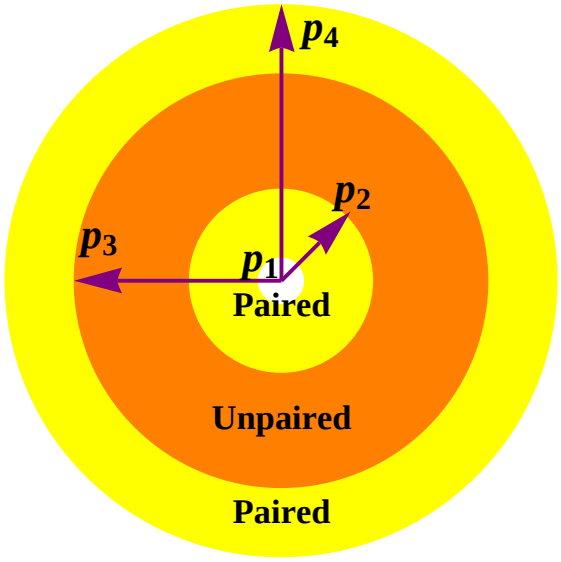

Figure 5.5: Three-shell structure for population-imbalanced system

shell one can be found out by noting the maximum number of frequencies that the system can generate : for a three-shell configuration it is three, and for a two-shell configuration it is two.

5.8 Probing by an Oscillatory Drive

Let us add a small oscillatory component to the Feshbach magnetic field H, so that it becomes $H(1+\epsilon e^{i\Omega t})$.Here $\epsilon << 1$. This is equivalent to replacing the factor $(2\nu - \mu_B)$ by $(2\nu - \mu_B)(1+\epsilon e^{i\Omega t})$. We can make a perturbative expansions: $\tilde{\phi}(t) = \phi^0 + \epsilon\phi'$ and $\tilde{O}_{\mathbf{p}}(t) = {O_{\mathbf{p}}}^0 + \epsilon {O_{\mathbf{p}}}'$

Where ϕ^0 and ${O_{\mathbf{p}}}^0$ are the values of $\tilde{\phi}(t)$ and $\tilde{O}_{\mathbf{p}}(t)$ when there is no oscillatory part in the coupling.

$$\begin{aligned} i\hbar\frac{\partial({O_{\mathbf{p}}}^0 + \epsilon {O_{\mathbf{p}}}')}{\partial t} &= \epsilon_{\mathbf{p}}({O_{\mathbf{p}}}^0 + \epsilon {O_{\mathbf{p}}}') + g\sum_{\mathbf{p}}({O_{\mathbf{p}}}^0 + \epsilon {O_{\mathbf{p}}}') + g_2(\phi^0 + \epsilon\phi') \\ i\hbar\frac{\partial(\phi^0 + \epsilon\phi')}{\partial t} &= g_2\sum_{\mathbf{p}}({O_p}^0 + \epsilon {O_p}') + (2\nu - \mu_B)(1+\epsilon e^{i\Omega t})(\phi^0 + \epsilon\phi') \end{aligned} \tag{5.37}$$

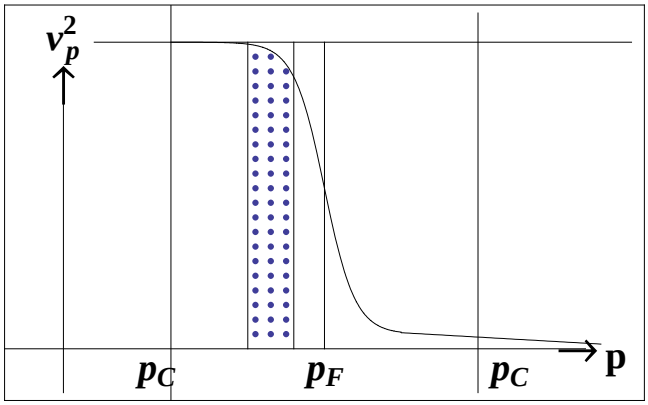

Figure 5.6: Plot of occupation probability v_p^2 vs. momentum p for the three-shell structure

Noting that $\phi^0 = \phi_1 e^{i\omega_1 t}$, it follows that

$$\begin{aligned} i\hbar\frac{\partial O_{\mathbf{p}}{}'}{\partial t} &= \epsilon_{\mathbf{p}} O_{\mathbf{p}}{}' + g\sum_{\mathbf{p}} O_{\mathbf{p}}{}' + g_2\phi' \\ i\hbar\frac{\partial \phi'}{\partial t} &= g_2\sum_{\mathbf{p}} O_{\mathbf{p}}{}' + (2\nu - \mu_B)\phi' + (2\nu - \mu_B)\phi_1 e^{i(\Omega+\omega_1)t} \end{aligned} \tag{5.38}$$

Taking Fourier Transforms as before, we find that $\phi'(\omega)$ is non-zero only when $\omega = \omega_1 + \Omega$ and its value at that particular frequency is

$$\phi'(\omega) = \frac{-(2\nu - \mu_B)\phi_1 2\pi}{\hbar(\Omega + \omega_1) - g_2^2 f1(\omega_1 + \Omega))} \tag{5.39}$$

There is a resonance when the denominator becomes zero, i.e., $\hbar(\Omega + \omega_1) - g_2^2 f1(\omega_1 + \Omega) = 0$. But we know, $\hbar\omega_1 - g_2^2 f1(\omega_1) = 0$. Subtracting,

$$\hbar\Omega + g_2^2(f1(\omega_1) - f1(\omega_1 + \Omega)) = 0 \tag{5.40}$$

Since Ω is associated with the Feshbach resonance, by tuning the frequency of the time-dependent magnetic field, we can control Ω. If, for a particular Ω the above equation is satisfied, then we have a sharp resonance in the fluctuation is ϕ.

If, $\phi^0 = \phi_1 e^{i\omega_1 t} + \phi_2 e^{i\omega_2 t}$, following the same treatment, we can say that resonance will take place when Ω satisfies either of the equations:

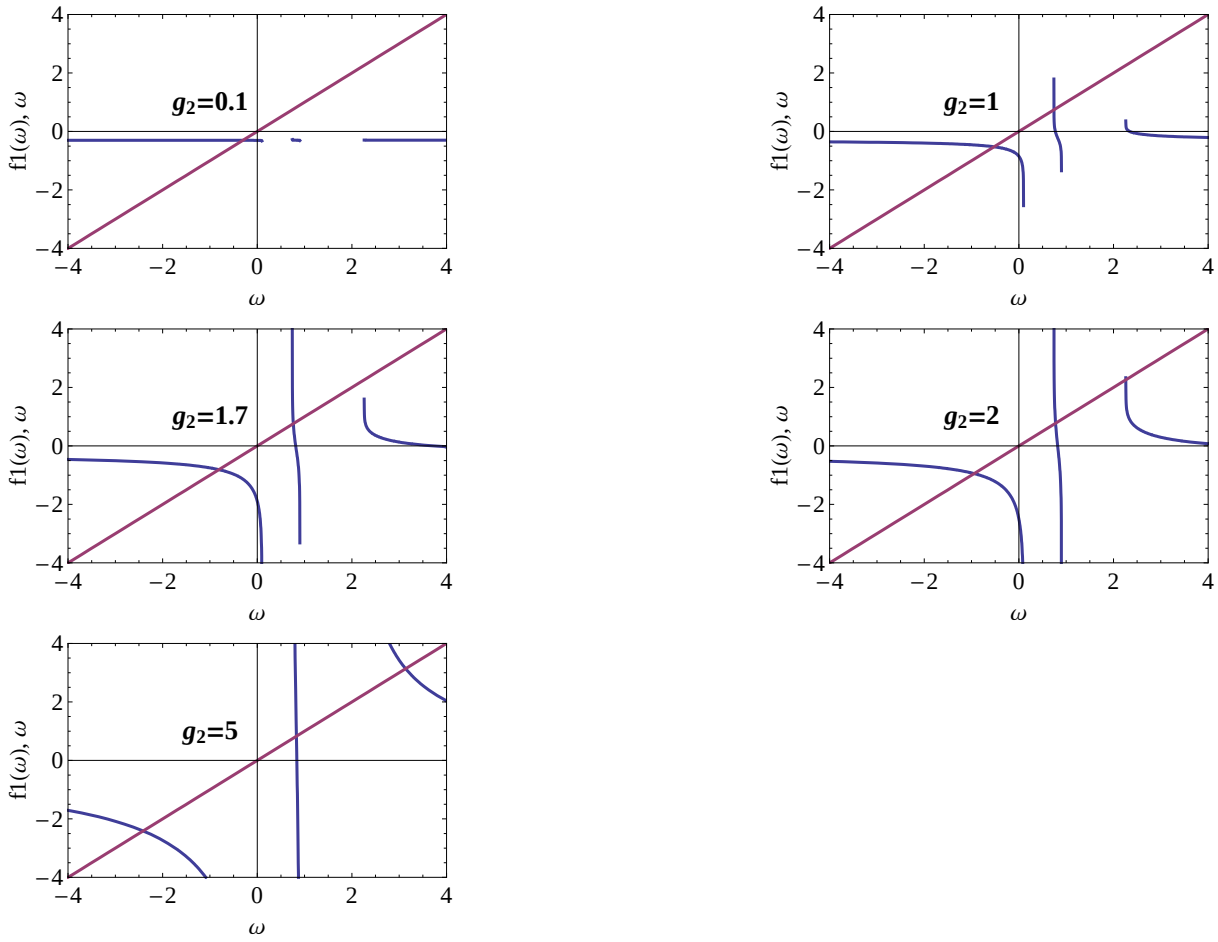

Figure 5.7: Variation of $f1(\omega)$ with ω and solutions for $f1(\omega) = \omega$ for different values of g_2 for the three-shell structure

$$\begin{aligned} \hbar\Omega + g_2^2(f1(\omega_1) - f1(\omega_1 + \Omega)) = 0 \\ \hbar\Omega + g_2^2(f1(\omega_2) - f1(\omega_2 + \Omega)) = 0 \end{aligned} \tag{5.41}$$

It is obvious that $\Omega = 0$ is a trivial solution of the equations. Again we take resort to graphical solutions to find out whether non-zero real solutions exist for Ω.

If there are 3 frequencies of oscillation, there is one additional equation:

$$\hbar\Omega + g_2^2(f1(\omega_3) - f1(\omega_3 + \Omega)) = 0 \tag{5.42}$$

Let $(f1(\omega_1) - f1(\omega + \Omega)) = f'(\Omega)$

We plot Ω along X-axis and both $f'(\Omega)$ and Ω along Y-axis. The blue lines(curved lines) correspond to $f'(\Omega)$ and the red lines (straight lines) mark Ω. As before, the solutions correspond to their intersections.

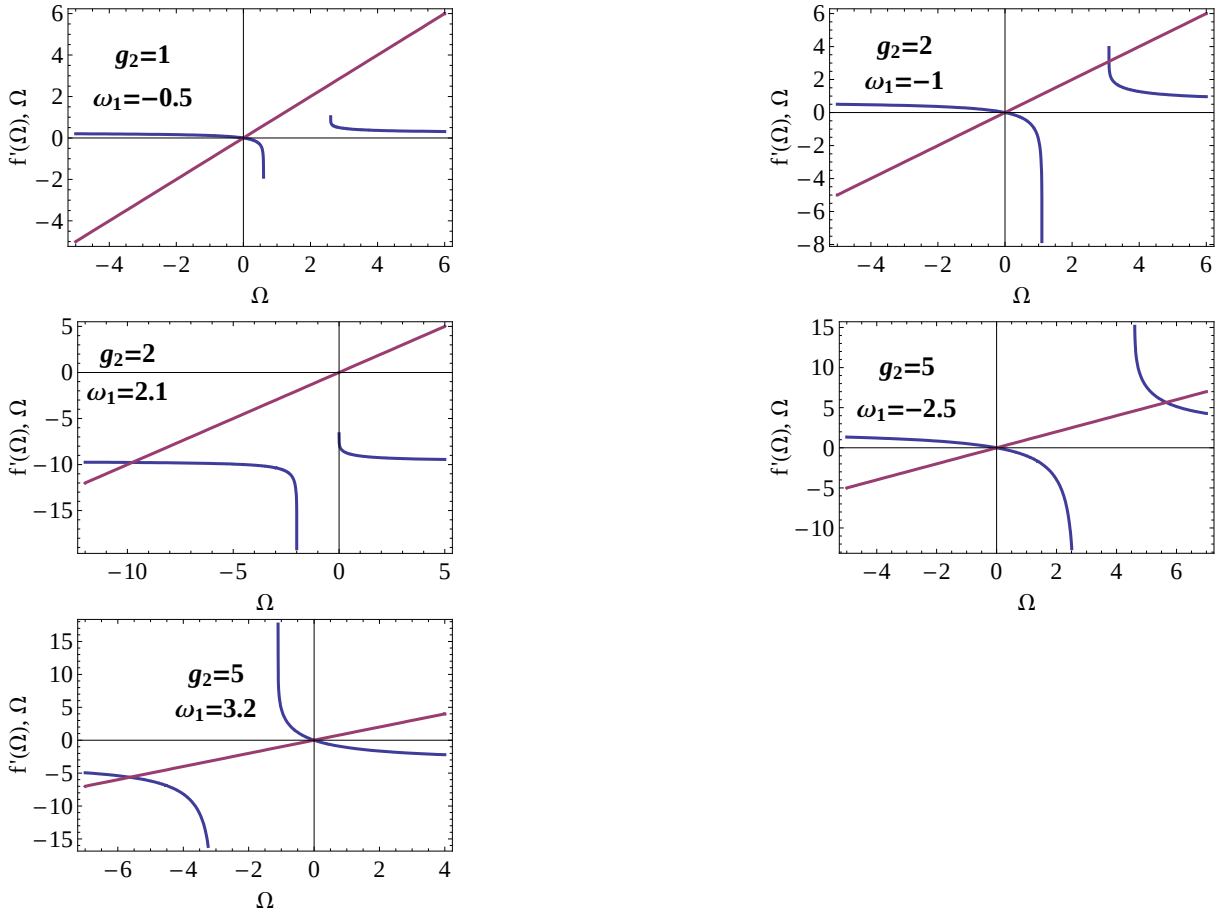

Figure 5.8: Variation of $f'(\Omega)$ with Ω and solutions for $f'(\Omega) = \Omega$ for different values of g_2 and corresponding ω.

Experimentally one can detect the oscillation frequencies. We have already noted that if an oscillatory component is added to the Feshbach coupling, and its frequency is tuned, then at a particular frequency there is a sharp resonance in the condensate fraction. We propose an algorithm for determining the imbalance: for a two-shell configuration choose a p_1 (p_2 is set to 1 because at zero temperature it is the Fermi momentum of the majority species, by which all momenta are scaled) so that the numerically computed oscillation

frequencies match with those obtained in the experiment. Then use those frequencies and the external resonant frequency to calculate p_1. If this doesn't match with the initial p_1, use the new values as input for the first step. Iterating the process a number of times, one should arrive at the actual value of the breaching point, or the point which marks the separation of the two phases in the momentum space.

The same algorithm can be applied to the three-shell configuration as well, but then one has to provide initial estimates for p_2 and p_3 separately. Whether the structure is a two-shell or a three-shell one can be found by noting the number of maximum frequencies that the system can generate.

5.9 Summary and Discussion

Here we have studied the natural dynamics of a population-imbalanced two-species fermionic system. The system is capable of making a BCS-BEC crossover, and form Bose condensate via Feshbach resonance. We have shown that the fluctuation in the condensate fraction displays a periodic or a quasi periodic oscillation, depending on the value of the Feshbach coupling. There is a critical coupling below which the oscillation is always periodic, and its value depends on the population imbalance. When the coupling exceeds this critical value, two frequencies of oscillations appear in the system.

We have shown that if there is an additional oscillatory component is present in the Feshbach term, one can achieve a sharp resonance in the condensate fraction by tuning the frequency of the external magnetic field. The breached momentum region can be calculated from this frequency value. Thus it proves to be an indirect method of experimentally determining the momentum space structure of the imbalanced Fermi system. If we remember how difficult it is to detect these novel phases experimentally, and how much problematic it would be to resolve their momentum space structures, we can understand the importance and the promise such an indirect method holds.

This treatment can be extended to detect more complicated structures in the momentum space, too. In case the bosons have a non-zero momentum pairing as in (Eq. 5.1), the same method can be used to study the system. Only, the sum of the squares of the additional momenta will enter the denominator $2\epsilon_{\mathbf{p}} + \hbar\omega$ in the expression of $\sum_{\mathbf{p}} O_{\mathbf{p}}(\omega)$

(Eq. 5.33), and that will result in a shift in the position of the resonant frequencies. The FFLO state, which arises due do finite momentum pairing thus can also get reflected in a similar dynamical study.

Bibliography

[1] R. A. Barankov, L. S. Levitov, and B. Z. Spivak , Phys. Rev. Lett. **93**, 160401 (2004).

[2] A. V. Andreev, V. Gurarie, and L. Radzihovsky, Phys. Rev. Lett. **93**, 130402 (2004).

[3] M. H. Szyman'ska, B. D. Simons, and K. Burnett, Phys. Rev. Lett. **94**,170402 (2005).

[4] A. L. Fetter and J. D. Walecka, Quantum Theory of Many-Particle Systems, Dover Publications, New York, 2003.

[5] P. F. Bedaque, H. Caldas, and G. Rupak, Phys. Rev. Lett. **91**, 247002 (2003).

[6] S-T. Wu and S. Yip, Phys. Rev. A **67**, 053603 (2003).

[7] Bimalendu Deb, Amruta Mishra, Hiranmaya Mishra, and Prasanta K. Panigrahi, Phys. Rev. A **70**, 011604(R)

[8] H. Caldas, C.W. Morais and A.L. Mota, Phys. Rev. D **72**, 045008 (2005)

[9] M. Iskin and C. A. R. S de Melo, Phys. Rev. Lett. **97**, 100404 (2006).

[10] M. Iskin and C. A. R. S de Melo , Phys. Rev. A **76**, 013601 (2007).

[11] W. Yi and L.-M. Duan, Phys. Rev. Lett. **97**, 120401 (2006).

[12] R. Dasgupta, Phys. Rev. A **80**, 063623 (2009).

[13] Y. Shin, M. W. Zwierlein, C. H. Schunck, A. Schirotzek, and W. Ketterle, Phys. Rev. Lett.**97**, 030401 (2006).

[14] C. J. Pethick and H. Smith, Bose-Einstein Condensation in Dilute Gases, Cambridge Univ. Press 2002.

Chapter 6

Conclusions and Future prospects

In this Chapter, we shall summarize this thesis by highlighting our important findings and also discuss the future prospects of our study.

Our aim was to investigate some of the the static and dynamic properties of ultracold atom systems, in the light of "pairing" and "condensation" phenomena in cold quantum gases. Here the simplest form of "pairing" was the Cooper pairing as in the BCS theory. We also considered exotic pairing states that can take place in population-imbalanced systems. By "condensation" we mostly implied the Bose Einstein condensation (BEC). The fact that the cold atom system can shuttle between BCS end and BEC as the coupling is varied played a key role in our research.

In the following section, we briefly describe our journey: the questions we addressed, the methods that were employed and the results obtained.

6.1 Concluding Remarks

In Chapter 1 we have presented an overview of the novel features of ultracold quantum gases. We have given an account of the existing theories and experimental achievements in this field, that served as the motivation for our work. We have discussed BCS-superfluidity and Bose-Einstein Condensation (BEC), and shown how they are connected via a single phenomenon : "BCS-BEC Crossover". We have also talked about population-imbalanced fermions and the novel pairing states that can arise from such an imbalance. The importance of dynamical studies of ultracold atom systems was underlined as well.

Chapter 2 concerned the effect of three-body scattering processes on BCS-BEC Crossover. We started with a two-species ultracold Fermi gas, where there are either two different fermionic atoms (e.g., ^{6}Li and ^{40}K), or two hyperfine states of the same fermion (e.g., states $|F = 1/2, m_F = 1/2\rangle$ and $|F = 1/2, m_F = -1/2\rangle$ of ^{6}Li atoms). The fermions pair up in the standard BCS fashion. Now, if the coupling between the fermions is increased via the Feshbach magnetic field, the Cooper-paired fermions tend to come closer in the real space and start to form bosonic molecules. Our assumption was that, in addition to the fermion-fermion two-body interaction, there is a three-body interaction as well in the form of boson-Cooper pair scattering. This interaction becomes important near resonance as all cooper pairs do not get converted into tightly bound molecules at the same time : Cooper pairs and molecules can coexist at that point. Our motivation was to find out if this additional interaction can bring any qualitative change in the crossover picture. We have shown that if the newly formed molecules scatter the fermion-fermion pairs, a variational mean-field calculation leads to multiple crossover routes, including the usual one. The system now has the option to follow either of these paths. We plotted the energy surface to find out which amongst these crossover routes corresponds to the minimum of energy and hence is more probable. We observed that if the two-body interaction is attractive, then irrespective of whether the three-body interaction is attractive or repulsive, the crossover process becomes a non-reversible one. Starting from a stable BEC system the BCS state can be reached via Feshbach resonance, but the path cannot be reversed : a start from the BCS side can only end up in an alternative route that represents metastable BEC state (and not the stable one).

In Chapter 3, we discuss exotic superfluid states in a population-imbalanced two-species ultracold Fermi gas. The thrust is on the "Breached Pair state" or "Sarma Phase", a special kind of novel superfluid state that accommodates the excess unpaired fermions in a region where pairing is "breached". Thus, there are both gapped and gapless zones in the momentum-space. It is known that for weak coupling BCS theory, this gapless breached pair state marks the maximum of the thermodynamic potential, and thus, cannot be the stable ground state of the system. This is the well-known Sarma instability. We wanted to find out whether there is a region of stability if the entire BCS-BEC crossover path is considered, and to identify the conditions for stability. From the criterion that the

superfluid density must be positive, we showed that the breached state is stable only when the chemical potentials of the two species bear opposite signs. Solving the gap equation and the number equation, we arrived at analytical expression for the Feshbach magnetic field that serve as the boundary values for the stable region. We used data obtained in experiments with population-mismatched fermions to obtain the exact values of the magnetic field for a typical experiment with unequal mixture of two spin states of ^{6}Li atoms. The conclusion was : the breached pair state can become stable only in a narrow window near the resonance on the BEC side.

The first part of Chapter 4 focuses on sudden quench Dynamics in a BCS-paired ultracold atom system. We started with a superfluid in the BCS regime. The four-point coupling can be tuned via Feshbach resonance. The coupling is abruptly changed, and then the subsequent evolution is controlled by the final Hamiltonian which also a BCS one. We observed that quantities characteristic of this quench like the fidelity susceptibility and defect density follow power law equations when plotted against the change in the coupling amplitude. In the remaining part of this chapter we addressed periodic quench, as the chemical potential has a sinusoidal time dependent part. The condition for self-consistency of the gap parameter invokes a nonlinearity in the system. We studied the evolution of the effective magnetization and defect density. It was found that nonlinear coupling results in a rapid decay of the response to a stabilized well-defined mean value with very small oscillations around that point.

In Chapter 5, we reported our work on the natural dynamics of a two-species fermionic system that is capable of undergoing BCS-BEC Crossover. The motivation was to probe whether the dynamical studies can be used to probe momentum-space structures in the population-imbalanced Fermi system. We found that the oscillation of the condensate fraction is periodic or quasi periodic, depending on the value of Feshbach coupling.There is a critical coupling below which the oscillation is always periodic, and its value depends on the population imbalance. Moreover, these frequencies of oscillations are found to be sensitive to the nature of pairing in the momentum space. We proposed that this method can be employed to map the momentum-space structure of the novel pairing states characteristic of population-imbalanced systems. In our view, this is a really important approach, since it is extremely difficult to detect the exotic pairing states like the FFLO

and Breached Pair state experimentally. The ability to resolve their momentum space structures, therefore, is beyond the scope of present-day experiments. We felt that an indirect experimental method can be of great significance, and our dynamical studies suggested a technique for the same. We showed that if there is an additional oscillatory component present in the Feshbach magnetic field, one can achieve a sharp resonance in the condensate fraction by tuning its frequency. The boundary values of the breached momentum region, or the region that hosts the excess unpaired fermions, can be calculated from this frequency value. Thus it proves to be an indirect method of experimental determination of the momentum space structure of the imbalanced Fermi gas.

6.2 Future Directions

We have addressed some of the important issues in the context of ultracold atom gases. The results we obtained also open up newer possibilities. We plan to look at the following problems in future:

- To extend our work on dynamical studies to cover Fermi systems with a finite-momentum pairing, i.e, the FFLO state, and to probe whether the value of the pairing momenta can be deduced from the oscillation in the condensate fraction.
- To study BCS-BEC crossover in the presence of disorder, and find out whether disorder itself can be the driving factor that causes the crossover if three-body interactions are considered.
- To link the study of periodic quench with two-level systems and find out how the Landau Zener probability of transition is affected by the periodic drive.
- To look for competing instabilities in ultracold atom systems, e.g the pairing and magnetic instability, using dynamical studies.

The study of ultracold atom systems is important not only from the perspective of cold atoms, but from other branches of physics as well. The techniques and concepts which we came across while studying ultracold atoms have greater applicability : they can be used

to explore untrodden areas in nuclear physics and condensed matter physics. Ultacold atom physics is an useful test bed for studying interacting many-body systems, because the unparallelled tunability of system parameters in cold atom systems allows one to experimentally simulate standard condensed matter Hamiltonians. The knowledge from the study of cold quantum gases can be applied to understand superfluidity in nuclear matter, too. We foresee some of our works to be directed along condensed matter physics and nuclear physics, using the fundamental ideas of "pairing" and "condensation".